

NASA  
TP  
1911  
c.1

**NASA  
Technical  
Paper  
1911**

March 1982

# Design Criteria for Flightpath and Airspeed Control for the Approach and Landing of STOL Aircraft

James A. Franklin,  
Robert C. Innis,  
Gordon H. Hardy,  
and Jack D. Stephenson

LOAN COPY: RETURN TO  
AFWL TECHNICAL LIBRARY  
WRIGHT-PATTERSON AFB, N. M.



**NASA**

**NASA  
Technical  
Paper  
1911**

1982

TECH LIBRARY KAFB, NM



0067686

# Design Criteria for Flightpath and Airspeed Control for the Approach and Landing of STOL Aircraft

James A. Franklin,  
Robert C. Innis,  
Gordon H. Hardy,  
and Jack D. Stephenson  
*Ames Research Center  
Moffett Field, California*

**NASA**

National Aeronautics  
and Space Administration

Scientific and Technical  
Information Branch



## TABLE OF CONTENTS

	Page
CHARACTERISTICS OF GLIDE-SLOPE CONTROL .....	2
CHARACTERISTICS OF FLARE CONTROL .....	10
Flare with Pitch Rotation .....	10
Flare with Thrust .....	14
DESCRIPTION OF FLIGHT RESEARCH PROGRAM .....	14
Research Aircraft .....	14
Evaluation Configurations .....	26
Evaluation Task .....	30
Data Acquisition .....	33
DISCUSSION OF RESULTS .....	34
Glide-Slope Control .....	34
Flare Control .....	45
IMPLICATIONS FOR DESIGN CRITERIA .....	58
Glide-Slope Control .....	58
Flare Control .....	61
CONCLUSIONS .....	63
APPENDIX A – TURBULENCE RESPONSE RELATIONSHIPS .....	64
APPENDIX B – DOCUMENTATION OF EVALUATION CONFIGURATIONS .....	66
APPENDIX C – SUMMARY OF PILOT COMMENTS AND RATINGS .....	80
APPENDIX D – SYMBOLS .....	90
REFERENCES .....	93



# DESIGN CRITERIA FOR FLIGHTPATH AND AIRSPEED CONTROL FOR THE APPROACH AND LANDING OF STOL AIRCRAFT

James A. Franklin, Robert C. Innis, Gordon H. Hardy, and Jack D. Stephenson

Ames Research Center

*A flight research program was conducted to assess requirements for flightpath and airspeed control for glide-slope tracking during a precision approach and for flare control, particularly as applied to powered-lift, short takeoff and landing (STOL) aircraft. In some instances, the results are also pertinent to other types of aircraft that execute steep approaches to a flare and landing at low airspeeds. Ames Research Center's Augmentor Wing Research Aircraft was used to fly approaches on a 7.5° glide slope to landings on a 30 × 518 m (100 × 1700 ft) STOL runway. The aircraft's research flight control system made it possible to evaluate a wide range of flightpath and airspeed control characteristics. The dominant aircraft response characteristics that influence flying qualities for approach path tracking were determined to be flightpath overshoot, flightpath-airspeed coupling, and the initial flightpath response time. The significant contribution to control of the landing flare using pitch attitude was the short-term flightpath response. The limiting condition for initial flightpath response time for flare control with thrust was also identified. In general, the range of these characteristics that encompasses satisfactory to unacceptable flying qualities for the approach and landing was determined. Considering these data, as well as results of other flight and ground-based simulator programs, it is possible to define flying-qualities design criteria for glide-slope and flare control based on the aforementioned response characteristics.*

Military flying-qualities specifications (refs. 1, 2), civil airworthiness regulations (refs. 3, 4), and other design criteria for short takeoff and landing (STOL) transport aircraft (refs. 5, 6), contain little information on flightpath and airspeed control requirements for the approach and landing phase. In recent years, analytical studies, ground-based simulation and flight experiments have contributed to a basic understanding of those characteristics of STOL aircraft that influence flightpath and airspeed control; they have also served to define the pilot's control behavior that is necessary to the execution of precision STOL approaches and landings. The flight experiments that are described in this report were the culmination of a research program conducted at Ames Research Center to identify the pertinent flightpath and airspeed control characteristics that affect precision approach path control and flare capability and to establish with flight data the range of these characteristics that encompasses satisfactory to unacceptable flying qualities for the approach and landing task.

An analytical study and ground-based simulation experiments were conducted as part of the program at Ames Research Center (ref. 7). That effort concentrated on glide-slope tracking for a powered-lift aircraft through control of engine thrust; it identified the characteristics of flightpath and airspeed response to thrust that seemed most important to the pilot in performing precision instrument approaches to minimum decision heights. A number of other analyses

and simulation experiments of the flare and landing, as well as for glide-slope tracking have been also conducted (refs. 8-11); a summary of the flight-test results presented here is contained in reference 12. Data from flight experiments with the Princeton Variable Stability Navion, concerned with flightpath control for the approach and landing, are presented in references 10 and 13. Together, these various programs provide a variety of criteria based on open-loop time response characteristics or closed-loop frequency response that can be of use in the design of an aircraft or in definition of new flying-qualities specifications or airworthiness standards. In fact, tentative flying-qualities specifications and certification criteria have been published in references 14 and 15 as a consequence of these programs, as well as from experience (as yet unpublished) gained from the U.S. Air Force's Advanced Medium STOL Transport prototype flight-test program.

This report describes in detail a flight research program conducted at Ames Research Center and presents design criteria based on these data as well as data extracted from the sources noted previously. Background information regarding the aircraft response characteristics selected for evaluation of glide-slope tracking and flare control in these flight experiments is presented first. The experiment, including the research aircraft, the experimental configuration setup, the evaluation task, and the data acquisition and analysis, is described and flight-test results are discussed,

primarily in terms of interpretations of pilot opinion ratings and commentary. Supporting data extracted from time histories of the aircraft's response and the existing wind and atmospheric turbulence are included. Design criteria for glide-slope and flare control are also defined. The results are considered applicable to glide-slope control during precision approaches along steep flightpaths for powered-lift aircraft and for low-wing-loading aircraft that use direct-lift control devices; the results are also applicable to the flare and landing of any type of STOL aircraft.

### CHARACTERISTICS OF GLIDE-SLOPE CONTROL

Analytical studies, ground-based simulation experiments, and some limited flight research programs (refs. 7-10) have defined the characteristics of flightpath and airspeed response that are likely to be crucial to glide-slope tracking and to maintaining safety margins during a precision landing approach. In general, these characteristics establish control authority and sensitivity, dynamic response, and cross-coupling between flightpath and airspeed response to the pitch attitude and throttle controls and response to longitudinal and vertical winds and turbulence. It is typical to assume that adequate pitch attitude control is provided, generally by a form of control augmentation such as an attitude-command or pitch rate-command/attitude-hold system. Because these aircraft invariably operate on the back side of the drag curve, the glide-slope tracking control technique involves flightpath control with thrust and airspeed control with pitch attitude.

The flightpath and airspeed response characteristics to these controls that are of interest may be described in either the time or frequency domains. Figure 1 illustrates a typical time response of flightpath and airspeed to the throttle control. As indicated in references 7 and 9, the significant characteristics are

- Control authority, described by  $\Delta\gamma_{ss}$
- Initial time response, arbitrarily described by  $t_{0.5\Delta\gamma_{max}}$ , that determines how quickly flightpath responds to the throttle input
- Overshoot in flightpath response, described by  $(\Delta\gamma_{max}/\Delta\gamma_{ss})\Delta T$  that determines how well the pilot can anticipate a stabilized flightpath correction based on the short-term response
- Steady-state coupling between flightpath and airspeed, described by  $(\Delta u_{ss}/\Delta\gamma_{ss})\Delta T$ , that determines the attention the pilot must devote to maintaining airspeed during a flightpath correction.

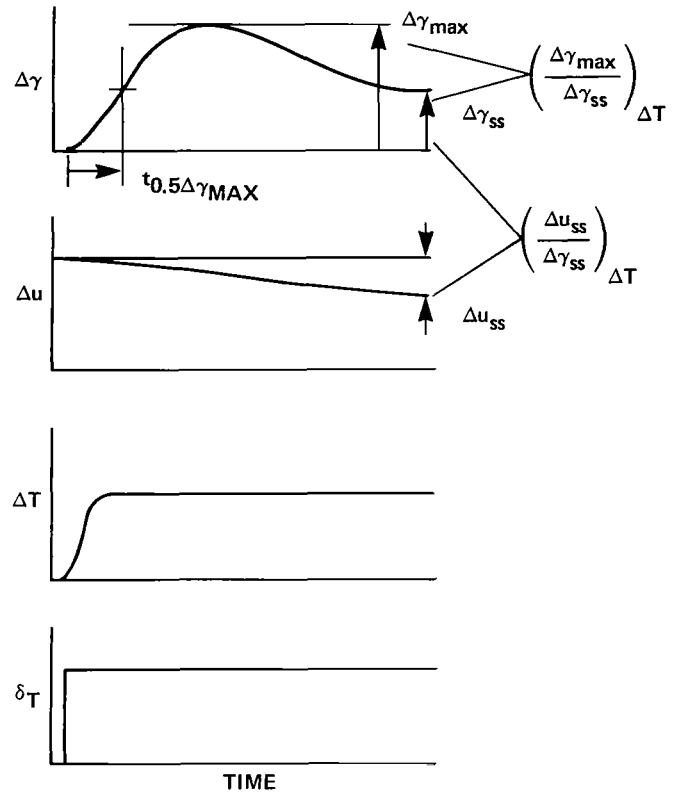


Figure 1.— Characteristics of flightpath and airspeed response to throttle for constant pitch attitude.

Although not explicitly illustrated in figure 1, throttle control sensitivity, exemplified by the slope of the initial flightpath response per unit throttle input or by the derivative  $Z_{\delta T}$ , is also an important influence on flightpath control with thrust.

Short-term airspeed response to the throttle is of little consequence because the pilot typically is concerned with long-term speed variations and does not choose to maintain tight speed control. Speed control with pitch attitude is correspondingly of interest in the steady-state, and is characterized by the speed-to-attitude sensitivity  $\Delta u_{ss}/\Delta\gamma_{ss}$ . Flightpath response to attitude is not of concern because attitude is not used directly for flightpath control; attitude only influences the flightpath indirectly in the long-term in conjunction with its use to control speed. It is generally considered that as long as sufficient flightpath control authority exists in response to thrust, any long-term path variations resulting from pitch control activity can be readily managed with the throttles.

In the frequency domain, the primary concern, as noted in references 9 and 10, is with the phase margin available for flightpath response to the throttle to insure adequate closed-loop stability for control of flightpath at bandwidths in the range of 0.5 to 0.8 rad/sec (ref. 10).

Each of the characteristics noted in the foregoing discussion may be related to the aircraft's primary stability and control derivatives for purposes of defining design criteria by the transfer functions of flightpath and airspeed response to throttle, assuming constant pitch attitude:

$$\frac{\gamma}{\delta T}(s) = \frac{A_{\gamma T}(s + 1/T_{\gamma T})}{\left(\frac{s^2}{\omega_E^2} + \frac{2\xi_E}{\omega_E}s + 1\right)} \Delta\theta = \text{const}$$

$$\frac{u}{\delta T}(s) = \frac{A_{uT}(s + 1/T_{uT})}{\left(\frac{s^2}{\omega_E^2} + \frac{2\xi_E}{\omega_E}s + 1\right)} \Delta\theta = \text{const}$$

$$\Delta\theta = \text{const} = s^2 + 2\xi_\theta\omega_\theta s + \omega_\theta^2 \quad \text{or} \quad (s + 1/T_{\theta_1})(s + 1/T_{\theta_2})$$

The transfer-function parameters can, in turn, be described as functions of the aircraft's longitudinal and vertical force perturbation derivatives resulting from longitudinal and vertical velocity and thrust control:

$$X_u, X_w, X_{\Delta T}$$

$$Z_u, Z_w, Z_{\Delta T}$$

In figure 2, examples of flightpath response to step throttle inputs, normalized in time with respect to the appropriate frequency parameter ( $\omega_\theta$  or  $1/T_{\theta_2}$ ), are shown to illustrate the influence of various transfer-function parameters on time-response characteristics. It is apparent that engine dynamic response  $\omega_E$  and the numerator and denominator time constants ( $T_{\gamma T}$  and  $T_{\theta_1}$ ) have a substantial effect on the shape of the initial flightpath response. In particular, increasing the engine response time (reducing  $\omega_E/\omega_\theta$ ) has the effect of significantly increasing the lag in flightpath response to throttle. Increasing the time constant  $T_{\theta_1}$  with respect to  $T_{\theta_2}$  also increases the flightpath lag, particularly as the transient response approaches its steady-state value. Flightpath overshoot is influenced to a considerable extent by the ratio of the numerator to denominator roots ( $1/T_{\gamma T}\omega_\theta$  or  $T_{\theta_1}/T_{\gamma T}$ ).

Figures 3 and 4 present a more detailed summary of the effects on the nondimensional initial time response and on flightpath overshoot. It can be seen in figure 3 that, as the engine response time approaches that of the airframe flightpath response ( $\omega_E \rightarrow \omega_\theta$  or  $1/T_{\theta_2}$ ), the initial path response time increases significantly, although not in inverse proportion. Variations in the ratio of the path response numerator time constant  $T_{\gamma T}$  to the path response mode  $\omega_\theta$  or  $T_{\theta_1}$ , produce directly proportional changes in

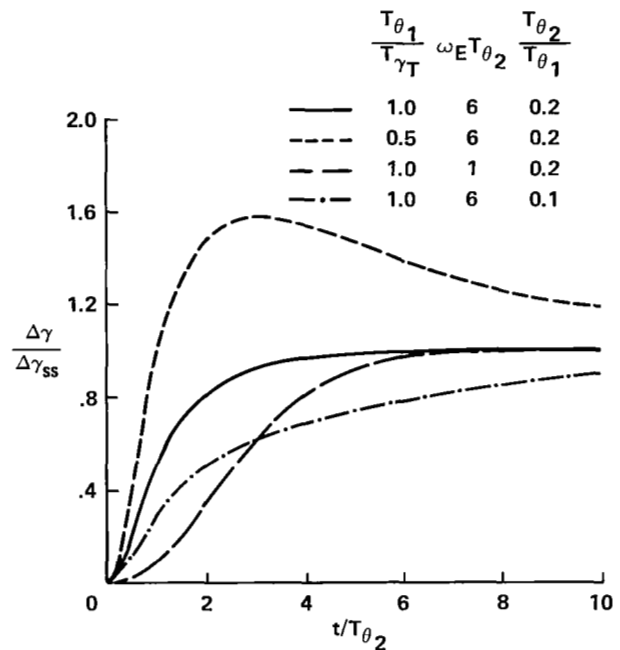
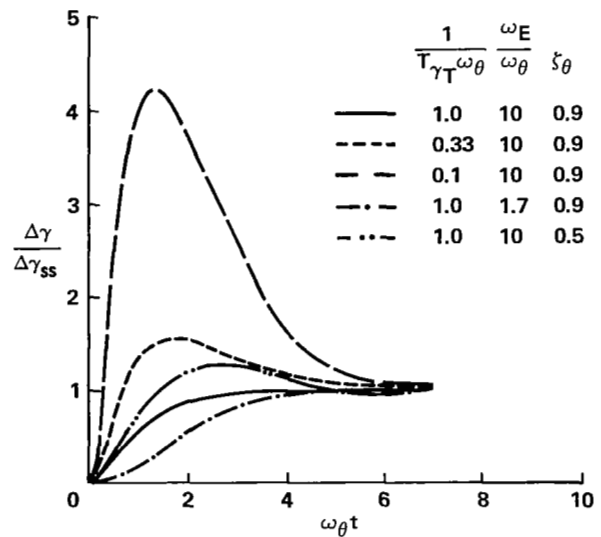
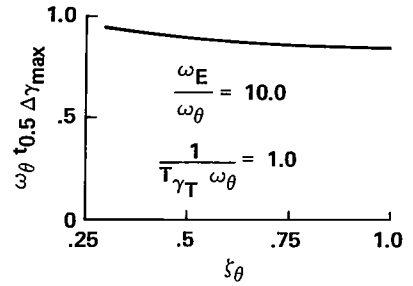
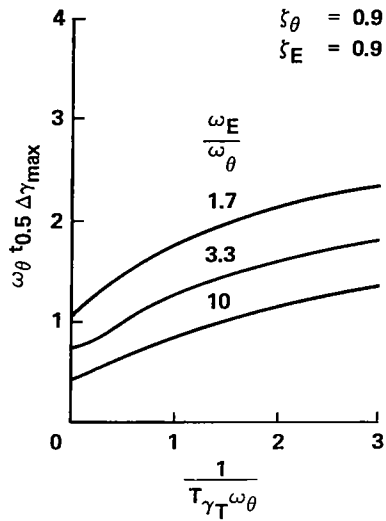
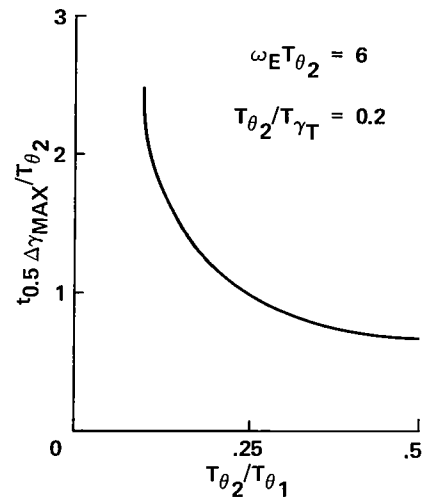
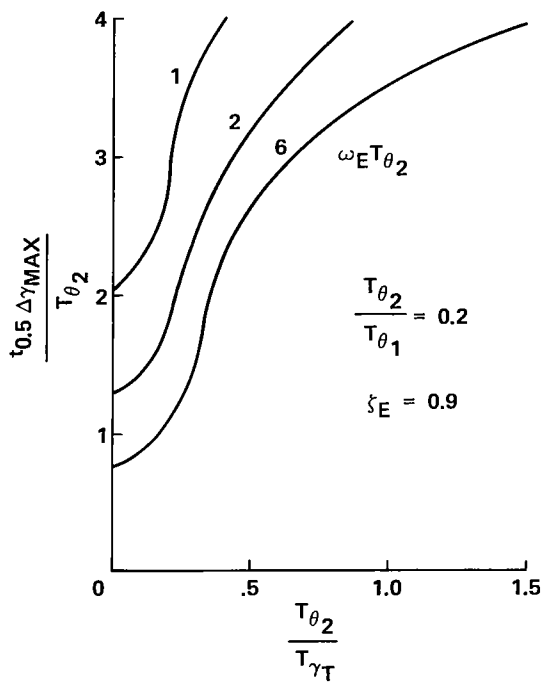


Figure 2.— Normalized flightpath time histories in response to a step throttle input.

the initial response,  $t_{0.5}\Delta\gamma_{\text{max}}$ . The ratio of the flightpath and airspeed-mode time constants ( $T_{\theta_2}/T_{\theta_1}$ ) has a nearly inversely proportional influence on the initial response time (fig. 3(b)) and path-mode damping ratio  $\xi_\theta$  has little effect (fig. 3(a)). Thus, the dominant contributions to the initial response time come from the path-mode bandwidth ( $\omega_\theta$  or  $1/T_{\theta_2}$ ), the speed-mode bandwidth ( $1/T_{\theta_1}$ ), the path-response numerator time constant ( $1/T_{\gamma T}$ ), and the engine response time ( $\omega_E$ ). In figure 4, it is apparent that flightpath overshoot can become substantial when the ratio of



(a) Complex characteristic roots.



(b) Real characteristic roots.

Figure 3.— Influence of transfer-function factors on initial flightpath time response to a step throttle input.

$$\frac{\omega_E}{\omega_\theta} = 10.0 \quad \zeta_E = 0.9$$

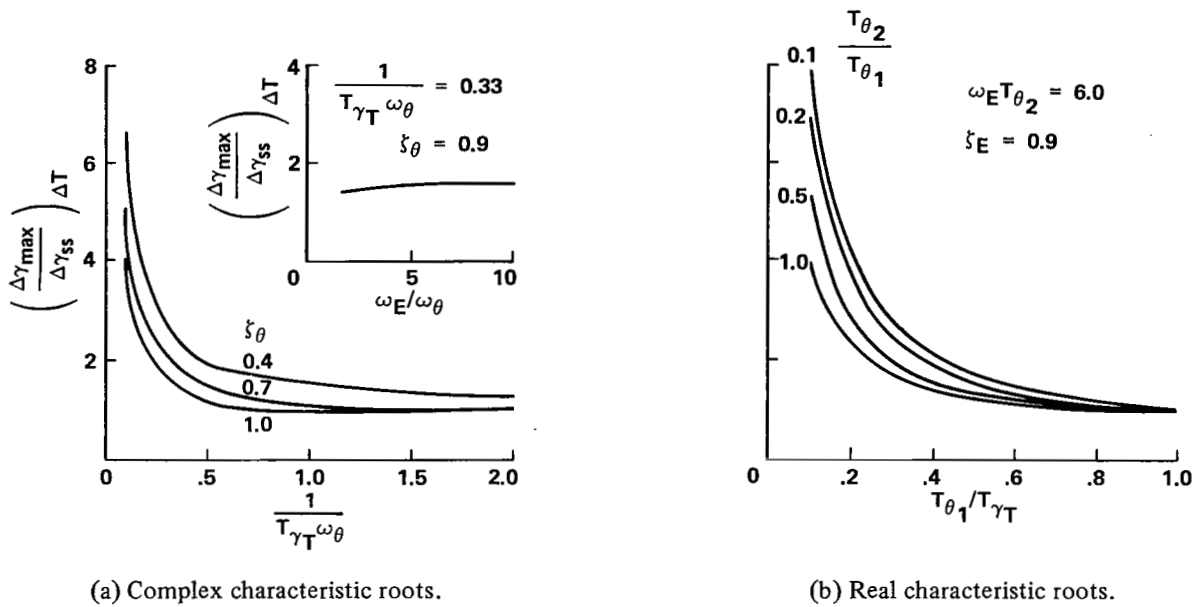


Figure 4.— Influence of transfer-function parameters on flightpath overshoot.

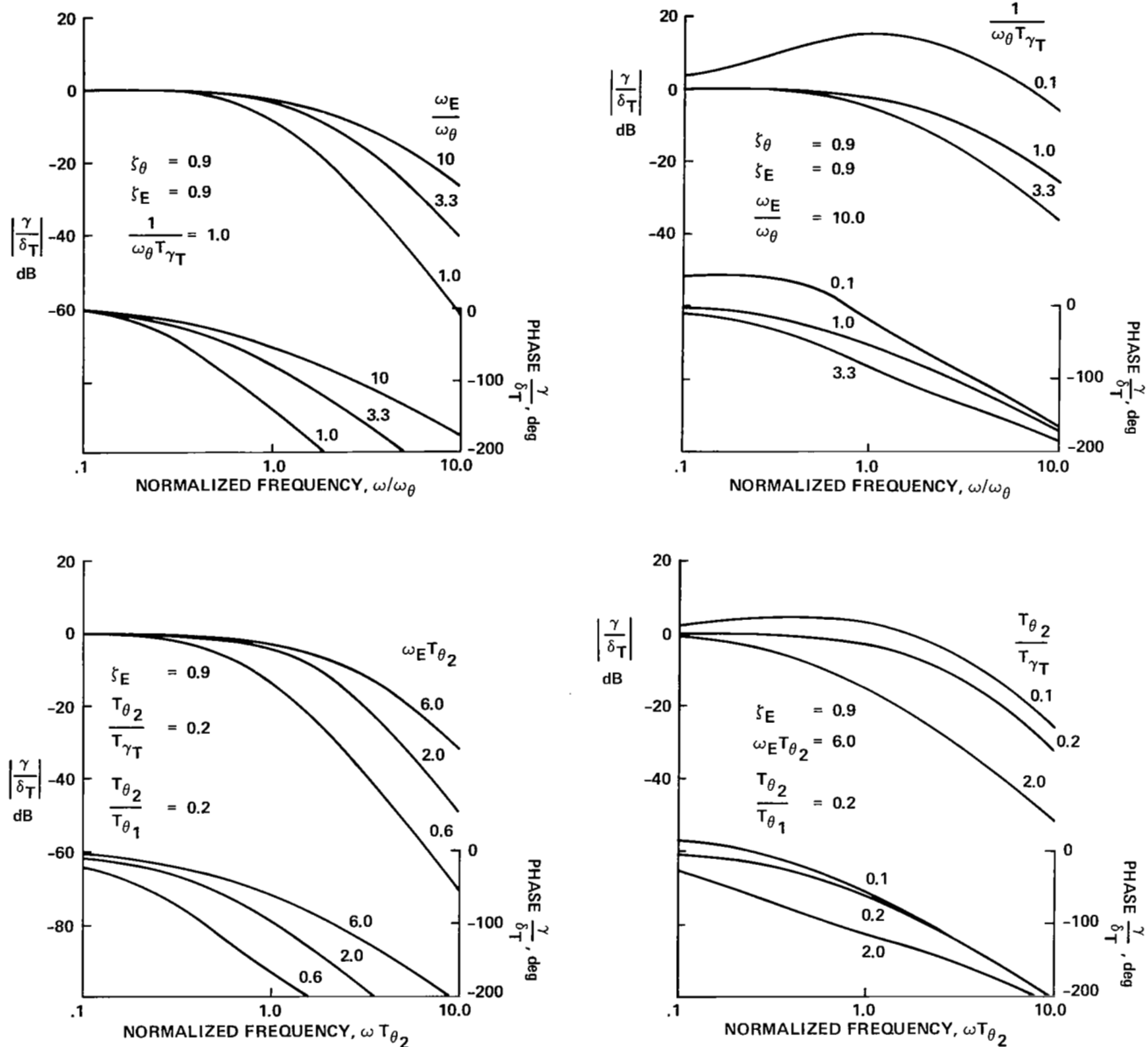
the flightpath numerator factor  $1/T_{\gamma T}$  to  $\omega_\theta$  or  $1/T_{\theta_1}$  is less than one half. Path-mode damping  $\zeta_\theta$  also has an influence on overshoot, as might be expected (fig. 4(a)). However, engine dynamic response  $\omega_E$  has little effect in this regard.

Contributions to frequency response characteristics are illustrated in figure 5. It can be seen that phase margin for flightpath control at or above the path-mode frequencies  $\omega_\theta$  or  $1/T_{\theta_2}$  is quite sensitive to variations in engine dynamics (fig. 5(a)) and somewhat less so to variations in the path-mode numerator (fig. 5(b)), path-mode damping (fig. 5(c)), or the speed-mode time constant (fig. 5(d)). The effect of the numerator time constant on amplification of the path response at the path-mode frequencies ( $\omega_\theta$  or  $1/T_{\theta_2}$ ) is also evident. These contributions are summarized in figures 6(a) and 6(b). The diagrams at the upper right in figures 6(a) and 6(b) show that as the engine response bandwidth approaches that of the flightpath response ( $\omega_E \rightarrow \omega_\theta$  or  $1/T_{\theta_2}$ ), phase margins for control of flightpath with throttles is reduced significantly. As shown in the graphs at the upper left of these figures, the flightpath numerator adds noticeable lead for ratios of  $1/T_{\gamma T} \omega_\theta$  or  $T_{\theta_2}/T_{\gamma T}$  much less than 1. From the graphs at the bottom of figures 6(a) and 6(b) it is apparent that any reduction in the aircraft's path-response frequency below the pilot's nominal path-control bandwidth ( $\omega_\theta/\omega_{BW}$  or  $1/T_{\theta_2} \omega_{BW} < 1$ ) is accompanied by a significant reduction in phase margin. Consequently, when the pilot attempts to

control flightpath at frequencies greater by a factor of 2 or more than the aircraft's basic response mode, the phase margin for flightpath response will be reduced to values that are unacceptable for closed-loop control (less than  $45^\circ$  to  $60^\circ$ ). For acceptable phase margins for control of glide-slope deviations (the integral of flightpath) control bandwidths of the order of the basic aircraft mode or less are indicated.

Concerning flightpath airspeed coupling, it was noted in reference 7 that the coupling ratio  $(\Delta u_{ss}/\Delta \gamma_{ss})\Delta T$  was strongly influenced by the relationship of the path-response numerator root to the path-response mode ( $1/T_{\gamma T} \omega_\theta$ ) and by the path-response bandwidth  $\omega_E$ . Figure 7 shows this relationship graphically and also presents an example of the time response for extreme values of the airspeed numerator root location. Although for the case in which the numerator root is negative (nonminimum phase) the initial and final response are of opposite sign, this characteristic of the dynamic response of airspeed, as well as the effective time constant of the response is of little interest to the pilot. Since speed is not being controlled tightly in the short term, the steady-state value of speed in relation to the flightpath correction being accomplished with thrust is of the most significance.

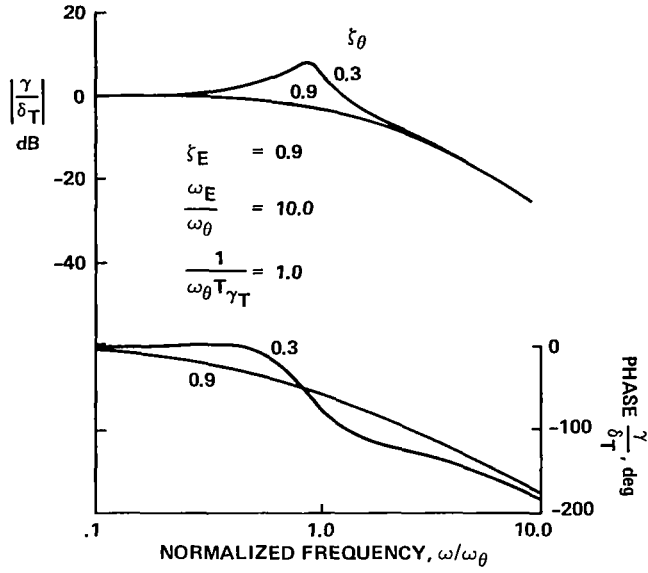
It is worthwhile to review the influence of the aircraft's dynamic stability derivatives on the transfer-function factors that, in turn, most prominently affect the flightpath



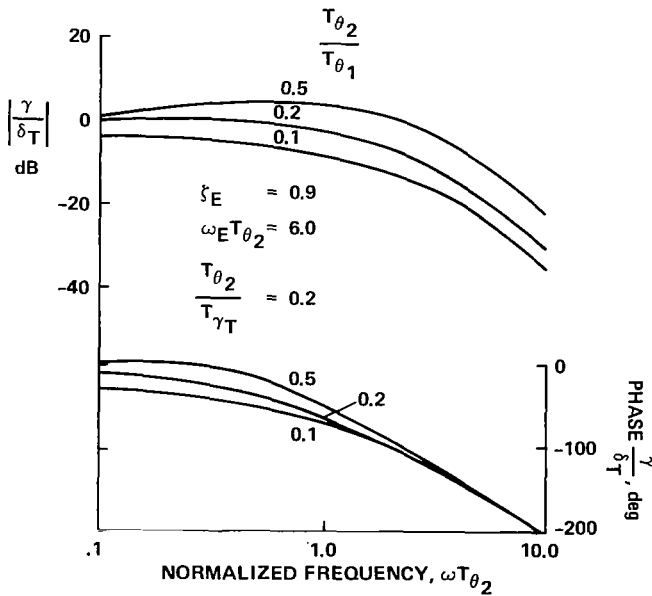
(a) Effect of engine dynamics.

(b) Effect of numerator root.

Figure 5.— Frequency response characteristics of flightpath to throttle control.



(c) Effect of damping ratio.



(d) Effect of speed response mode,  $1/T_{\theta_1}$ .

Figure 5. — Concluded.

and airspeed response characteristics of interest. These transfer-function factors and their relation to the aircraft's derivatives are as follows.

- Flightpath response bandwidth:

$$\omega_{\theta}^2 \text{ or } \frac{1}{T_{\theta_1}T_{\theta_2}} = (X_u Z_w - X_w Z_u)$$

- Flightpath damping:

$$2\zeta_{\theta}\omega_{\theta} \text{ or } \frac{1}{T_{\theta_1}} + \frac{1}{T_{\theta_2}} = -(X_u + Z_w)$$

- Flightpath numerator root:

$$\frac{1}{T_{\gamma T}} = -X_u + \frac{X_{\Delta T}}{Z_{\Delta T}} Z_u$$

- Engine-response bandwidth:  $\omega_E$

- Flightpath-airspeed coupling ratio:

$$\left( \frac{\Delta u_{ss}}{\Delta \gamma_{ss}} \right)_{\Delta T} = \frac{T_{\gamma T} \omega_{\theta}^2}{Z_u/V_0} \left( 1 + \frac{Z_w}{T_{\gamma T} \omega_{\theta}^2} \right)$$

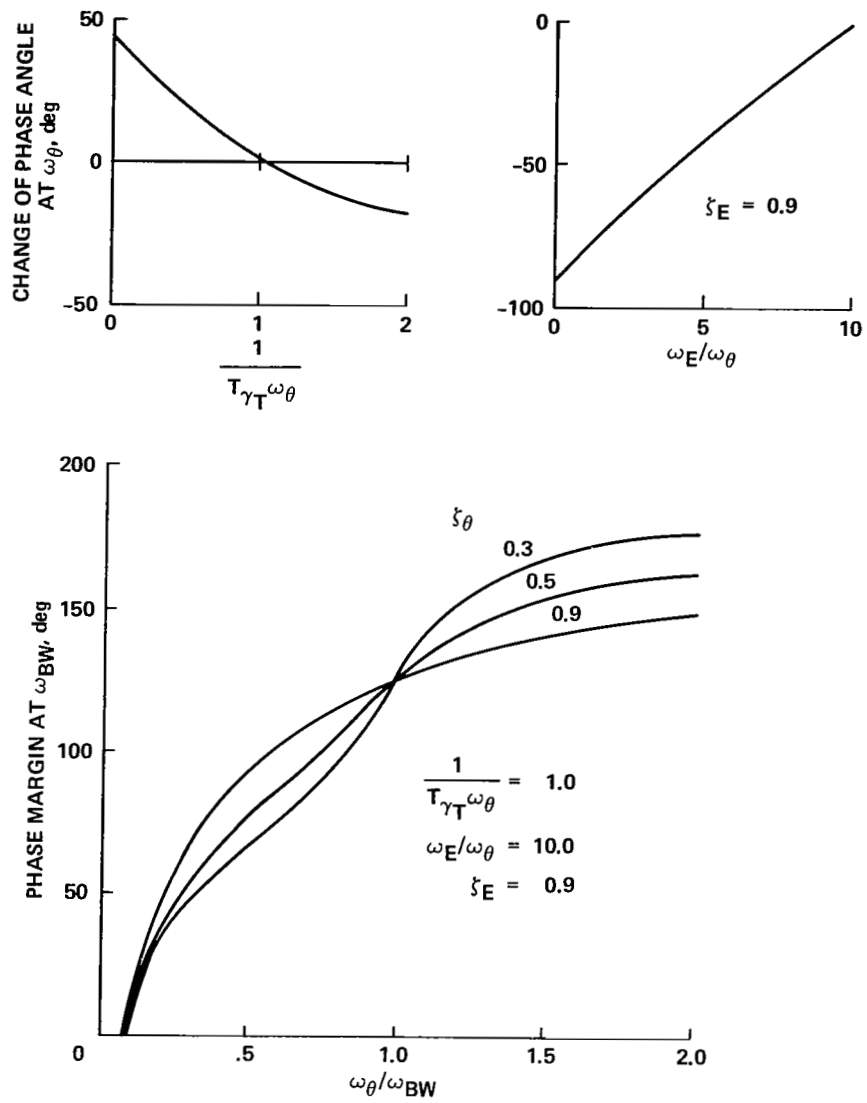
- Airspeed numerator root:

$$\frac{1}{T_{uT}} = -Z_w + \frac{Z_{\Delta T}}{X_{\Delta T}} X_w$$

These relationships illustrate the influence of such factors as vertical velocity damping  $Z_w$ , axial velocity damping  $X_u$ , lift and drag cross-coupling  $Z_u$  and  $X_w$ , and effective thrust turning  $\theta_T = \tan^{-1}(-Z_{\Delta T}/X_{\Delta T})$  on the response characteristics and provide a link to the aircraft configuration for eventual determination of design criteria for flightpath control.

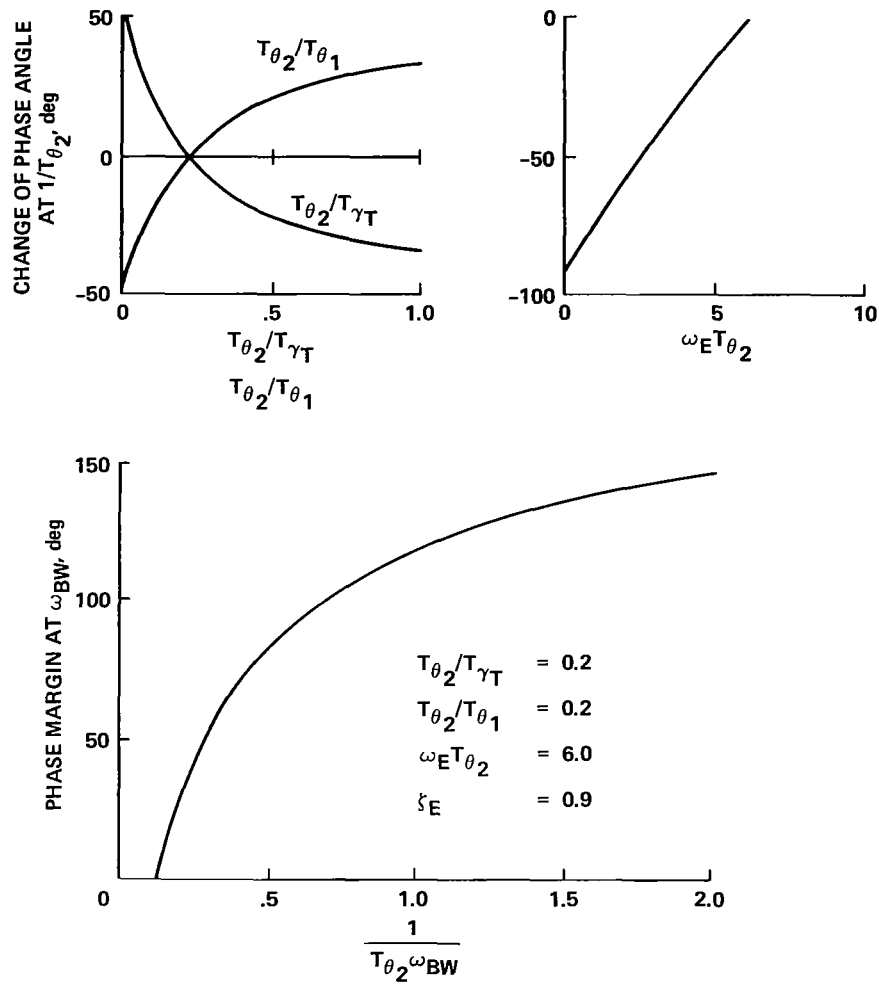
In the flight research program, evaluations of glide-slope tracking were conducted to provide data for determining satisfactory through adequate flying qualities associated with variations in

- Initial flightpath time response,  $t_{0.5} \Delta \gamma_{\max}$
- Flightpath overshoot  $(\Delta \gamma_{\max}/\Delta \gamma_{ss}) \Delta T$
- Flightpath-airspeed coupling  $(\Delta u_{ss}/\Delta \gamma_{ss}) \Delta T$



(a) Complex characteristic roots.

Figure 6.— Contribution of transfer-function factors to phase margin of flightpath response to throttle.



(b) Real characteristic roots.

Figure 6.— Concluded.

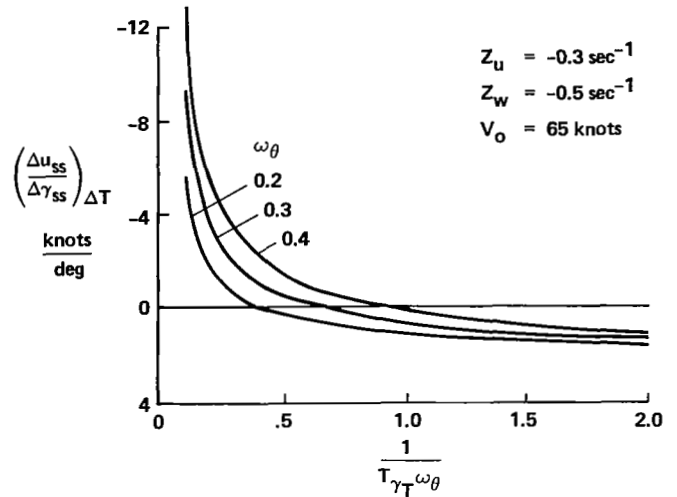
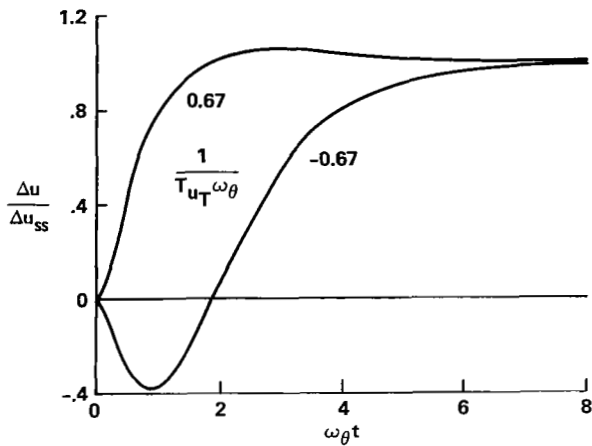


Figure 7.— Influence of transfer-function factors on airspeed response to a step throttle input.

Flightpath control authority has been assessed and reported in references 9 and 15 and substantiated in flight experiments, the results of which are in the process of publication. Throttle control sensitivity was kept constant at the value of the basic aircraft. Airspeed response to pitch was not investigated independently because the results of reference 7 indicated that approach flying qualities were not sensitive to variations over a wide range of  $-1.0 \leq \Delta u_{ss}/\Delta \theta_{ss} \leq -4.0$  knots/deg. Turbulence response was maintained substantially at the level of the basic aircraft as dominated by the derivative  $Z_u$  (refs. 9 and 10 and appendix A). Wind-shear response varied in proportion to the aircraft's flightpath-to-airspeed gradient at constant thrust,  $d\gamma/du$ , based on the relationship derived in appendix A.

### CHARACTERISTICS OF FLARE CONTROL

The landing flare maneuver with a STOL aircraft may put few demands on the pilot or it may require a coordinated application of the controls for orienting the aircraft for touchdown and arresting its sink rate. It is possible that no flare action would be required of the pilot if the aircraft were designed to absorb high sink rates and if ground effects were favorable for cushioning the landing without inducing floating tendencies. The complexity of the pilot's control application can range from an open-loop control of pitch attitude or thrust to partially arrest the rate of sink, to continuous, closed-loop modulation of the pitch and thrust controls and even use of an auxiliary lift control device (such as an independent direct lift control). It should be clear that the no-flare and open-loop flare require little

design consideration in terms of pilot controllability. The purpose of this investigation is to consider the requirements for performing a flare to a reasonably low sink rate while using either the pitch or thrust controls. This maneuver could conceivably require closed-loop control of the aircraft through the flare to make adjustments for achieving a reasonable and repeatable touchdown point and sink rate. Hence, the dynamic response of the aircraft to either pitch or thrust controls should be considered in defining the aircraft's flare characteristics.

### Flare with Pitch Rotation

Both open-loop time response and open or closed-loop frequency response characteristics have been suggested as measures of flare-control behavior in response to pitch-attitude inputs. In reference 12, the nature of the open-loop time response of flightpath to a step change in pitch attitude was considered, particularly as it affects the maximum change in the initial flightpath response and the time required for this initial response to decay to some fraction of its maximum value. The initial flightpath response to pitch determines the ability to substantially reduce the rate of descent without an excessive requirement for pitch rotation. The rate at which the initial path correction can be developed also might be considered to be important; however, this characteristic can also be dominated by the rate of the pitch maneuver. For aircraft that are operated near to or on the backside of the drag curve, the initial change in flightpath following a step change in pitch attitude cannot be sustained and will subsequently decay to some lesser value (for operation on the backside of the drag curve, the path correction will eventually reverse in

sign and the steady flightpath will be steeper than the initial path). The ability to sustain the flightpath correction for a duration required to complete the flare was considered to be a factor of possible significance to the pilot for landing precision. It is possible that too rapid a washout of the path correction could lead to hard landings, and that too little washout could induce floating and lead to excessive landing distances.

Reference 9 also presented open-loop time-response measures, such as normal acceleration capability or vertical velocity damping, as potential descriptors of the maneuver. Closed-loop control characteristics were described extensively in reference 10, with flightpath frequency and damping playing a major role in the assessment of flightpath response. Figure 8 presents an example time history of response to a step change in pitch attitude that illustrates the characteristics of flightpath response for this maneuver. The initial response is characterized by the maximum value of the response and the time to reach a fraction of this maximum. In the long term, the response can be described by the decay time and the steady-state flightpath angle, if the response stabilizes within a reasonable period of time.

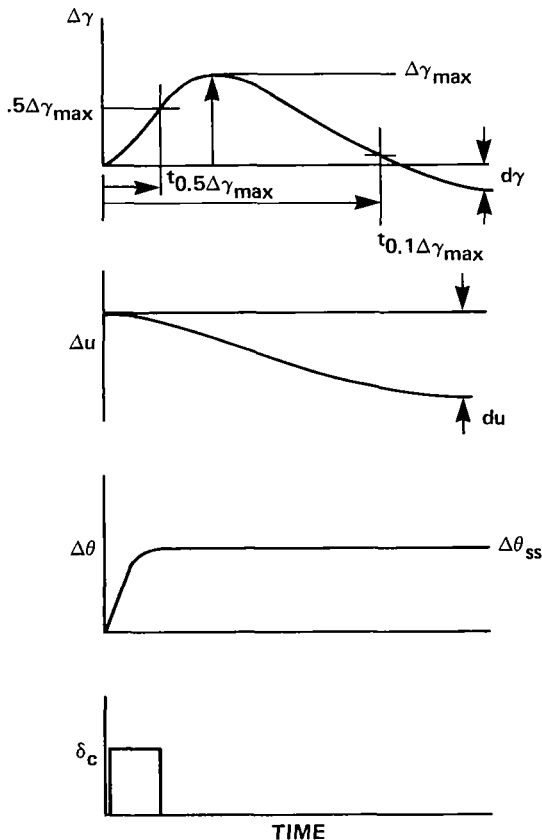


Figure 8.— Characteristics of flightpath and airspeed response to pitch attitude for constant thrust.

The particular measures associated with these characteristics are the ratio of the maximum flightpath increment to the step change in pitch attitude ( $\Delta\gamma_{\max}/\Delta\theta_{ss}$ ), the initial response time increment ( $t_{0.5\Delta\gamma_{\max}}$ ), and the decay time ( $t_{0.1\Delta\gamma_{\max}}$ ). Closed-loop control characteristics noted in reference 10 are the same as those noted in the previous section; namely, the frequency ( $\omega_\theta$ ) and damping ratio ( $\zeta_\theta$ ).

In a manner similar to that of the flightpath-thrust response relationship, the flightpath-attitude relationship can be described by a transfer function of the form (refs. 7, 9, 10)

$$\frac{\gamma}{\theta_c}(s) = \frac{A_{\gamma\theta}(s + 1/T_{\gamma_1})}{\Delta\theta = \text{const}}$$

In figure 9, examples of flightpath response to a step change in pitch attitude are plotted against a nondimensional time parameter to illustrate the contributions of the transfer-function parameters. For the range of parameters shown, there is little variation in the initial time increment  $t_{0.5\Delta\gamma_{\max}}$ , except in proportion to changes in  $\omega_\theta$  or  $1/T_{\theta_2}$ . The magnitude of the initial peak is affected somewhat by the ratio of the numerator factor to the characteristic roots ( $1/T_{\gamma_1}\omega_\theta$  and  $T_{\theta_2}/T_{\gamma_1}$ ); it scales in direct proportion to the gain constant  $A_{\gamma\theta}$ . The decay time can be seen to be most affected by the ratio of the numerator and characteristic roots ( $1/T_{\gamma_1}\omega_\theta$  and  $T_{\theta_2}/T_{\gamma_1}$ ) and varies to a lesser degree as a function of  $T_{\theta_2}/T_{\theta_1}$ .

Figures 10 and 11 provide a more detailed summary of the contributions to the initial response magnitude and the response decay time. Since the initial response time varies predominantly in proportion to  $\omega_\theta$  or  $1/T_{\theta_2}$ , it is not included in these plots. Trends of  $t_{0.5\Delta\gamma_{\max}}$  would be identical to those shown in figure 3. From figure 10, it can be seen that the initial response magnitude  $\Delta\gamma_{\max}/\Delta\theta_{ss}$  is influenced to the first order by the gain factor  $A_{\gamma\theta}/\omega_\theta$  or  $A_{\gamma\theta}T_{\theta_2}$ . The ratio of the speed and path modes  $T_{\theta_2}/T_{\theta_1}$  has less effect on the initial magnitude; the path damping,  $\zeta_\theta$ , and the ratio of the numerator root  $1/T_{\gamma_1}$  to  $\omega_\theta$  or  $1/T_{\theta_2}$  have very little influence. Response decay time scales in direct proportion to  $\omega_\theta$  or  $1/T_{\theta_2}$  and is strongly influenced by the ratio of the numerator root to the path mode roots ( $1/T_{\gamma_1}\omega_\theta$  or  $T_{\theta_2}/T_{\gamma_1}$ ). The magnitude of the numerator root is directly associated with the steady-state flightpath to airspeed gradient  $d\gamma/du$  by the relationship

$$\frac{1}{T_{\gamma_1}} = -g \frac{d\gamma}{du} \doteq \frac{1}{3} \frac{d\gamma}{du} \frac{\text{deg}}{\text{knot}}$$

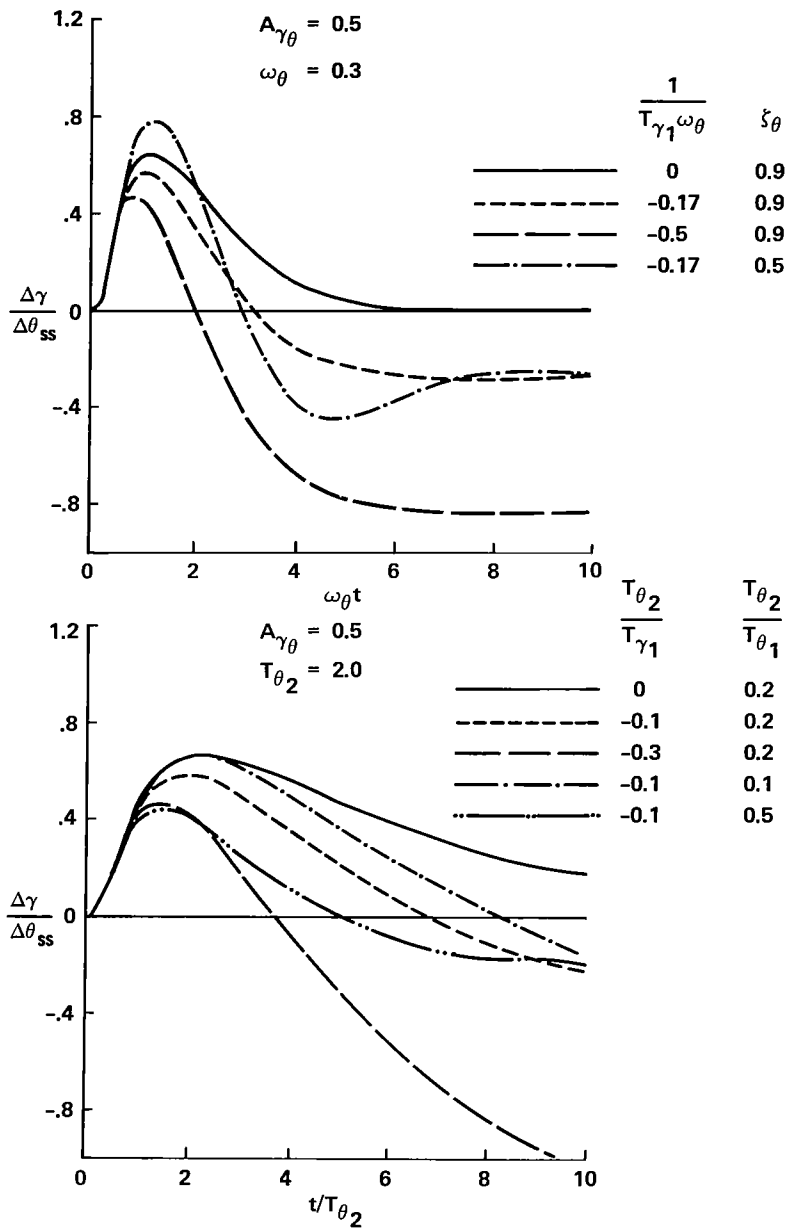


Figure 9.— Influence of transfer-function factors on flightpath response to a step change in pitch attitude.

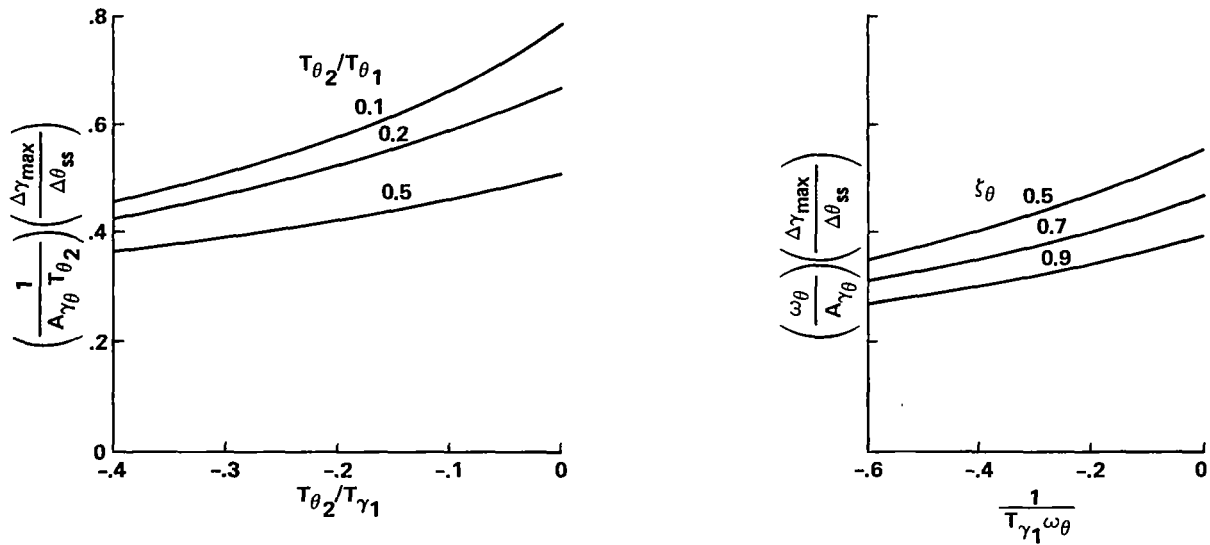


Figure 10.— Effect of transfer-function factors on initial flightpath response to pitch attitude.

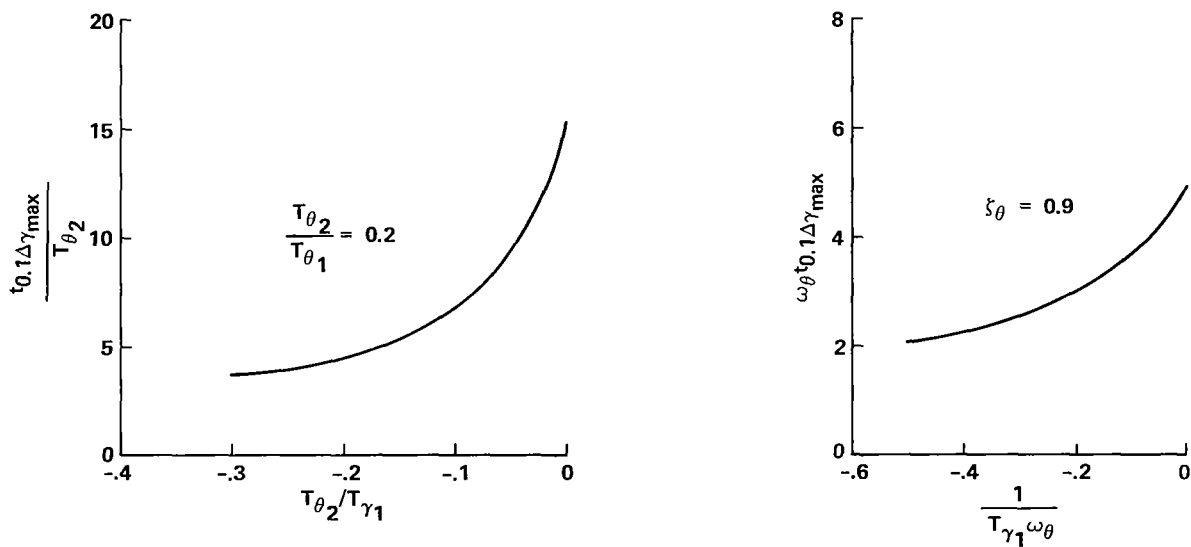


Figure 11.— Effect of transfer-function factors on long-term flightpath response to pitch attitude.

where  $d\gamma/du$  is positive for operating conditions on the backside of the drag curve. Thus, it can be seen from this relationship and from the trend of the curve in figure 11 that the time for the initial flightpath response to decay is substantially reduced as the gradient  $d\gamma/du$  (or  $1/T_{\gamma_1}$ ) increases, which is associated with operation further on the backside of the drag curve.

The influence of the aircraft's dynamic derivatives on the transfer-function factors that dominate the aircraft's

flightpath response to pitch attitude may be summarized as follows.

- Flightpath response bandwidth and damping are the same as noted previously for flightpath control with thrust
- Response sensitivity gain factor:

$$A_{\gamma\theta} = -Z_w + \frac{g}{V_0} \sin \gamma_0$$

- Flightpath numerator root:

$$\frac{1}{T\gamma_1} = -g \frac{d\gamma}{du}$$

$$= -X_u + Z_u \frac{X_w - \frac{g}{V_0} \cos \gamma_0}{Z_w - \frac{g}{V_0} \sin \gamma_0}$$

The relationships illustrate the influence of vertical velocity damping ( $Z_w$ ), axial velocity damping ( $X_u$ ), lift and drag cross-coupling ( $X_w$  and  $Z_u$ ), and the degree of operation on the backside of the drag curve on the aircraft's flare characteristics with pitch attitude. It is also worth noting that the relationship of normal acceleration to pitch rate is described by a transfer function nearly identical to that for flightpath response to pitch attitude, differing only by a factor equal to the initial airspeed (i.e.,  $(n_z/\dot{\theta})(s) = V_0(\gamma/\theta)(s)$ ). This means that the initial normal acceleration in response to an abrupt change in pitch rate, which provides the pilot strong cues regarding flare authority, scales in proportion to the maximum flightpath response to a step change in attitude (i.e.,  $n_{z\max}/\Delta\dot{\theta}_{ss} = V_0(\Delta\gamma_{\max}/\Delta\theta_{ss})$ ). Thus, these two metrics that influence the pilot's impression of flare control capability are strongly interrelated, and in fact are dominated by the derivative  $Z_\alpha$ .

### Flare with Thrust

Control of the flare with thrust can be treated conceptually in the same manner as glide-slope control with thrust. Response of the aircraft to a step application of thrust was previously illustrated in figures 1 and 2. Concerns for flare control which can be identified therein are

- How quickly the initial flightpath correction can be accomplished as indicated by  $t_{0.5} \Delta\gamma_{\max}$
- Short-term flightpath increment related to the increment in thrust,  $\Delta\gamma_{\max}/\Delta T$
- Degree to which the initial path correction washes out ( $\Delta\gamma_{\max}/\Delta\gamma_{ss})\Delta T$

Concerns similar to those expressed for flare response to pitch may be associated with these characteristics; namely, can the sink rate be substantially reduced within a short time and can this reduction be sustained for a sufficient duration to accomplish the flare. The question of being able to achieve a sufficient reduction in sink rate within operational thrust limits is, of course, analogous to the requirement for checking the sink rate within acceptable attitude limits.

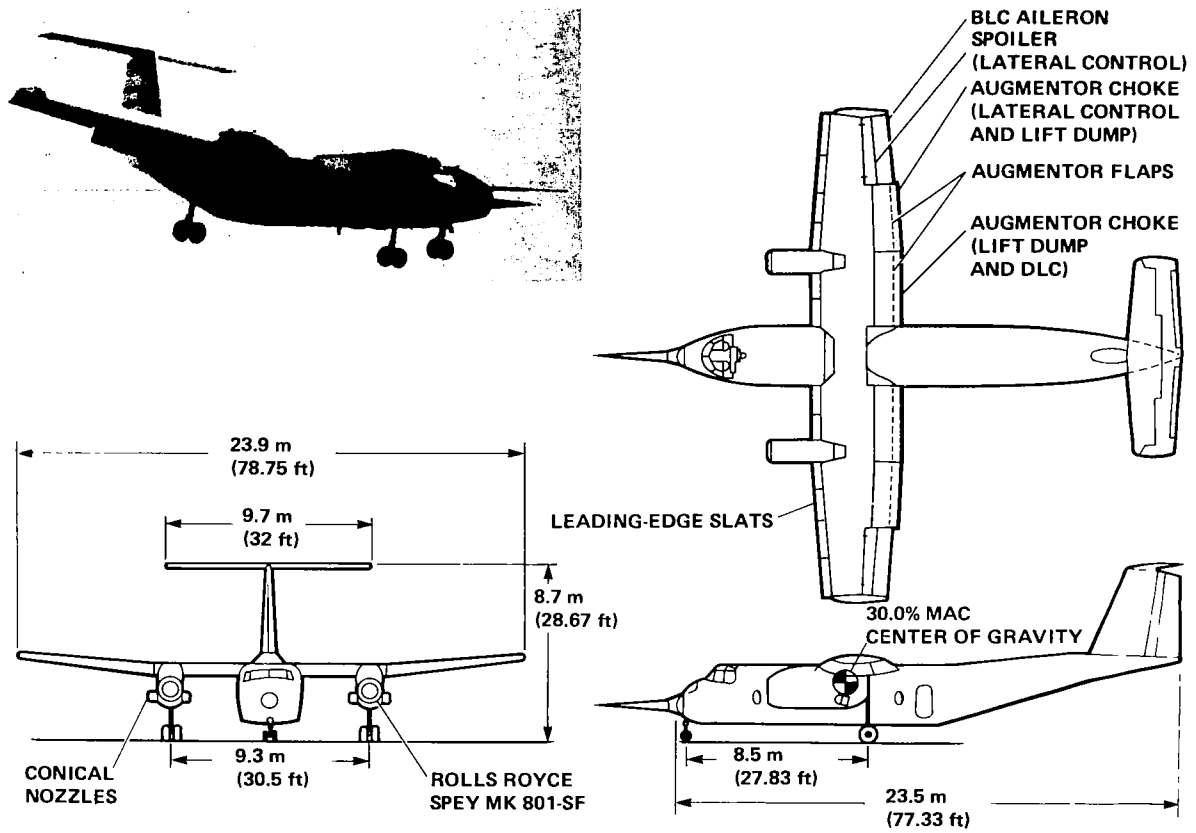
The significant transfer-function factors and their relationship to the aircraft's dynamic derivatives are the same as those noted in the preceding section.

## DESCRIPTION OF FLIGHT RESEARCH PROGRAM

### Research Aircraft

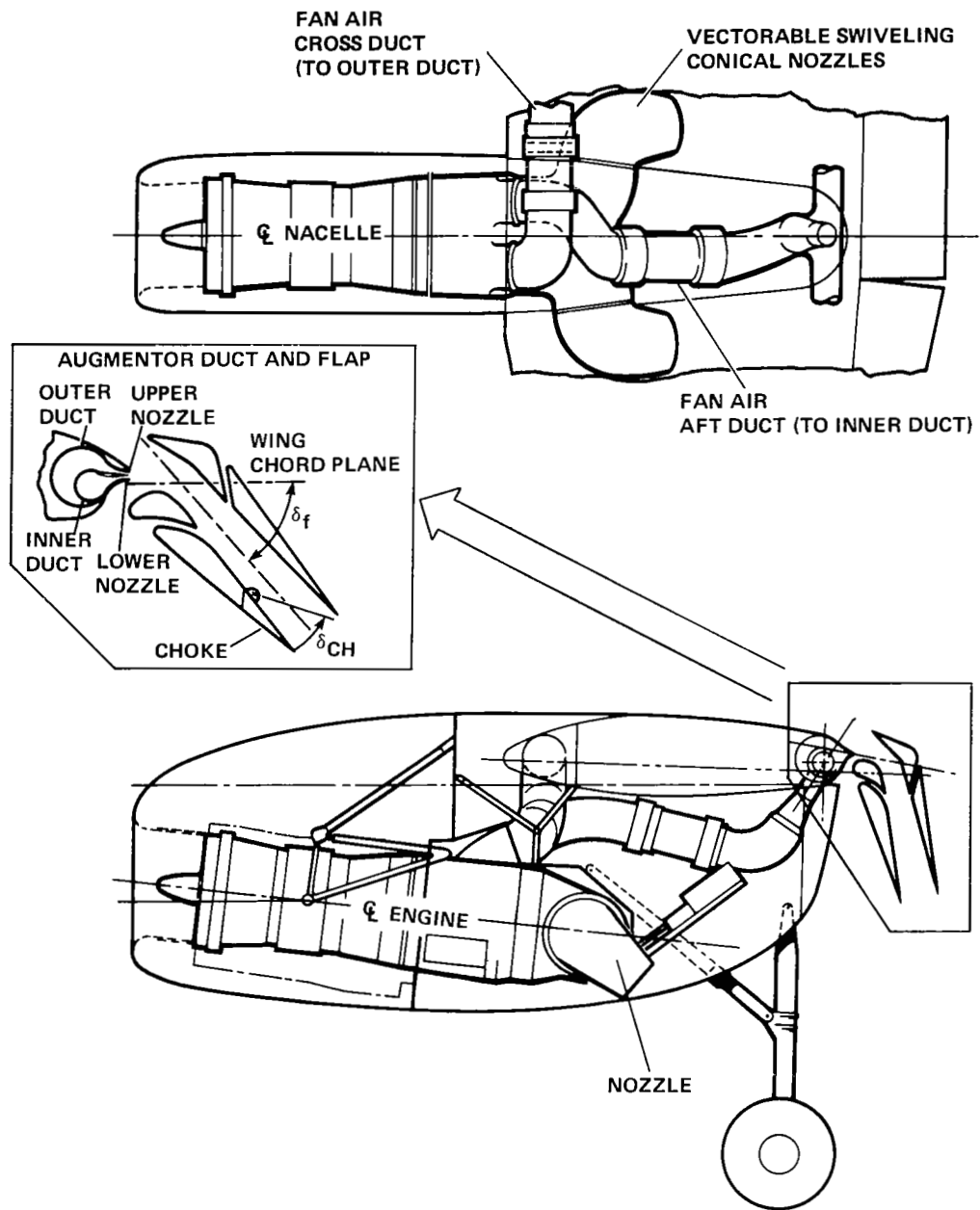
The flight experiments were conducted with Ames Research Center's Augmentor Wing Research Aircraft (fig. 12), a modified de Havilland C-8A Buffalo. The modification — to incorporate a propulsive-lift system — was performed by the Boeing Company, de Havilland of Canada, and Rolls Royce of Canada, as part of a joint research program between NASA and the Canadian Department of Industry, Trade, and Commerce. The aircraft is described in detail in references 16 and 17. It has a maximum gross weight of 21,792 kg (48,000 lb) and a range of operational wing loadings of 215–272 kg/m<sup>2</sup> (44–55 lb/ft<sup>2</sup>). The propulsive-lift system uses an augmentor jet flap designed for physical flap deflections up to 72°. Two Rolls Royce Spey MK 801-SF (split flow) engines, having 46,280 N (10,400 lb) thrust each, power the aircraft. Fan air is distributed through bypass ducts to the flaps to augment the basic wing aerodynamics. The flow from each engine is split to supply air through the inner and outer bypass ducts to both right and left flaps, thus maintaining symmetric lift in the event of an engine failure. Hot flow from the engine core passes out of the conical nozzles, which can be rotated through 98° (6° to 104° relative to the fuselage centerline) to deflect the direct thrust component.

*Flight control System*— The primary flight controls are fully powered hydraulically. They consist of a single-segment elevator; ailerons, spoilers, and outboard augmentor flap chokes; a two-segment rudder; hot thrust exhaust nozzles; and inboard augmentor flap chokes. The elevator is used for both pitch maneuvering and trim and has a total deflection of -15° to +24° at normal STOL landing approach speeds. Ailerons, spoilers, and outboard augmentor chokes are programmed for roll control in response to wheel command inputs. The ailerons have boundary-layer control, and droop as a function of flap position. They can be deflected to ±19° about the nominal droop position for the approach flap angle. The spoilers deflect up to 48°, and outboard chokes deflect to close off up to 55% of the augmentor flap exit area. Full rudder deflection is ±25° for the forward segment, where the aft panel to forward panel gearing ratio is 2:1. The inboard augmentor chokes are controlled symmetrically to modulate lift in flight and to dump lift when on the ground. Their full deflection is 65%



(a) Three views of the aircraft.

Figure 12.- Augmentor Wing Research Aircraft.



(b) Augmentor jet flap and propulsion system.

Figure 12.— Concluded.

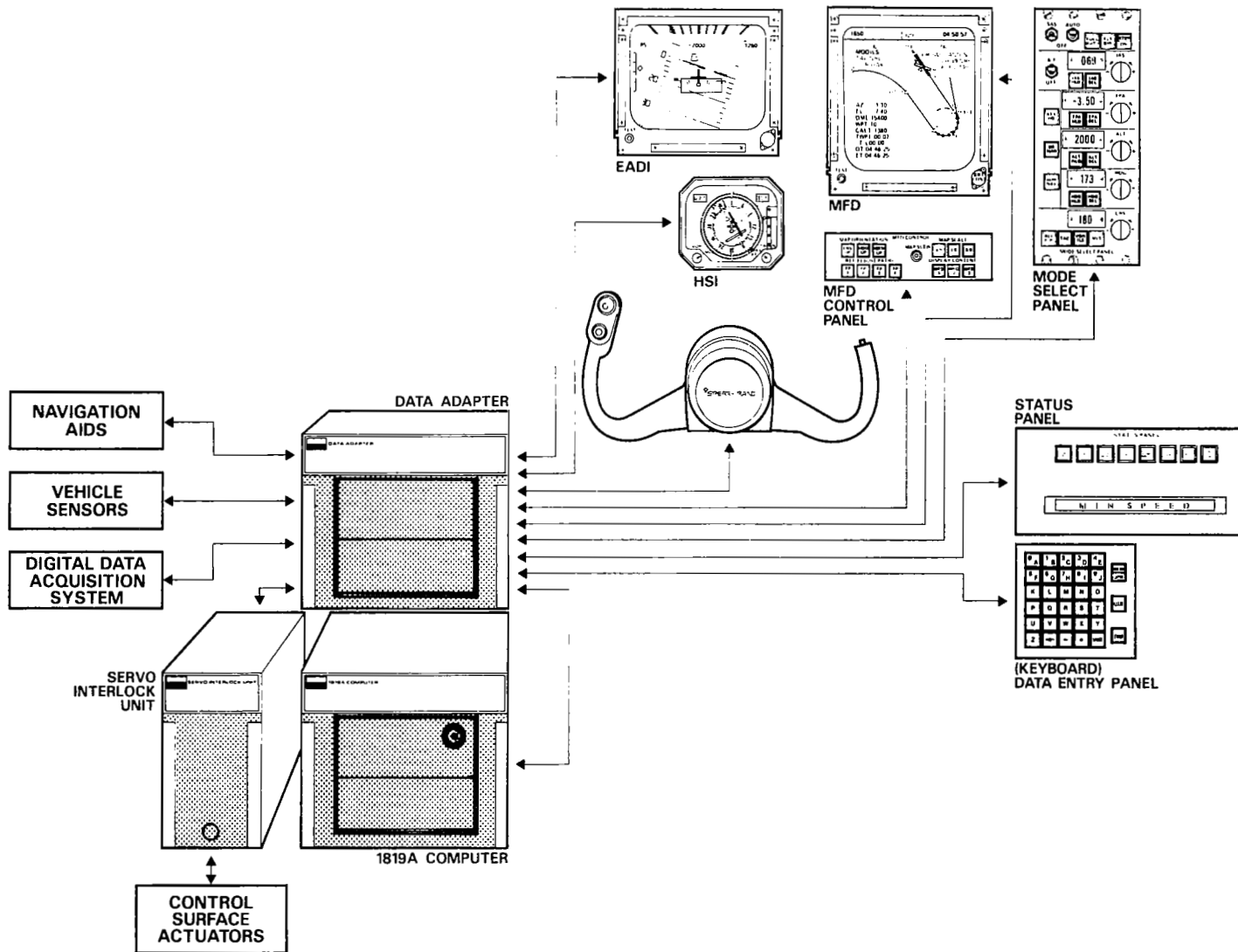


Figure 13.— STOLAND system block diagram.

closure of the flap exit area for the approach flap configuration.

The aircraft's primary flight controls (described previously) can be driven through servos commanded by an experimental digital avionics system (STOLAND) that is installed in the aircraft. This system, which was developed by Sperry Flight Systems, is described in reference 18. A block diagram of the system is presented in figure 13; the major components are a Sperry 1819A general-purpose digital computer, a data adapter, and the aircraft's sensors, controls, displays, and navigation aids. Sensor information pertinent to this program was provided by body axis linear accelerometers, attitude and rate gyros, pitot-static airspeed, barometric and radio altimeters, control column force and wheel position, and engine rpm. Servo controls were provided for the elevator, blended lateral controls, rudder, nozzles, and inboard augmentor chokes. Limited-authority series electro-hydraulic servos drove the elevator, lateral controls, and rudder, with authorities of 40%, 27%, and 40%, respectively. The inboard augmentor flap chokes have full mechanical authority (65% closure of the augmentor flap) and are also driven by electro-hydraulic servos. In the approach configuration, their authority corresponds to  $\pm 0.12$  g. The exhaust nozzles of the Spey engines are driven by electromechanical parallel servos that may be overridden, if desired, by the pilot. Longitudinal acceleration effectiveness of the nozzles in the approach configuration is approximately 0.0037 g per degree for nozzle deflections between  $50^\circ$  and  $104^\circ$ .

Because this research program was concerned with evaluating flightpath and airspeed control, the pitch, roll, and yaw characteristics of the basic aircraft were augmented to provide satisfactory flying qualities in these axes for the approach and landing task. In this regard, the elevator, lateral controls, and rudder were used to provide command augmentation (SCAS) for pitch attitude, bank angle, and sideslip control. Rate-command/attitude-hold functions were incorporated for pitch and roll control; they are described in detail in reference 19. A block diagram for the pitch SCAS is shown in figure 14, and a time history of pitch response to a longitudinal control force input is shown for the approach configuration in figure 15. Pitch rate follows the pilot's command with a sensitivity of  $0.09^\circ/\text{sec}/\text{N}$  ( $0.4^\circ/\text{sec}/\text{lb}$  neglecting the column breakout force of 6 lb); there is little or no attitude overshoot in the response. With this system operating, pilot ratings of 2 were obtained for attitude control appropriate to a precision instrument approach. Block diagrams for the roll and yaw SCAS systems are shown in figure 16; they are accompanied by a time history response to the pilot's lateral control wheel input, as presented in figure 17. Roll rate responds to the wheel input with a sensitivity of  $0.94^\circ/\text{sec}/\text{N}$  ( $4.2^\circ/\text{sec}/\text{lb}$ ); little or no bank angle overshoot appears. The system acts to increase the Dutch roll frequency and damping and to improve turn coordination.

Consequently, directional oscillations are nonexistent and sideslip excursions are effectively suppressed ( $\Delta\beta/\Delta\phi = 0.1$ ). Pilot ratings of 3 were obtained for lateral-directional control during a precision instrument approach.

The inboard augmentor chokes and the engine exhaust nozzles provide independent normal and axial force control when the aircraft is configured in the landing approach configuration ( $\delta_f = 65^\circ$ ,  $\nu = 80^\circ$ ). These two controls were driven as shown in figure 18. The purpose was to alter the basic aircraft's lift and drag characteristics, as a function of airspeed, angle of attack, and engine thrust, so as to encompass a range of flightpath and airspeed responses to variations in pitch attitude and throttle controls and to low-frequency axial wind disturbances. Feedbacks of pitch attitude, engine rpm, and complementary filtered airspeed and vertical velocity were used to drive the chokes and nozzles to achieve the desired lift and drag variations. These inputs were processed through the 1819A computer at a cycle time of 50 msec to produce commands to the appropriate control servos.

*Cockpit arrangement*— The general arrangement of cockpit instrument displays, flight controls, and system mode controls available to the pilot are shown in figure 19. Specific instruments are designated in figure 20. An electronic attitude director indicator (EADI) presents pitch and roll attitude, aerodynamic flightpath angle, and raw glide-slope and localizer deviation, as well as calibrated airspeed, vertical velocity, and radar altitude in digital readouts. A three-cue flight director could be selected by the pilot as desired. An electromechanical horizontal situation indicator (HSI) presented aircraft heading and bearing to the navigational aid as well as glide-slope and localizer deviation. The pilot's cockpit controls consist of a yoke and wheel, rudder pedals, and overhead throttle, and nozzle-control levers. A mode-select panel provided switches for engaging SCAS modes and the flight director. The keyboard and status display on the center console permit manual entry and readout of inputs to the digital computer.

A horizontal bar representing aerodynamic flightpath angle in the vertical plane was available on the EADI, superimposed on the pitch attitude scale. This display was useful in providing lead information for glide-slope acquisition and tracking and for alerting the pilot to incipient glide-slope deviations caused by variation in horizontal and vertical winds and turbulence.

Final approach guidance was provided by a prototype microwave landing guidance system (MODILS). Raw data glide-slope and localizer deviation from MODILS were presented on the HSI. The sensitivity of the glide-slope needle was reduced from the nominal  $0.3^\circ/\text{dot}$  for a  $3^\circ$  ILS glide slope; this was done to account for the steep approach path angle. Sensitivity was set at  $1^\circ/\text{dot}$  for both the glide slope and localizer.

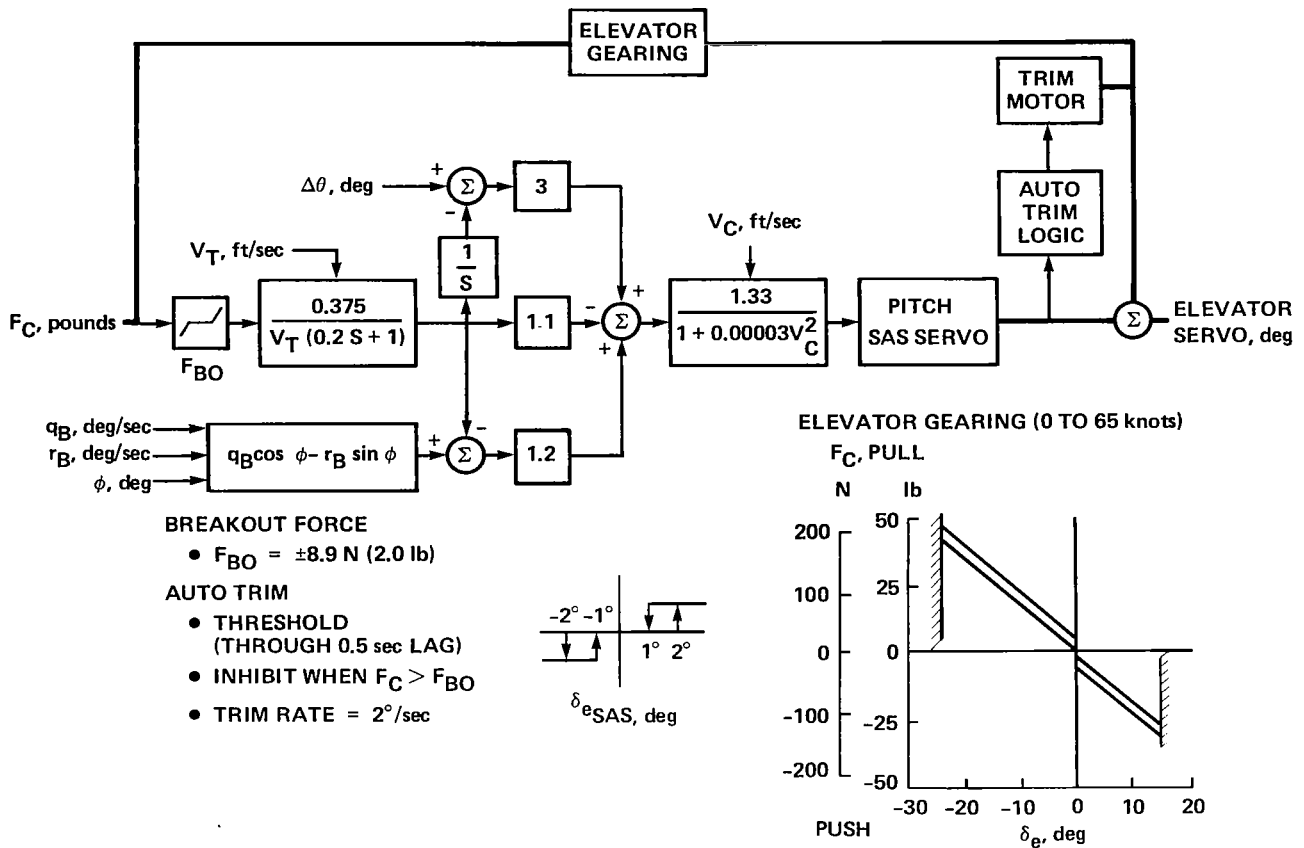


Figure 14.— Pitch SCAS block diagram.

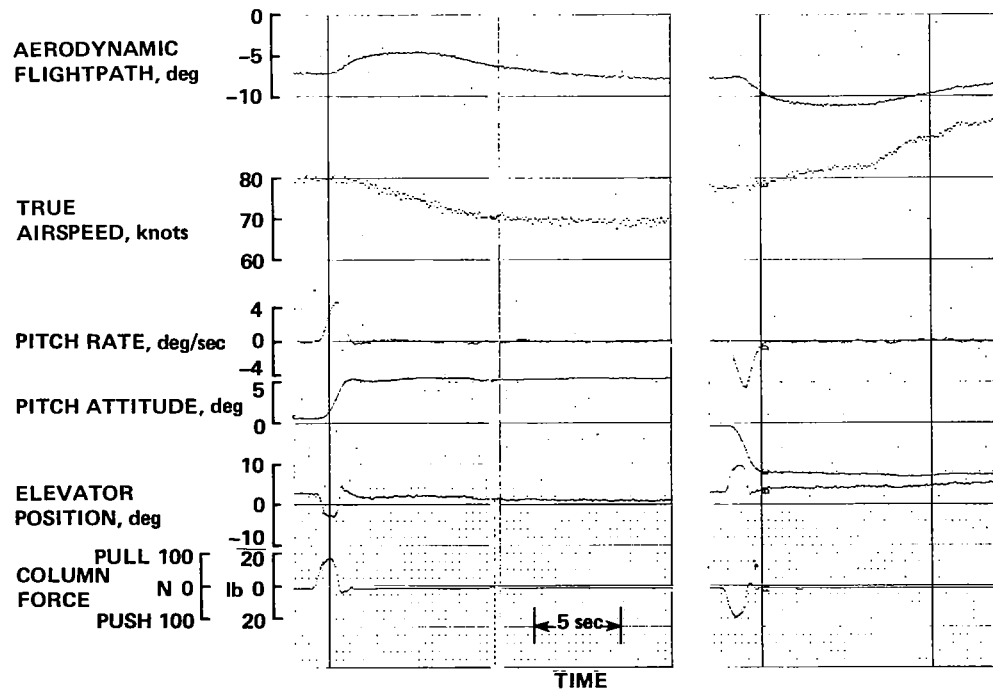


Figure 15.— Longitudinal response to attitude control — rate-command-attitude-hold system on.

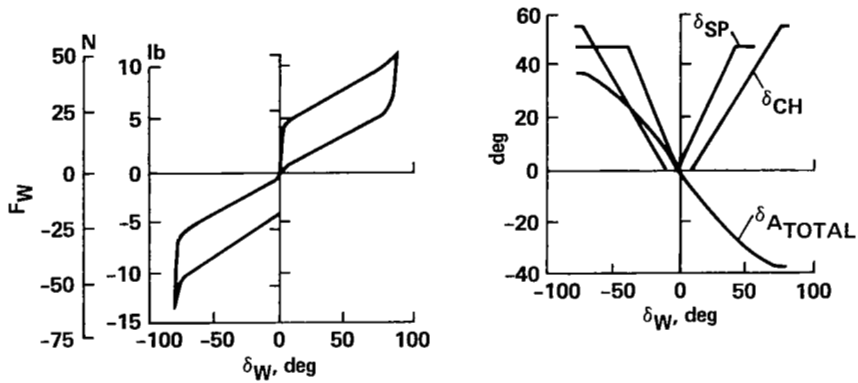
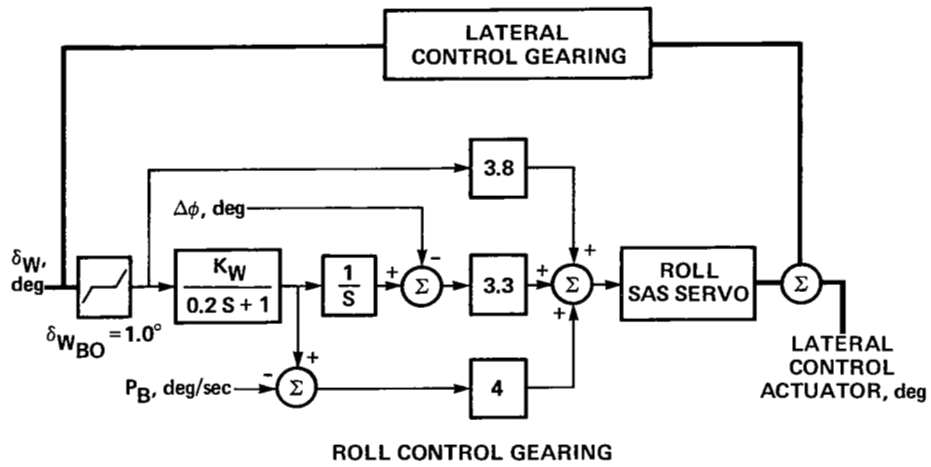
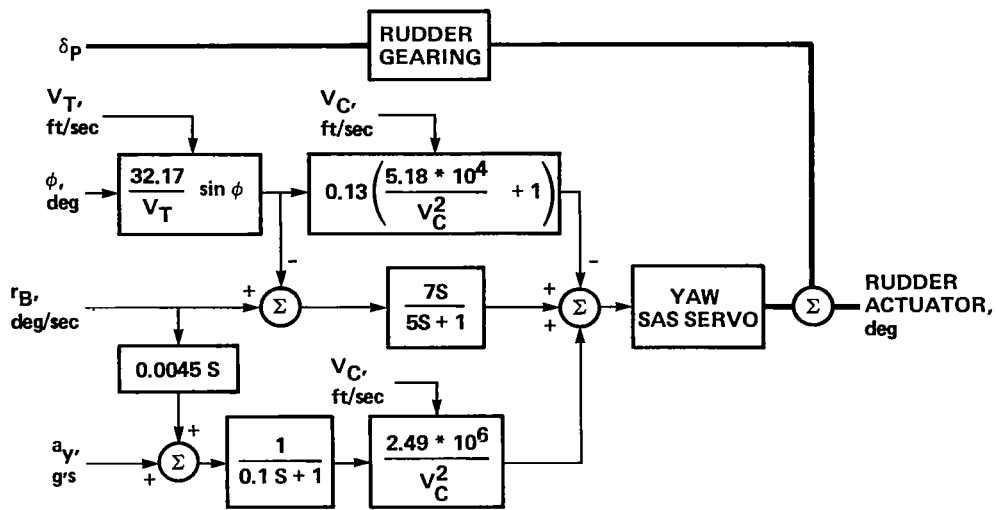
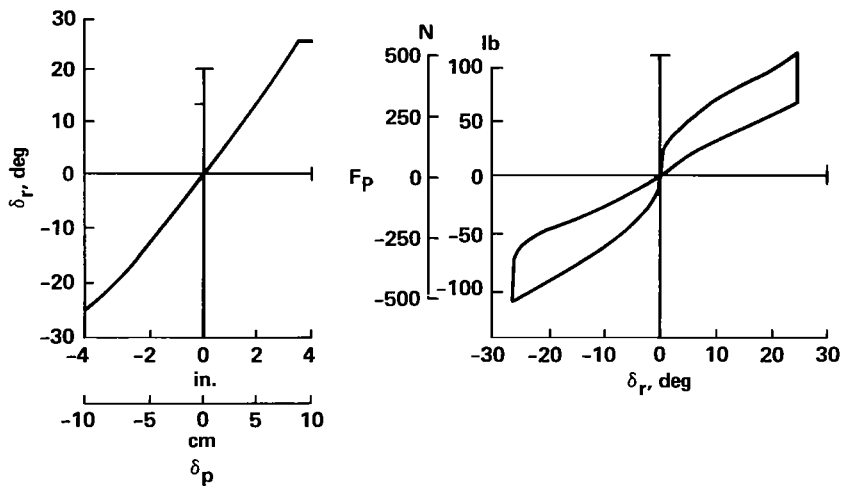


Figure 16.— Lateral-directional SCAS block diagrams.



RUDDER GEARINGS



(b) Yaw SCAS.

Figure 16.— Concluded.

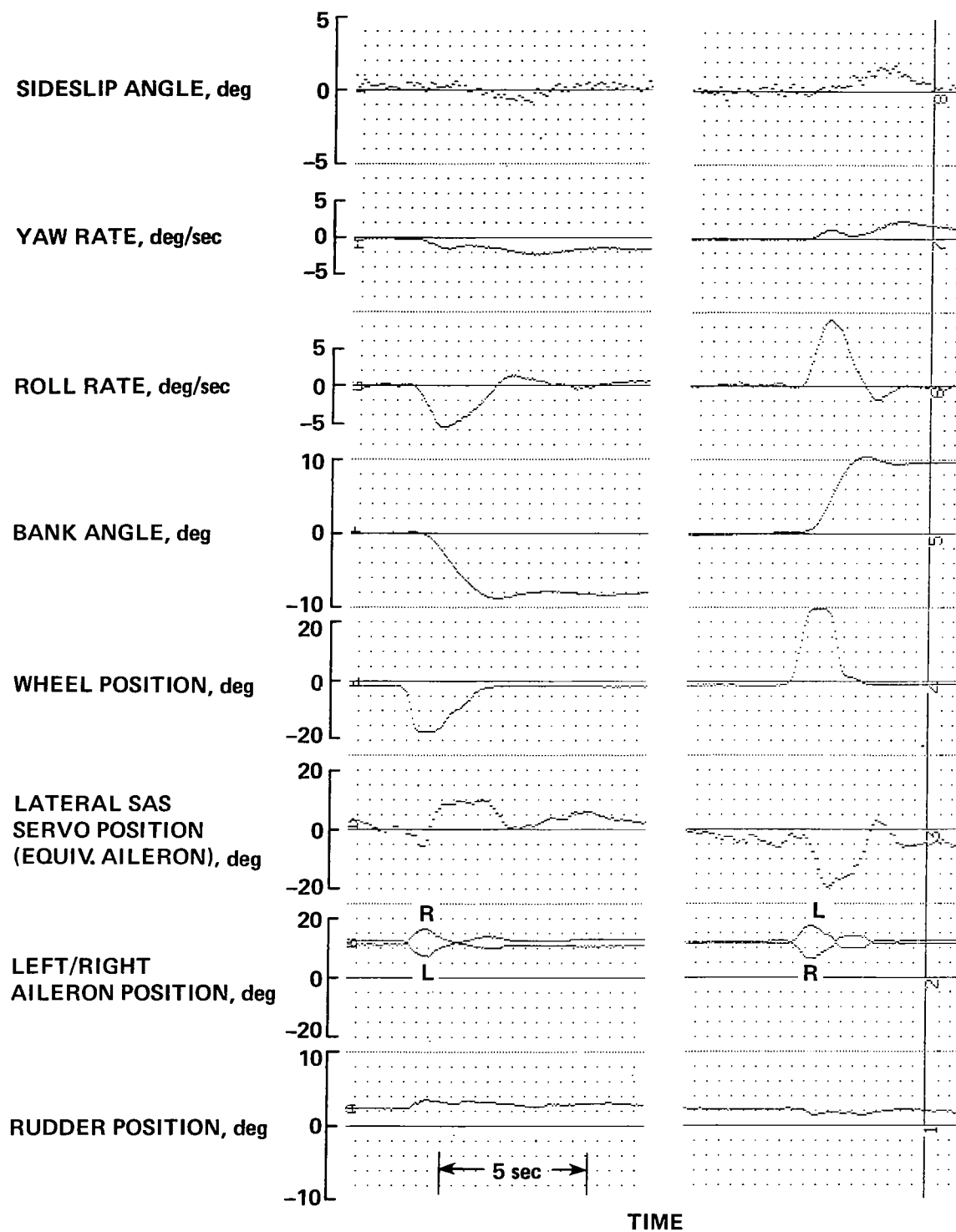
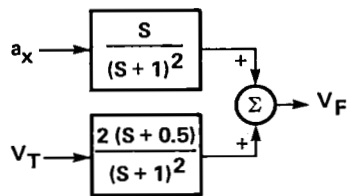


Figure 17.— Lateral-directional response to roll control — roll-yaw SCAS on.

**AIRSPED COMPLEMENTARY FILTER**



**SINK RATE COMPLEMENTARY FILTER**

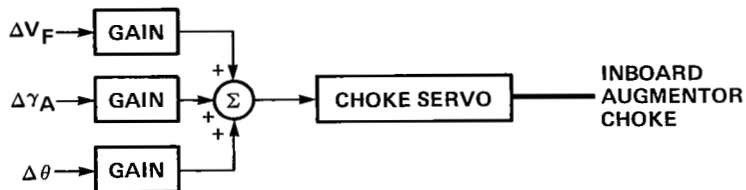
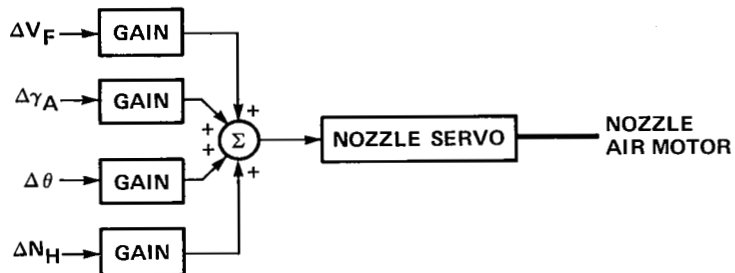
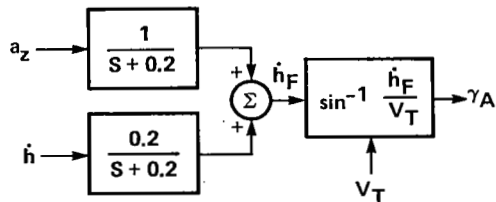


Figure 18.— Block diagram of nozzle and inboard augmentor choke controls.

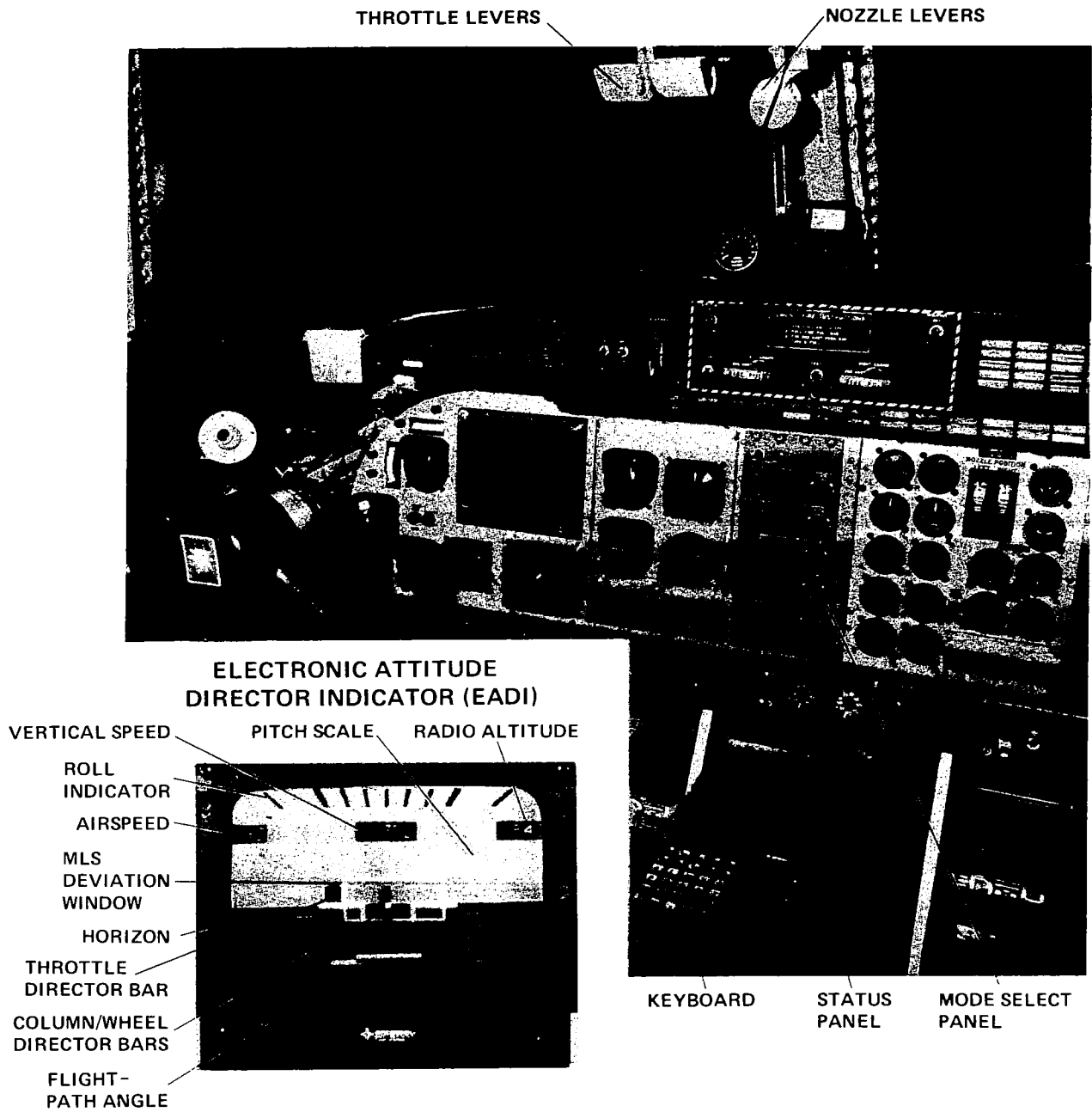
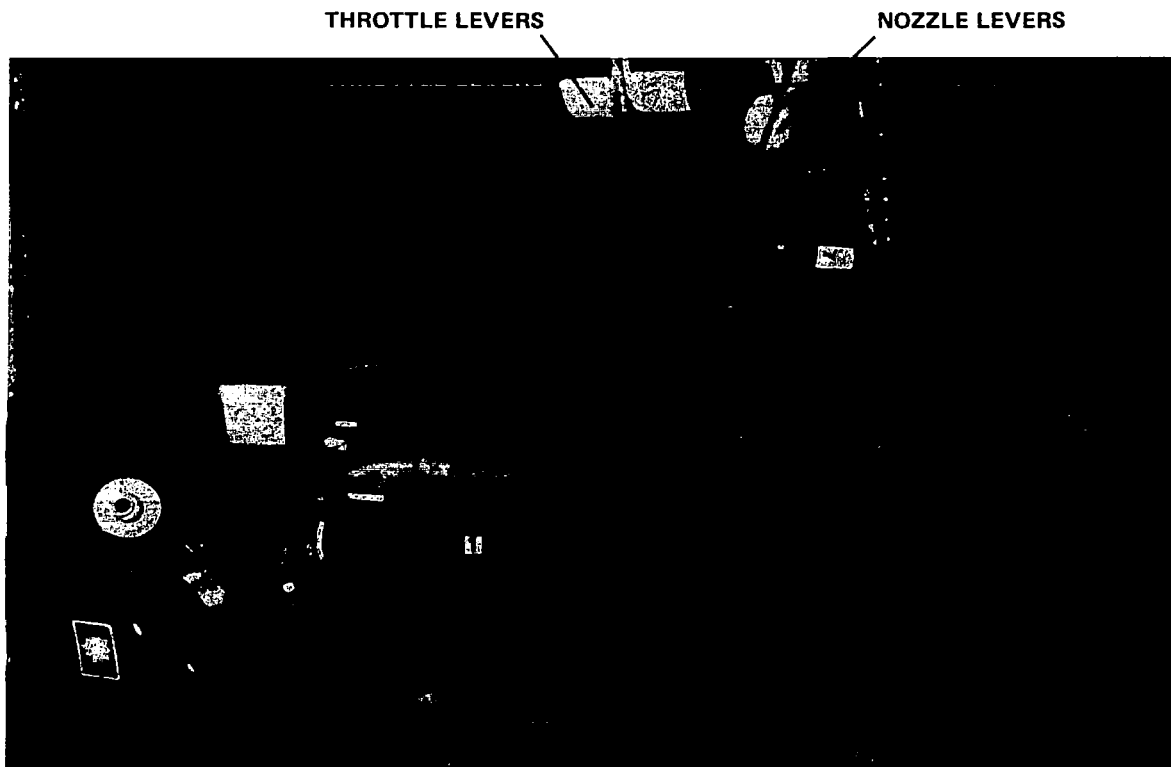


Figure 19.— Flight control and instrument arrangement.



**COCKPIT INSTRUMENTS**

1. EADI
2. HSI
3. AIRSPEED
4. COARSE ANGLE-OF-ATTACK
5. FINE ANGLE-OF-ATTACK
6. SIDESLIP ANGLE
7. BAROMETRIC ALTITUDE
8. RADAR ALTITUDE
9. IVSI
10. NORMAL ACCELERATION
11. AILERON, SPOILER,  
OUTBOARD CHOKE POSITIONS
12. ELEVATOR POSITION
13. INBOARD CHOKE POSITIONS
14. NOZZLE PRESSURE RATIO
15. HIGH PRESSURE COMPRESSOR SPEED
16. EXHAUST GAS TEMPERATURE
17. FUEL FLOW
18. LOW PRESSURE COMPRESSOR SPEED
19. NOZZLE POSITIONS
20. OUTBOARD FLAP POSITIONS
21. INBOARD FLAP POSITIONS
22. TIME CODE



KEYBOARD

STATUS  
PANEL

MODE SELECT  
PANEL

Figure 20.— Cockpit instruments.

The three-cue flight director consisted of centrally located column and wheel (pitch and roll) command bars and a throttle command bar located on the left wing of the aircraft symbol. These directors provide for vertical- and lateral-path tracking and for maintaining the desired airspeed and safe angle-of-attack margins. This flight director, which was designed for the Augmentor Wing Aircraft by Systems Technology, Inc., is described in detail in references 19 and 20. For this program, the director was configured for the backside control technique in which the throttle is used for glide-slope tracking, the column for maintaining airspeed and performing discrete pitch attitude changes, and the wheel for localizer tracking.

### Evaluation Configurations

*Glide-slope control*— The flightpath and airspeed response characteristics related to thrust control that were selected for evaluation in the flight research program, were flightpath overshoot, initial flightpath time response, and flightpath-airspeed coupling. As noted in the previous section and in reference 7, flightpath overshoot is strongly influenced by thrust turning angle,  $\theta_T = \tan^{-1}(-Z_{\Delta T}/X_{\Delta T})$ , because of its contribution to the flightpath-throttle numerator root  $1/T\gamma_T$ . Thus, it was possible to vary the magnitude of overshoot by changing the longitudinal force derivative due to thrust,  $X_{\Delta T}$ . However, in so doing, the airspeed-throttle numerator was also changed, resulting in a variation of the magnitude of steady-state flightpath-airspeed coupling in conjunction with the change in overshoot ratio. As shown in reference 7, for a practical range of powered-lift STOL aircraft characteristics, it is difficult to achieve an independent variation of path-speed coupling and overshoot ratio. Hence, they were not independently controlled in this experiment.

The initial flightpath time response is governed to a large extent by the response bandwidth associated with  $\omega_\theta$  or  $1/T\theta_2$  and the engine dynamics, and to a lesser extent by the flightpath numerator root  $1/T\gamma_T$ . The choice was made to alter the initial response by correspondingly varying bandwidth either through changes in vertical velocity damping ( $Z_w$ ) or in the numerator root by varying thrust turning through the derivative  $X_{\Delta T}$ . In the former case, the initial response time and bandwidth are varied with little or no change in path overshoot or path-speed coupling. In the latter case, the variation in initial time response is accompanied by a change in path-speed coupling and may or may not be associated with a change in overshoot. Otherwise, no alterations in the effective engine response dynamics were attempted ( $\omega_E = 2.7$  rad/sec,  $\zeta_E = 1.0$  for a second-order model, or  $\tau_E = 0.8$  sec for a first-order model). Furthermore, since throttle control sensitivity for the basic aircraft was nearly ideal, based on existing criteria (refs. 7, 21) and

by the judgment of the evaluation pilots for this program, it was also not altered ( $Z_{\delta T} = -0.04$  g/cm or  $-0.1$  g/in.).

A listing of the experimental configurations designed for evaluation of flightpath and airspeed control during glide-slope tracking is provided in table 1. Stability derivatives, transfer-function factors, and pertinent response characteristics are provided therein. The actual response characteristics achieved in flight are documented in appendix B in the form of time histories of flightpath and airspeed response to throttle. A summary of these characteristics, compared with those of the initial experimental design, is shown in table 2. In general, the flight-measured values compare well with those predicted in the experimental design. Time histories of the quality required to define the appropriate response characteristics were not obtained for all cases. In those instances (e.g., configuration 3) where acceptable flight data did not exist, the configuration parameters for use in subsequent analysis and interpretation of pilot ratings and comments have been determined by correcting the predicted value based on interpolation of flight-derived parameters from adjacent configurations. Another distinction between the flight and predicted response characteristics is the nonlinear character of the flight data. This behavior was expected because the aerodynamic nonlinearities associated with the approach operating condition are well recognized (e.g., those associated with strong induced-drag effects). For the purposes of data interpretation in this report, the configurations will be defined in terms of the most adverse values of their response parameters. As an example, path overshoot and path-speed coupling are, in most cases, more severe for increases (as opposed to reductions) in thrust, and the large values of  $(\Delta\gamma_{\max}/\Delta\gamma_{ss})\Delta T$  and  $(\Delta u_{ss}/\Delta\gamma_{ss})\Delta T$  will be adopted to describe these configurations. This approach will also define the characteristics associated with the most critical glide-slope corrections, those initiated to recapture the glide slope from below.

Configurations 1-4 (table 1) were designed to provide for a large variation of path overshoot with minimal change in the initial response time ( $1.7 \leq t_{0.5} \Delta\gamma_{\max} \leq 2.5$  sec). Flightpath-airspeed coupling also varies over a large range for this group. Configurations 1, 5, and 6 provide for variation of initial response through the range  $1.7 \leq t_{0.5} \Delta\gamma_{\max} \leq 3.7$  sec with minimal flightpath overshoot and for essentially decoupled flightpath and airspeed response. These alterations were made through changes in vertical velocity damping from  $-0.21 \leq Z_w \leq -0.82$  sec<sup>-1</sup>. Variations in this time response were also made by appropriately changing the longitudinal force derivative  $X_{\Delta T}$ , i.e., by effectively changing the thrust inclination from 42° to nearly vertical. For  $\theta_T = 42^\circ$  (configuration 7), the initial time response is increased to  $t_{0.5} \Delta\gamma_{\max} = 5.1$  sec, and it is accompanied by a conventionally coupled flightpath-airspeed relationship  $(\Delta u_{ss}/\Delta\gamma_{ss})\Delta T = 1.2$  knots/deg. No overshoot is present in flightpath response for this

TABLE 1.—GLIDE-SLOPE CONTROL CONFIGURATIONS — STABILITY DERIVATIVES AND TRANSFER FUNCTION FACTORS

Config- uration	$X_{u'}$ sec <sup>-1</sup>	$X_{w'}$ sec <sup>-1</sup>	$X_{\delta T'}$ ft/sec <sup>2</sup> % $N_H$	$Z_{u'}$ sec <sup>-1</sup>	$Z_{w'}$ sec <sup>-1</sup>	$Z_{\delta T'}$ ft/sec <sup>2</sup> % $N_H$	$\frac{1}{T_{\theta_1}}$ , sec <sup>-1</sup>	$\frac{1}{T_{\theta_2}}$ , sec <sup>-1</sup>	$\xi_{\theta}$	$\omega_{\theta}$ , rad/sec	$\frac{1}{T_{\gamma_1}}$ , sec <sup>-1</sup>	$\frac{1}{T_{\gamma T}}$ , sec <sup>-1</sup>
1	-0.056	0.11	0.28	-0.36	-0.52	-0.894	0.169	0.408	---	---	-0.063	0.17
2	↓	.11	.0	↓	-.52	↓	.169	.408	---	---	-.063	.056
3	↓	.11	-.055	↓	-.52	↓	.169	.408	---	---	-.063	.034
4	↓	.11	-.122	↓	-.52	↓	.169	.408	---	---	-.063	.0068
5	↓	.08	.087	↓	-.82	↓	.095	.783	---	---	-.031	.091
6	↓	.145	.56	↓	-.21	↓	---	---	0.54	0.254	-.189	.283
7	↓	.11	.98	↓	-.52	↓	.169	.408	---	---	-.063	.45
8	↓	.18	.0	↓	-.21	↓	---	---	.494	.278	-.121	.056
9	↓	.11	.0	↓	-.21	↓	---	---	.603	.228	-.259	.056
10	↓	.11	.56	↓	-.37	↓	---	---	.867	.246	-.116	.283

case. Two additional configurations were included that provided combined variations in flightpath overshoot and initial time response (configurations 8 and 9). Overshoot ratios up to 3 for initial time response of approximately  $t_{0.5} \Delta\gamma_{\max} = 2.3$  sec were produced through variations in  $X_{\Delta T}$  and  $Z_{w'}$ . Path-speed coupling up to  $(\Delta u_{ss}/\Delta\gamma_{ss})\Delta T = -4.0$  knots/deg accompanied these configuration changes. For all of these configurations, overshoot and initial response times show good agreement with the initial configuration design. For configurations 8 and 9, flightpath-airspeed coupling is greater than predicted.

In accord with the backside control technique used during precision-approach path tracking for powered-lift aircraft, pitch attitude was the primary control for the reference approach airspeed. In this regard, the pilots chose to maintain control over approach airspeed ( $\Delta u = \pm 5$  knots) to provide margins for stall and wind-shear protection at the low end and reasonable stopping distance at the high end. Since reference 7 indicated that flying qualities for the approach were not significantly affected by variations in airspeed-attitude sensitivity ( $\Delta u_{ss}/\Delta\theta_{ss}$ ), this parameter was not varied independently during these flight experiments. The range of variations associated with other configurations encompasses approximately  $-0.8 \leq \Delta u_{ss}/\Delta\theta_{ss} \leq -3.6$  knots/deg.

**Flare control**— Flare-response characteristics associated with pitch rotation and thrust modulation were investigated in the flight experiments associated with the flare and landing. Evaluation of flightpath response to pitch rotation concentrated on effects of variations in the magnitude of the initial flightpath response ( $\Delta\gamma_{\max}/\Delta\theta_{ss}$ ) and the time required for the initial response to subside ( $t_{0.1} \Delta\gamma_{\max}$ ).

The initial magnitude is determined predominantly by the vertical velocity damping derivative, as noted in the preceding section; thus,  $\Delta\gamma_{\max}/\Delta\theta_{ss}$  was changed through variations in  $Z_{w'}$ . In accordance with previous discussions, it is recognized that this variable also strongly influences the rate of the initial response ( $t_{0.5} \Delta\gamma_{\max}$ ) and bandwidth and stability of path control. In this regard, it was left to the results of the flight experiment to discriminate between problems of sink-rate control authority and time response or closed-loop stability for regulation to the desired flare profile. The long-term time response has been tied strongly to the numerator time constant for path-to-pitch response, and thus to the steady-state path-speed gradient  $d\gamma/du$ . For the experiment, variations in degree of operation on the backside of the drag curve, ranging from the "drag bucket" to fairly steeply backside conditions were encompassed, with corresponding variations in the long-term subsidence time. These variations were accomplished by effectively changing  $X_{w'}$  through changes in the induced drag derivative  $D_{\alpha}$  (i.e.,  $X_{w'} = (g - D_{\alpha})/V_0$ ). Some evaluations were obtained for primary flare control with thrust in which the initial response time,  $t_{0.5} \Delta\gamma_{\max}$ , was the variable of interest. In this case, the initial response time was controlled through variations in vertical velocity damping.

Finally, it should be noted that contributions of ground effect have the potential of altering the characteristics of the flare. In this experiment, the lift and drag ground effects of the basic aircraft, as described in reference 22, were not modified. They consist of a slightly positive lift increment and a large drag decrement at wheel contact that act to provide a slight short-term and modest long-term cushioning of the sink rate prior to touchdown. Pitching

TABLE 2.— GLIDE-SLOPE CONTROL CONFIGURATION RESPONSE CHARACTERISTICS

CONFIG	$\left(\frac{\Delta\gamma_{\max}}{\Delta\gamma_{ss}}\right)_{\Delta T}$	$t_{0.5\Delta\gamma_{\max}}$ sec	$\left(\frac{\Delta u_{ss}}{\Delta\gamma_{ss}}\right)_{\Delta T}$ knots/deg	$\frac{\Delta\gamma_{\max}}{\Delta\theta_{ss}}$	$\frac{d\gamma}{du}$ deg/knot	$t_{0.1\Delta\gamma_{\max}}$ sec	$\frac{\Delta u_{ss}}{\Delta\theta_{ss}}$ knots/deg	STEADY-STATE PERFORMANCE
1 FLT PRED	1.0	2.5	0.38	0.55	0.19	10.5	-2.44	
	1.03 (+ΔT) 1.71 (-ΔT)	2.5 2.3	0.47 -2.62	0.53 (+Δθ) 0.53 (-Δθ)	0.1 0.062	12.8 10.1	-1.7 -2.7	
2 FLT PRED	1.9	1.8	-2.4	0.55	0.19	10.5	-2.44	
	1.8 (+ΔT) 1.4 (-ΔT)	2.0 2.2	-2.8 -2.2	0.53 (+Δθ) 0.53 (-Δθ)	0.1 0.062	12.8 10.1	-1.7 -2.7	
3 FLT PRED	2.92	1.7	-5.1	0.55	0.19	10.5	-2.44	
				0.53 (+Δθ) 0.53 (-Δθ)	0.1 0.062	12.8 10.1	-1.7 -2.7	
4 FLT PRED	13.5	1.7	-32.3	0.55	0.19	10.5	-2.44	
	14.5 (+ΔT) 2.2 (-ΔT)	1.7 1.8	-30.0 -3.53	0.53 (+Δθ) 0.53 (-Δθ)	0.1 0.062	12.8 10.1	-1.7 -2.7	
5 FLT PRED	1.02	1.7	0.01	0.70	0.093	15.8	-3.61	
				0.73 (+Δθ) 0.72 (-Δθ)	0.035 0.0	22.4 16.8	-2.6 -2.8	

TABLE 2.- Continued.

CONFIG	$\left(\frac{\Delta\gamma_{\max}}{\Delta\gamma_{ss}}\right)\Delta T$	$t_{0.5\Delta\gamma_{\max}}$ sec	$\left(\frac{\Delta u_{ss}}{\Delta\gamma_{ss}}\right)\Delta T$ knots/deg	$\frac{\Delta\gamma_{\max}}{\Delta\theta_{ss}}$	$\frac{d\gamma}{du}$ deg/knot	$t_{0.1\Delta\gamma_{\max}}$ sec	$\frac{\Delta u_{ss}}{\Delta\theta_{ss}}$ knots/deg	STEADY-STATE PERFORMANCE
6 FLT PRED	1.23	3.7	-0.04	0.23	0.57	6.9	-1.02	
	1.2 (+ΔT)	3.8	-0.31	0.29 (+Δθ) 0.53 (-Δθ)	0.27	8.8 13.6	-1.1	
7 FLT PRED	1.0	5.1	1.24	0.55	0.19	10.5	-2.44	
	1.0 (+ΔT)	5.2	1.2	0.53 (+Δθ)	0.1	12.8	-1.7	
	1.0 (-ΔT)	2.6	0.0	0.53 (-Δθ)	0.062	10.1	-2.7	
8 FLT PRED	3.24	2.2	-3.92	0.26	0.36	8.1	-0.84	
	3.33 (+ΔT)	2.4	-5.2					
	3.75 (-ΔT)	2.2	-7.5					
9 FLT PRED	2.5	2.4	-2.4	0.20	0.78	6.1	-1.31	
	2.9 (+ΔT)	2.0	-4.5					
10 FLT PRED	1.01	3.5	0.53	0.40	0.35	8.4	-1.96	
				0.38 (+Δθ)	0.5	6.0	-2.33	

moments in ground effect are suppressed by the pitch attitude SCAS and thus are not apparent to the pilot.

Detailed characteristics of the configurations for flare and landing evaluations are presented in table 3. They are documented from flight data in appendix B and are summarized in table 4. Configurations 11-14 include the variation of initial path response magnitude through a range  $0.2 \leq \Delta\gamma_{\max}/\Delta\theta_{ss} \leq 0.7$ , primarily by changing vertical velocity damping over  $-0.21 \leq Z_w \leq -0.82 \text{ sec}^{-1}$ . Minor adjustments were made in  $D_\alpha$  to reduce variations in  $d\gamma/du$  and the long-term path subsidence. In the cases in which the response to nose-up and nose-down attitude changes differ, the response to the nose-up attitude increment will be used to describe the configuration; this is done because the response to nose-up attitude is the most critical response (short term and long term) for flare with pitch. For configurations 11-13, the predicted and measured initial response compare well. Configuration 14 exhibited somewhat greater path response than predicted in the short term, but was still acceptable for the evaluation.

Configurations 11, 15, and 16 provide for evaluation of the long-term path response and cover a range from  $-0.04 \leq d\gamma/du \leq 0.36 \text{ deg/knot}$ . Minor variations in initial response magnitude ( $0.5 \leq \Delta\gamma_{\max}/\Delta\theta_{ss} \leq 0.6$ ) exist for these configurations. Combinations of variations in both initial and long-term response include a range of  $\Delta\gamma_{\max}/\Delta\theta_{ss}$  for both neutral and backside characteristics (configurations 17-19).

Evaluations of flare control with thrust were performed for configurations 13 and 14, which had characteristics

identical to those used for the glide-slope tracking experiment (configurations 10 and 6, respectively). To reiterate, the initial time response for these was approximately  $t_{0.5\Delta\gamma_{\max}} = 3.6 \text{ sec}$ . There was essentially no overshoot in flightpath response nor in flightpath-airspeed coupling for these configurations.

### Evaluation Task

Assessments of glide-slope tracking and flare and landing capability for the configurations described previously were obtained from landing approaches flown on a  $7.5^\circ$  glide slope at airspeeds from 65 to 70 knots to landing on a  $30 \times 518 \text{ m}$  ( $100 \times 1700 \text{ ft}$ ) STOL runway. Figure 21 shows the airfield layout; the runway orientation, including the STOL runway; and Ames Research Center's experimental flight facility at the Crows Landing Naval Airfield. The STOL runway is painted on the surface of runway 35, approximately halfway along the length from its threshold. As noted previously, approach guidance was provided by the MODILS system.

Straight-in approaches were initiated at altitudes between 450 and 600 m (1500 and 2000 ft). Both VFR and simulated IFR approaches were flown in calm- to light-wind conditions, and additional evaluations were made under surface conditions ranging from light tailwinds to strong headwinds and light-to-moderate turbulence. Two Ames Research Center pilots conducted all flight evaluations in this program. Pilot commentary and opinion ratings, based on the Cooper-Harper scale of reference 23, were obtained for all configurations.

TABLE 3.— FLARE-CONTROL CONFIGURATIONS — STABILITY DERIVATIVES AND TRANSFER-FUNCTION FACTORS

Config- uration	$X_w$ sec <sup>-1</sup>	$X_w'$ sec <sup>-1</sup>	$X_{\delta T}$ ft/sec <sup>2</sup> % $N_H$	$Z_w$ sec <sup>-1</sup>	$Z_w'$ sec <sup>-1</sup>	$Z_{\delta T}$ ft/sec <sup>2</sup> % $N_H$	$\frac{1}{T_{\theta_1}}$ sec <sup>-1</sup>	$\frac{1}{T_{\theta_2}}$ sec <sup>-1</sup>	$\xi_\theta$	$\omega_\theta$ rad/sec	$\frac{1}{T_{\gamma_1}}$ sec <sup>-1</sup>	$\frac{1}{T_{\gamma_T}}$ sec <sup>-1</sup>
11	-0.056	0.11	0.28	-0.36	-0.52	-0.894	0.169	0.408	---	---	-0.063	0.17
12	↓	.08	.087	↓	-.82	↓	.095	.783	---	---	-.031	.091
13	↓	.11	.56	↓	-.37	↓	---	---	0.867	0.246	-.116	.283
14	↓	.145	.56	↓	-.21	↓	---	---	.54	.254	-.189	.283
15	↓	.21	.45	↓	-.52	↓	---	---	.888	.325	.012	.238
16	↓	.035	.06	↓	-.52	↓	.085	.492	---	---	-.119	.082
17	↓	.035	.03	↓	-.82	↓	.073	.806	---	---	-.052	.069
18	↓	.21	.56	↓	-.21	↓	---	---	.461	.297	-.059	.283
19	↓	.11	.45	↓	-.21	↓	---	---	.602	.228	-.259	.238
20	↓	.11	.0	↓	-.21	↓	---	---	.602	.228	-.259	.056

TABLE 4.— FLARE-CONTROL CONFIGURATION RESPONSE CHARACTERISTICS

Configu- ration	$\left(\frac{\Delta\gamma_{\max}}{\Delta\gamma_{ss}}\right)_{\Delta T}$	$t_{0.5}\Delta\gamma_{\max}$ , sec	$\left(\frac{\Delta u_{ss}}{\Delta\gamma_{ss}}\right)_{\Delta T}$ , knots/deg	$\frac{\Delta\gamma_{\max}}{\Delta\theta_{ss}}$	$\frac{d\gamma}{du}$ , deg/knot	$t_{0.1}\Delta\gamma_{\max}$ , sec	$\frac{\Delta u_{ss}}{\Delta\theta_{ss}}$ , knots/deg
11. Predicted	1.0	2.5	0.38	0.55	0.19	10.5	-2.44
Flight	1.03 (+ $\Delta T$ )	2.5	.47	.53 (+ $\Delta\theta$ )	.1	12.8	-1.7
	1.71 (- $\Delta T$ )	2.3	-2.62	.53 (- $\Delta\theta$ )	.062	10.1	-2.7
12. Predicted	1.02	1.7	.01	.70	.093	15.8	-3.61
Flight				.73 (+ $\Delta\theta$ )	.035	22.4	-2.6
				.72 (- $\Delta\theta$ )	.0	16.8	-2.8
13. Predicted	1.01	3.5	.53	.40	.35	8.4	-1.96
Flight				.38 (+ $\Delta\theta$ )	.5	6.0	-2.33
14. Predicted	1.23	3.7	-.04	.23	.57	6.9	-1.02
Flight	1.2 (+ $\Delta T$ )	3.8	-.31	.29 (+ $\Delta\theta$ )		8.8	
				.53 (- $\Delta\theta$ )	.27	13.6	-1.1
15. Predicted	1.06	2.3	.26	.61	-.038	20.0	-1.55
Flight				.48 (+ $\Delta\theta$ )	-.03	12.8	-1.3
				.61 (- $\Delta\theta$ )	-.20		-1.6
16. Predicted	1.01	2.1	0.05	0.5	0.36	8.7	-4.14
Flight				.54 (+ $\Delta\theta$ )	.45	11.2	-2.8
				.59 (- $\Delta\theta$ )	.10		-5.4
17. Predicted	1.03	1.7	-.08	.69	.156	12.8	-4.63
18. Predicted	1.36	3.1	-.32	.30	.18	9.4	-.72
19. Predicted	1.18	3.8	.002	.20	.78	6.1	-1.31
20. Predicted	2.5	2.4	-2.4	.20	.78	6.1	-1.31
Flight	2.9 (+ $\Delta T$ )	2.0	-4.5				

For the landing approach task, the pilots' evaluations concentrated on both VFR and IFR tracking of the glide slope down to the point of flare initiation. Thrust was used as the primary control of flightpath for glide-slope tracking. Pitch attitude was selected as the primary approach flight reference to maintain adequate gust and maneuver margins. Choice of pitch attitude for the flight reference also provides a potential for reducing secondary control workload because attitude is stabilized by the pitch SCAS. Although it was not required to control airspeed precisely, some attention had to be devoted to speed control to achieve acceptable landing distances, to ensure adequate flare capa-

bility, and to suppress undesired flightpath coupling with airspeed.

Evaluations of the landing flare were obtained for both pitch rotation and thrust modulation as the primary means of sink-rate arrestment. In either case, it was permissible for the pilot to use the alternate control to assist in the initiation of the flare. The pilots' assessments of the acceptability of the flare and touchdown were based on the repeatability of the touchdown point and sink rate which could be achieved. The touchdown zone painted on the runway edge provided a target landing area and the pilots generally performed complete flares to touchdown at sink rates between

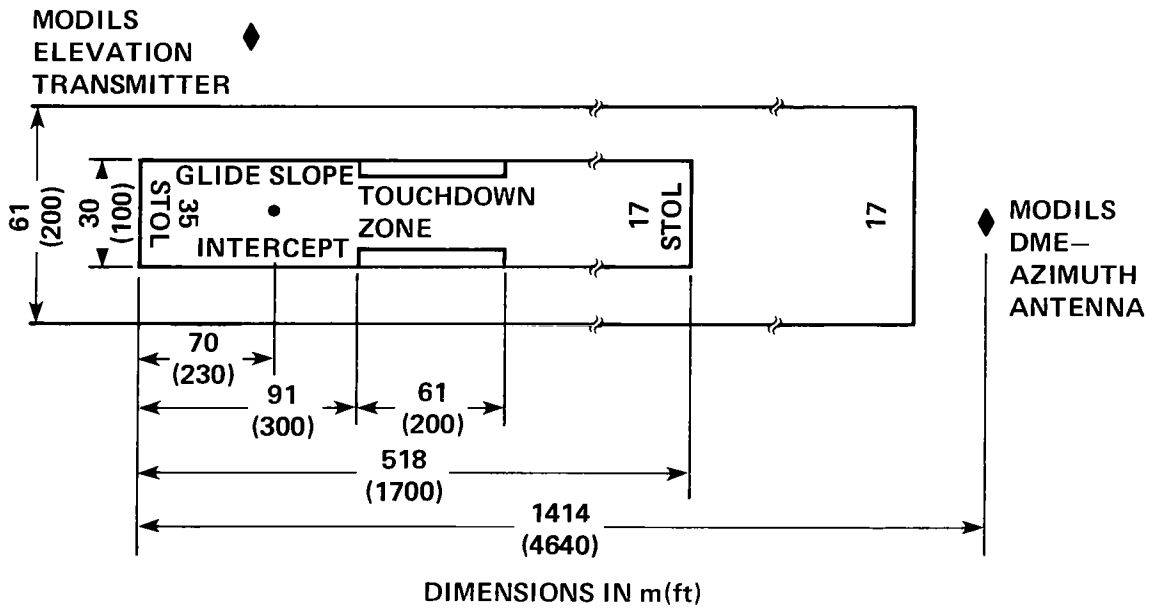
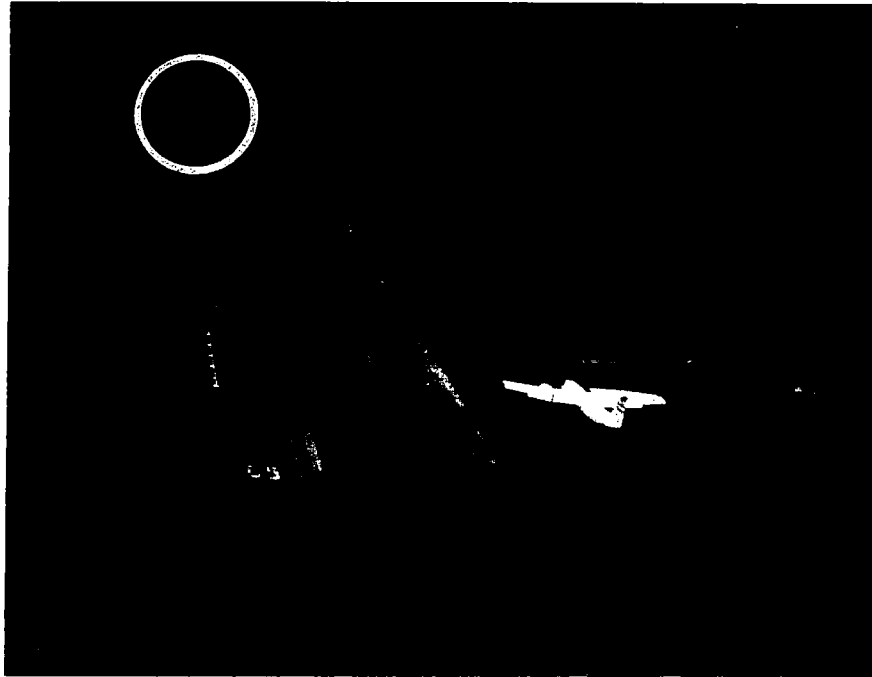


Figure 21.— Crows Landing flight research facility and STOL runway layout.

1 and 2 m/sec (3.3 and 6.6 ft/sec). However, consistency rather than ability to achieve a target point or sink rate was considered the figure of merit for the flare evaluation.

### Data Acquisition

Airborne and ground-based data acquisition capabilities were used in this research program. The airborne system provided for pulse code modulated (PCM) recording on board the aircraft and for PCM telemetry of data to the ground-based flight experiment facility at Crows Landing. Aircraft sensors provided attitudes, angular rates, linear accelerations, air data, engine performance, control position, approach path deviations, and digital control system discrete and computed variables. Video tape recordings were obtained of the pilot's instrument panel; included were a voice track of radio communications with the ground station and control tower and cockpit intercom conversation for use in postflight debriefing. Ground-based facilities include an experiment control station, telemetry data acquisition and on-line and postflight data processing equipment, strip-chart recorders, line printers, cathode ray tube data displays, and a wind recording device at the STOL runway location. Two Nike Hercules tracking radars provide three-dimensional, real-time data of aircraft position that is merged with the telemetered data for postflight processing.

Postflight data processing included generation of selected and conditioned time histories, landing perfor-

mance data, statistical results for selected parameters, stability derivatives from a parameter identification program, and the three components of wind velocity at the aircraft position on its flightpath. The wind velocity computation was performed using an analysis program developed by Dr. K-H. Doetsch of the National Research Council of Canada for operation with the Augmentor Wing Aircraft. This program is described schematically in the block diagram of figure 22. It combined radar position data (filtered and transformed into the aircraft body axis reference frame) with body axis linear accelerations in a third-order complementary filter to derive body axis components of inertial velocity. The radar position data were initially processed through a first-order washout filter with a time constant of 0.05 sec. The third-order complementary filter is of the form

$$\dot{X}_f = \frac{s(s+1)\ddot{X}_m + 0.33(s+0.11)\dot{X}_m}{(s+0.33)^3}$$

where

$$\dot{X}_f = \begin{Bmatrix} U_I \\ V_I \\ W_I \end{Bmatrix} \quad \dot{X}_m = \begin{Bmatrix} U \\ V \\ W \end{Bmatrix}$$

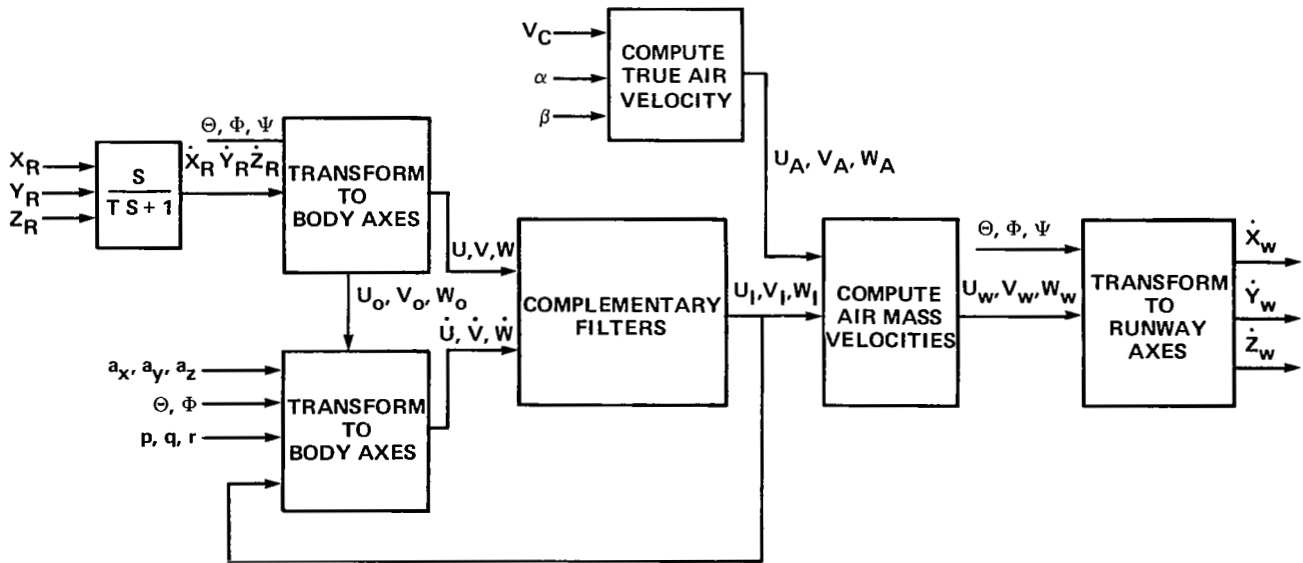


Figure 22.— Technique for extracting atmospheric motion.

Measurements of the three components of translational velocity with respect to the airmass were obtained from nose-boom-mounted pitot-static sensors and angle-of-attack and sideslip vanes; appropriate corrections were applied for aircraft angular rotation, configuration, and flight condition. The difference between the inertial- and air-data velocity components defined the individual components of the local wind velocity in the aircraft axis frame. Finally, these components were transferred back into an Earth-referenced axis system oriented with respect to the STOL runway. These runway oriented components are presented subsequently in this report.

## DISCUSSION OF RESULTS

### Glide-Slope Control

Results for that portion of the flight research program concerned with control of flightpath and airspeed for precision-approach path tracking down to the point of flare initiation are discussed in this subsection. The effects of variations in flightpath overshoot and flightpath-air-speed coupling, the influence of initial flightpath time response, and the collective effect of these characteristics are discussed in that order. Pilot ratings and commentary for each configuration are tabulated in appendix C.

*Effect of flightpath overshoot and flightpath-air-speed coupling*—Contributions of flightpath overshoot are illustrated in the trend of pilot ratings shown at the top of figure 23. Results for the two pilots are shown over a large range of overshoot ratios for initial time response in the range  $1.7 \leq t_{0.5\Delta\gamma_{\max}} \leq 2.5$  sec, and for both VFR and simulated IFR approaches. The pilots clearly preferred the configurations with minimal overshoot. Their objections to configurations with substantial overshoot related to the increased attention that was required for flightpath control to acquire the glide slope and to achieve adequate glide-slope tracking performance to the point of flare initiation. If the pilot maintained a constant flight reference throughout the approach, the flightpath washout following the initiation of a glide-slope correction made it difficult to anticipate the amount of control required to perform the correction so as to smoothly reacquire the glideslope. Consequently, the pilot was forced to monitor rate-of-descent or flightpath more closely while tracking the glide slope for the configurations with substantial overshoot, and the increased attention that was demanded produced a workload that was considered to be only marginally tolerable, if at all.

For these configurations, flightpath-air-speed coupling accompanied the flightpath overshoot and was also a factor

in the pilots' evaluations, as shown at the bottom of figure 23. The pilot could suppress the overshoot by adjusting pitch attitude to maintain constant airspeed during the flightpath correction. This action would also maintain speed closer to that desired for stall or wind-shear protection and for landing performance. However, this secondary task of speed control made a major contribution to pilot workload and correspondingly led to degraded ratings. Furthermore, due to the peculiar path-speed coupling (negative  $\Delta u_{ss}/\Delta\gamma_{ss})_{\Delta T}$ , the speed-control technique was unnatural, in that the pilot had to lower the nose to maintain speed when reducing the rate-of-descent, and vice versa.

A series of landing approach time histories (figs. 24-27) illustrates the differences in behavior between the configuration with no overshoot or coupling and one with only marginally acceptable values of these characteristics. Figure 24 shows an approach in light winds and turbulence for the configuration with no overshoot in which good glide-slope tracking performance and speed control are maintained with little control activity following the initial glide-slope capture. Even in the presence of significant turbulence and wind gradients (peak vertical gusts of 5.5 m/sec

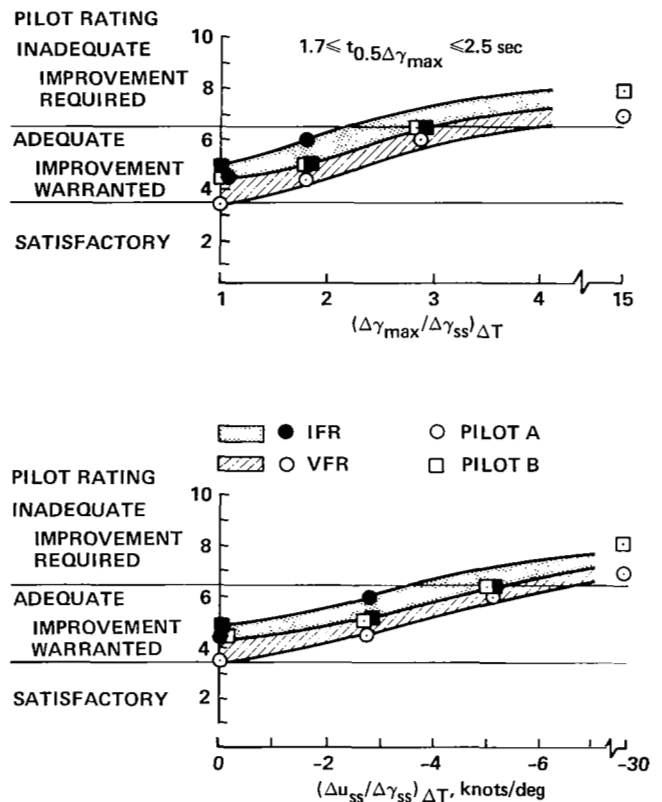


Figure 23.— Influence of flightpath overshoot and flightpath-air-speed coupling on pilot rating of glide-slope tracking (light winds, no turbulence).

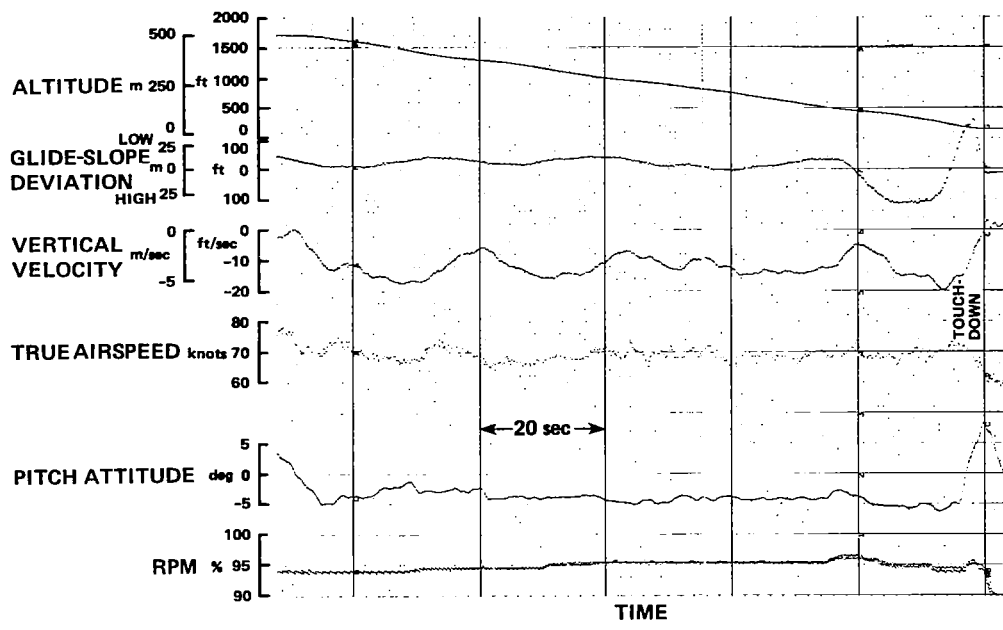


Figure 24.— Landing approach time history for configuration 1 (no flightpath overshoot or flightpath-airspeed coupling).

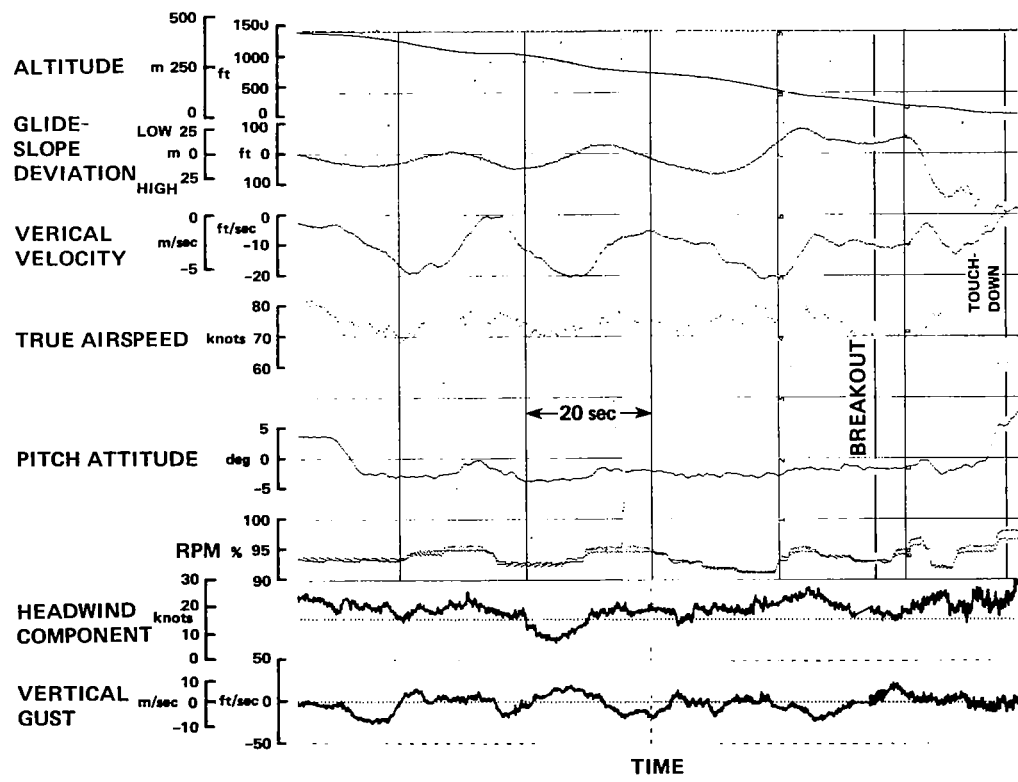


Figure 25.— Landing-approach time history in turbulence for configuration 1 (no flightpath overshoot or flightpath-airspeed coupling).

(18 ft/sec), wind shear 1.4 knots/sec sustained for 8 sec), as shown for the approach in figure 25, the pilots considered tracking performance to be acceptable; furthermore, the associated throttle control activity did not significantly increase pilot workload. Pilot ratings were degraded from 1/2 to 1 unit for this configuration under these conditions. For the configuration with large overshoot and coupling, figures 26 and 27 illustrate the difficulty with path and speed control. During the initial part of the approach in figure 26, the pilot is attempting to capture the glide slope from below and, following application of a substantial amount of thrust, finds that the aircraft has decelerated below an acceptable speed and still has not quite achieved the approach path. In the midst of this, the pilot makes a substantial nose-down attitude change to regain some airspeed and the aircraft again drops below the glide slope for some time. Toward the end of the approach, the pilot is finally able to establish position on the glide slope at a reasonable approach speed and successfully complete the landing. The opposite situation is illustrated in figure 27 where the pilot, in attempting to acquire the glide slope from above, substantially reduces thrust and allows the speed to build up substantially. In this case, the nominal speed is regained with modest adjustments of attitude following the large thrust application for glide-slope capture.

For both approaches, which were conducted in light winds and turbulence, the pilot had to make a number of adjustments in thrust and was continually changing attitude to correct to and maintain the desired airspeed.

The results of figure 23 indicate that the limits of flightpath overshoot that provide adequate flying qualities for the instrument approach range from 2.2 to 3.0. An approach under visual flight conditions would raise the allowable overshoot to 3.0 to 3.8. It should be noted that for these VFR approaches, the pilots still relied heavily on the MODILS guidance information, as well as on other status information in the cockpit. Corresponding levels of flightpath-airspeed coupling for these limiting conditions are -6.5 knots/deg VFR and -5.0 knots/deg IFR.

*Effect of initial time response*— The influence of the initial time response on the pilots' evaluations of flightpath control is evident in the trends of pilot rating with  $t_{0.5\Delta\gamma_{max}}$  shown in figure 28. Data are presented for initial time increments from  $1.7 \leq t_{0.5\Delta\gamma_{max}} \leq 3.8$  sec, with minimal flightpath overshoot and flightpath-airspeed coupling. As the initial response time approaches 4 sec, the pilots consider glide-slope tracking to be only marginally adequate, whereas for response times of 2 sec or less, satisfactory ratings can be achieved, at least for the VFR

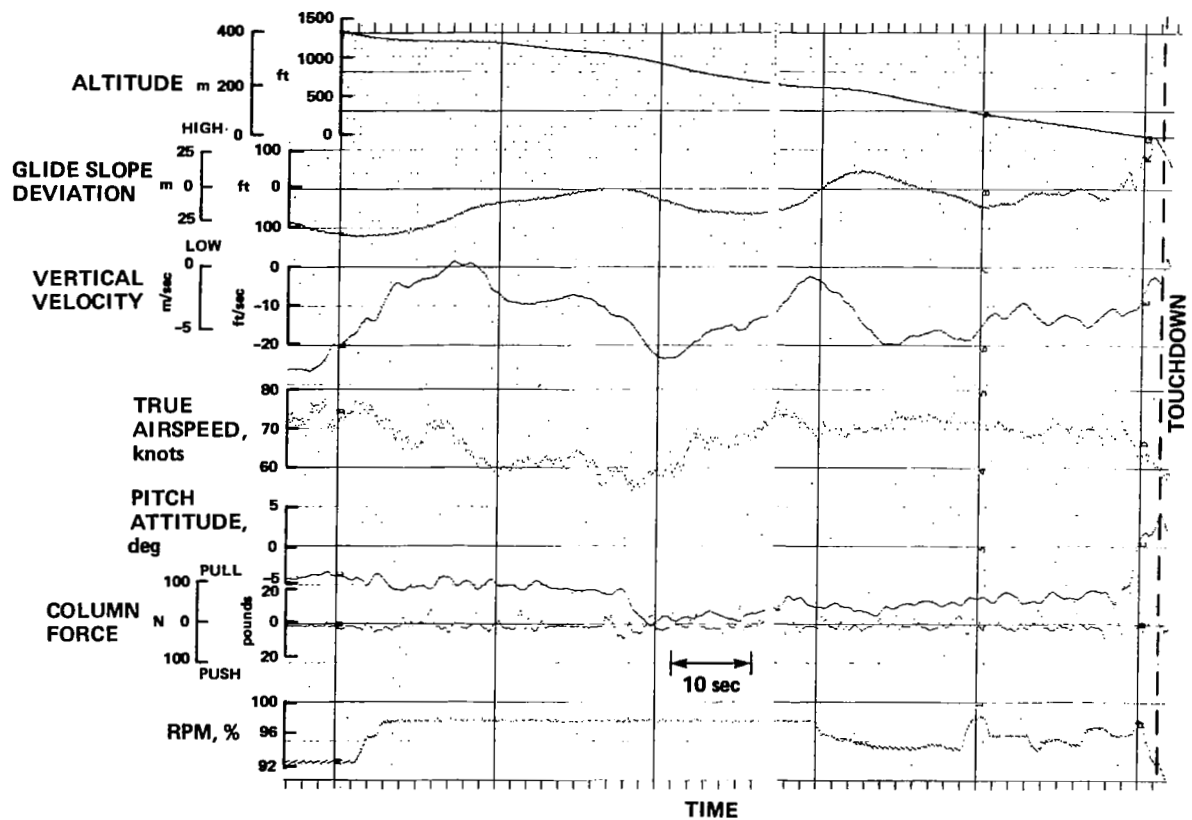


Figure 26.— Landing-approach time history for configuration 3 (large flightpath overshoot and flightpath-airspeed coupling).

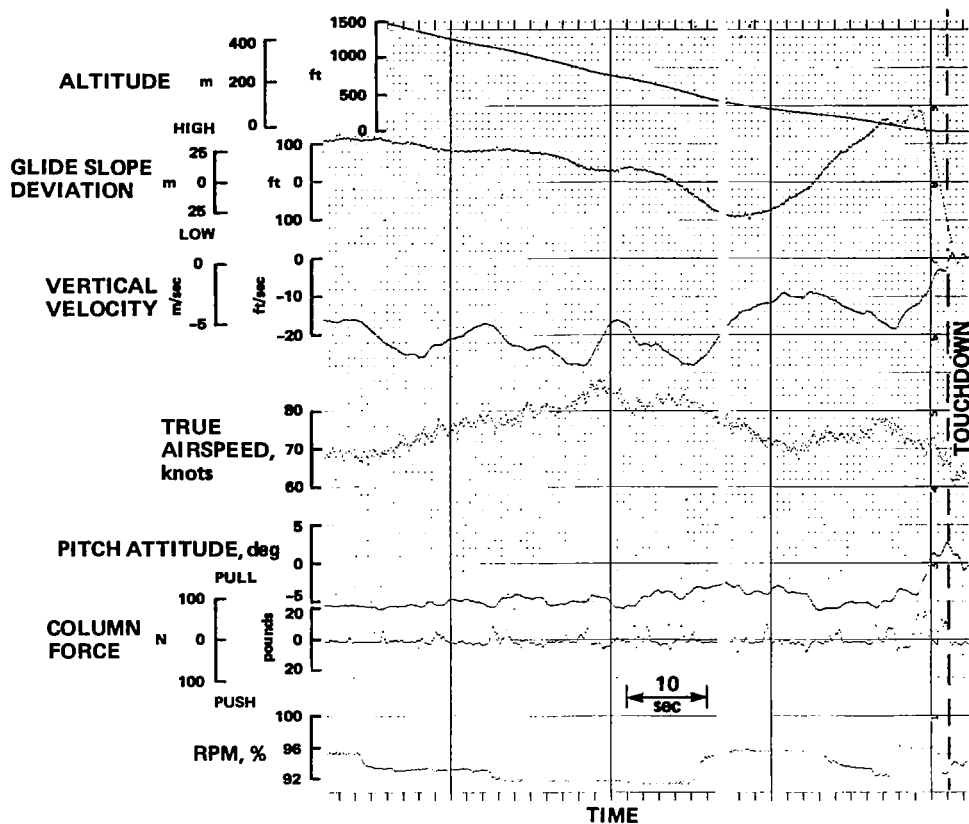


Figure 27.— Landing-approach time history of glide-slope capture for configuration 3 (large flightpath overshoot and flightpath-airspeed coupling).

approach. Recalling that these configuration variations were established through variations in vertical velocity damping, the configurations with slower initial response are those with the lowest level of damping. For these configurations, the pilots' objections concerned the difficulty they had in stabilizing the aircraft on the glide slope. It was necessary to pay close attention to glide-slope deviation and rate-of-descent and to anticipate the timing and magnitude of the throttle application for glide-slope corrections. Speed control generally presented no difficulty. Figure 29 provides a typical approach time history that illustrates the difficulty with glide-slope tracking for this configuration. It can be seen that even for an approach in light winds and turbulence, the pilot is never completely able to establish a steady condition on the glide slope, but continually chases it throughout the approach. Flightpath response to the pilot's throttle inputs also appears sluggish. For the approach in turbulence shown in figure 30 — up to 8.2 m/sec (27 ft/sec) vertical gusts; 4.3 knots/sec wind gradients — the aircraft continually wanders about the glide slope, flightpath response is oscillatory, and the pilot must make frequent large and abrupt throttle inputs to achieve even this level of performance. Pilot ratings for operation in turbulence of this magnitude were up to one rating unit

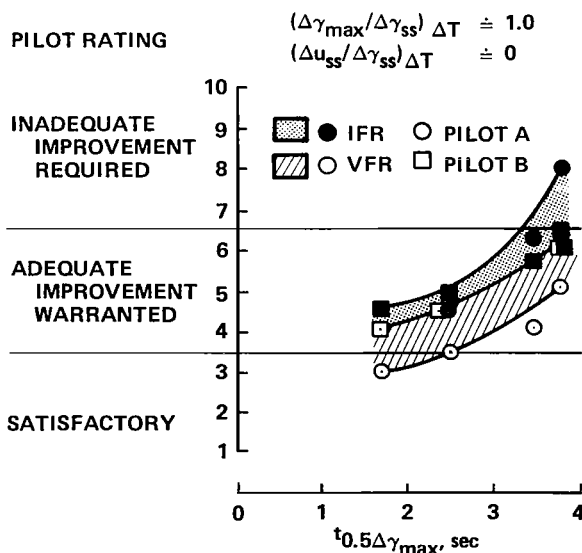


Figure 28.— Influence of initial flightpath time response on pilot rating of glide-slope tracking (light winds, no turbulence).

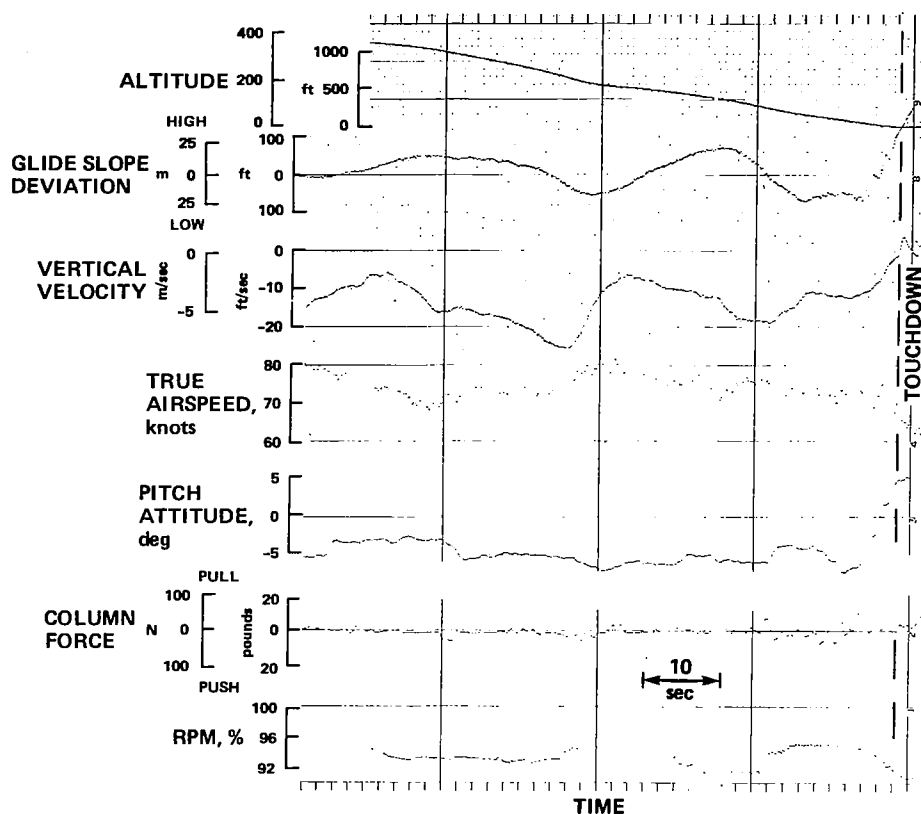


Figure 29.— Landing approach time history for configuration 6 (low heave damping, long initial time response).

worse than for the light wind and turbulence ratings shown in figure 28. In contrast, configuration 5 with the quickest flightpath response behaves much better during the approach. As an example, consider the approach time history for this configuration (fig. 31). In calm air, glide-slope tracking is smooth and precise, without much control activity on the part of the pilot. During an approach in turbulence (up to 6.4 m/sec (21 ft/sec) vertical gusts; 2.3 knots/sec wind gradients), glide-slope tracking is still good, as shown in figure 32, and proceeds without oscillatory flightpath behavior.

For the instrument approach task, flightpath time-response increments  $t_{0.5} \Delta \gamma_{\max} \leq 3.5$  sec would be required to obtain adequate flying qualities for glide-slope tracking. For visual approach, the corresponding time increment is about 4 sec.

Another group of data obtained during the flight program provides a somewhat different perspective of the influence of the initial response time on flightpath control. Figure 33 presents results of evaluating two configurations, for which the difference in initial time response was produced by changing the thrust inclination angle or, equivalently, the flightpath numerator time constant  $1/T\gamma_T$ . As the data indicate, initial response times somewhat greater than 5 sec can be tolerated while still retaining adequate

flying qualities for approach path tracking. For these configurations, no flightpath overshoot exists, but the increase in initial response time is accompanied by a conventional increase in flightpath-airspeed coupling (positive  $\Delta u_{ss}/\Delta \gamma_{ss}) \Delta T$ . Although the pilots objected to the excessive time required for a flightpath correction to stabilize for the poorest configuration, it was acceptable to assist the path correction with an adjustment in pitch attitude, which, in the short term, augmented flightpath response and, in the long term, maintained approximately constant airspeed. This coordinated use of the pitch and throttle controls is conventional (nose-up attitude to accompany an increment in thrust and vice versa) and allows the pilot to achieve acceptable glide-slope tracking performance. However, the secondary control task that required essentially simultaneous application of the throttle and pitch controls produced a workload level to which the pilots objected and led to flying qualities that were only marginally adequate for the task.

Figure 34 provides a typical time history of an approach for the configuration with the longest time response and conventional path-speed coupling. With little turbulence, glide-slope tracking is good and no oscillatory tracking tendencies are evident at altitudes approaching decision height. Airspeed control is also good; however, the coordinated

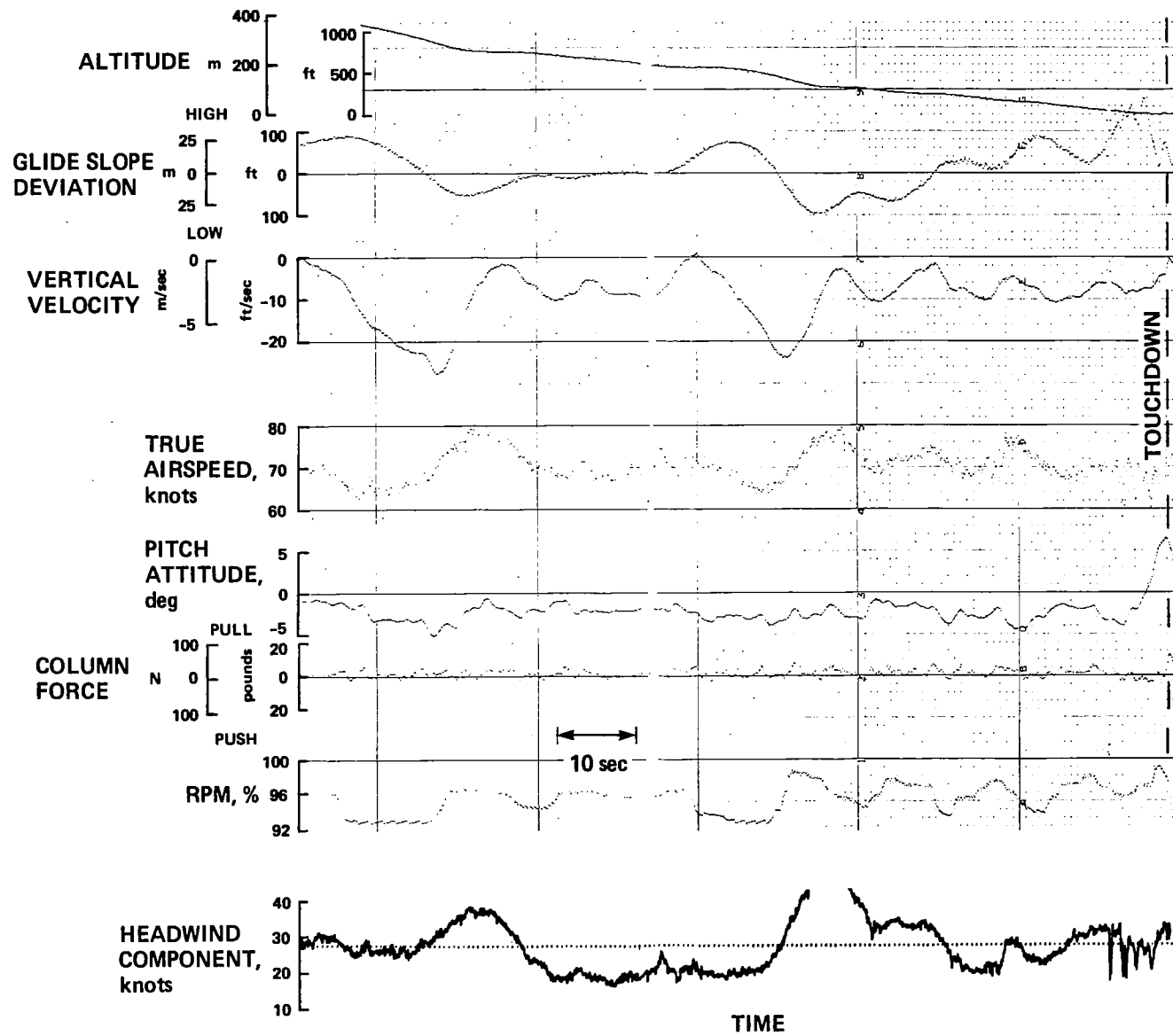


Figure 30.— Landing approach in turbulence for configuration 6 (low heave damping, long initial time response).

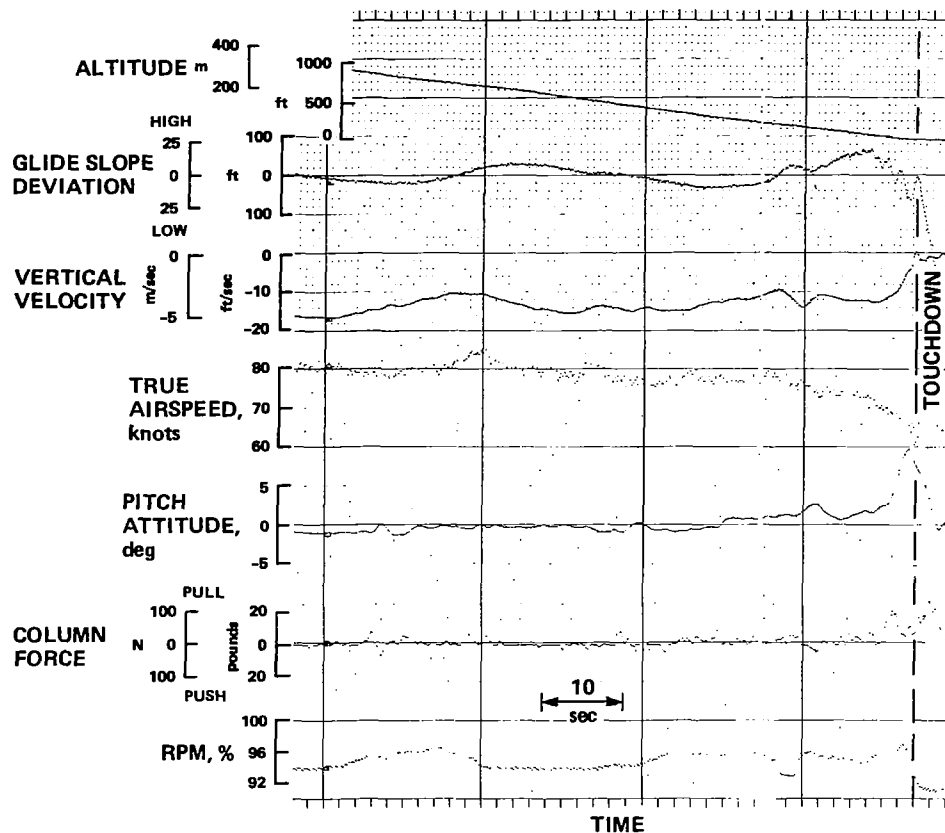


Figure 31.— Landing-approach time history for configuration 5 (high heave damping, short initial time response).

pitch and thrust control activity is apparent. during an approach in turbulence (fig. 35) — up to 5.5 m/sec (18 ft/sec) vertical gusts; 3.3 knots/sec wind gradients — glide-slope tracking performance is degraded and flightpath control is somewhat oscillatory. Pitch control is quite active to maintain speed in the presence of the flightpath corrections and turbulence. For this configuration, pilot ratings for this level of turbulence were from 1-1-1/2 units worse than for operation in calm air, as shown in figure 33.

*Combined effects of overshoot and time response*— The combined influence of flightpath overshoot and initial time response is shown in figure 36. In this case, three levels of flightpath overshoot are shown ( $\Delta\gamma_{\max}/\Delta\gamma_{ss}$  - 1.0, 1.8, and 3.0) for initial time response ranging from  $1.7 \leq t_{0.5} \Delta\gamma_{\max} \leq 3.8$  sec. The trend of degradation in pilot ratings with increased initial time response is somewhat more pronounced for the higher overshoot conditions. The combination of these adverse effects demands excessive pilot attention and compensation to achieve acceptable glide-slope tracking, even under visual flight conditions. An instrument approach would have been completely unacceptable and was not even attempted. Figure 37 illustrates the associated glide-slope control time history during

an approach in winds of 10-15 knots. The oscillatory nature of the glide-slope and flightpath behavior are evident. Continual thrust corrections were required to achieve this quality of approach-path control, even under these relatively light wind conditions.

It is evident from the data of figures 23, 28, and 33 that the best pilot ratings of the configurations that were evaluated were only marginally satisfactory. Furthermore, from the trends of the data with flightpath overshoot and initial time response, it is apparent that it would be difficult or impossible to improve those characteristics further. For the best of these configurations, it happens that the pilot's criticisms were not concerned with the flightpath response characteristics of the aircraft but were directed at the overall workload imposed by the raw data instrument scan required to achieve acceptable path tracking during the approach. One means of further reducing this workload is to provide the pilot with flight-director guidance for use in tracking the glide slope and localizer. In this regard, brief evaluations of the flight director described in the previous section were conducted for configurations 1 and 6 to see to what extent the flying qualities of those configurations could be improved for the landing approach.

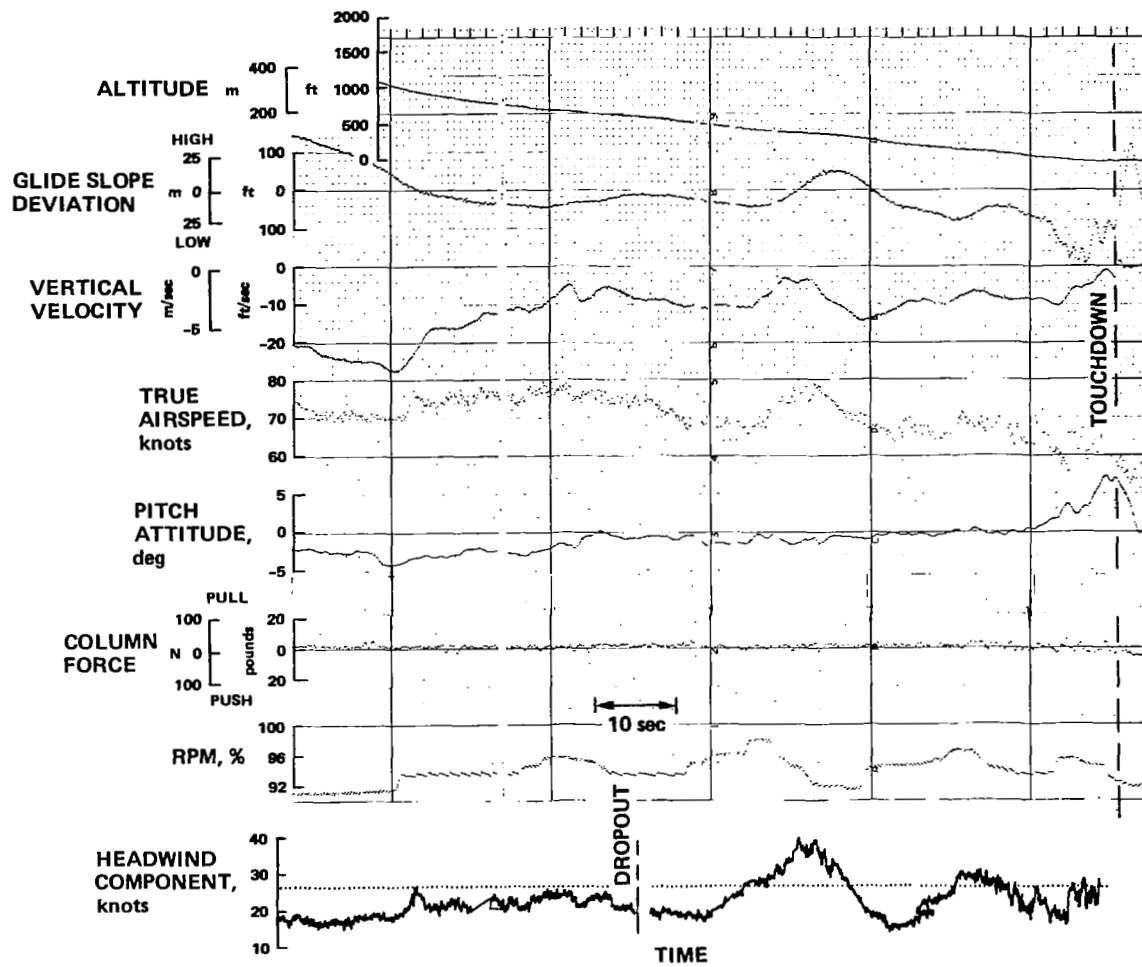


Figure 32.— Landing approach in turbulence for configuration 5 (high heave damping, short initial time response).

Figure 33.— Influence of initial flightpath time response and flightpath-airspeed coupling on pilot rating of glide-slope tracking (light winds, no turbulence).

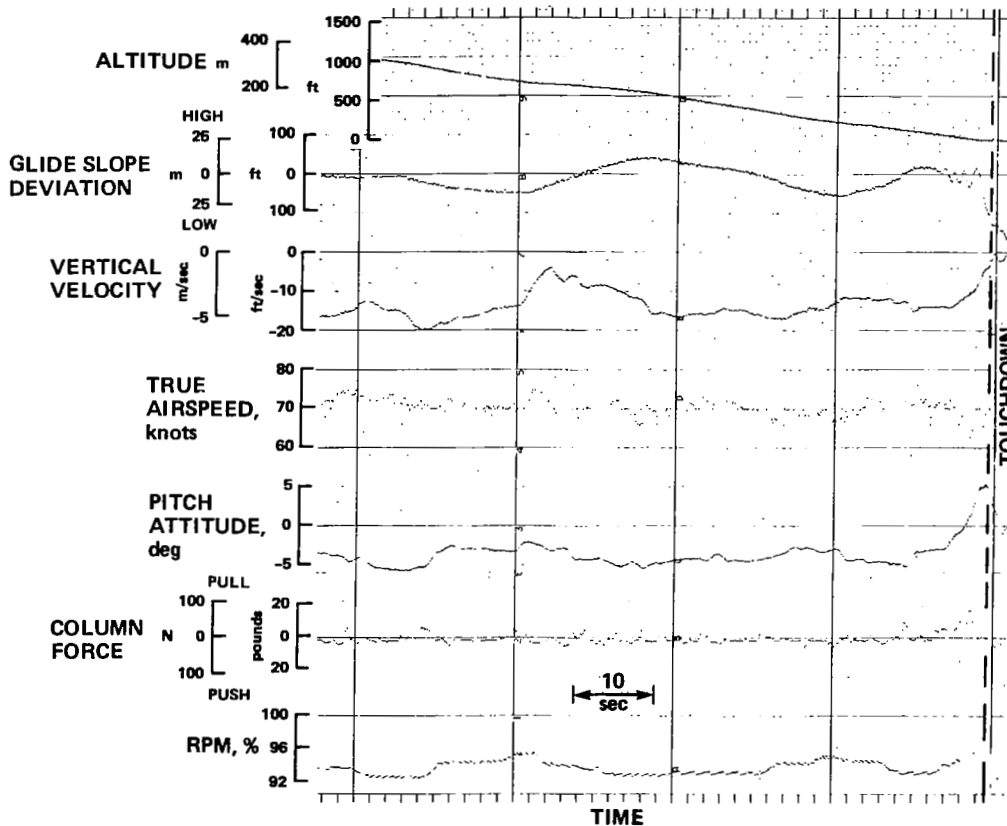
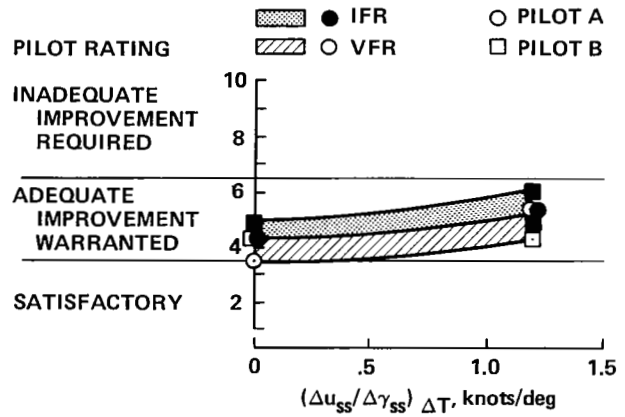
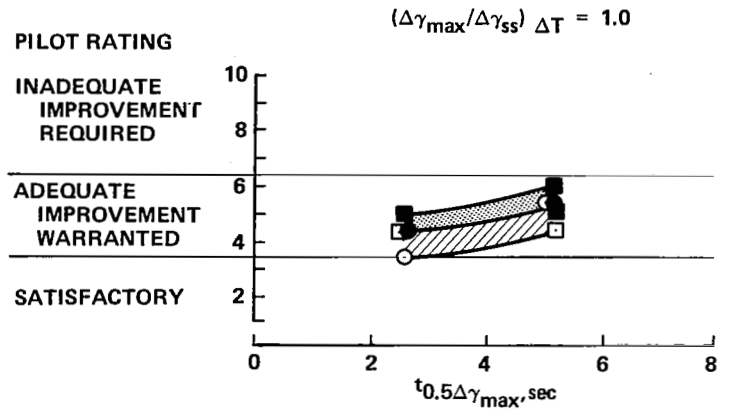


Figure 34.— Landing-approach time history for configuration 7 (long initial time response, conventional flightpath-airspeed coupling).

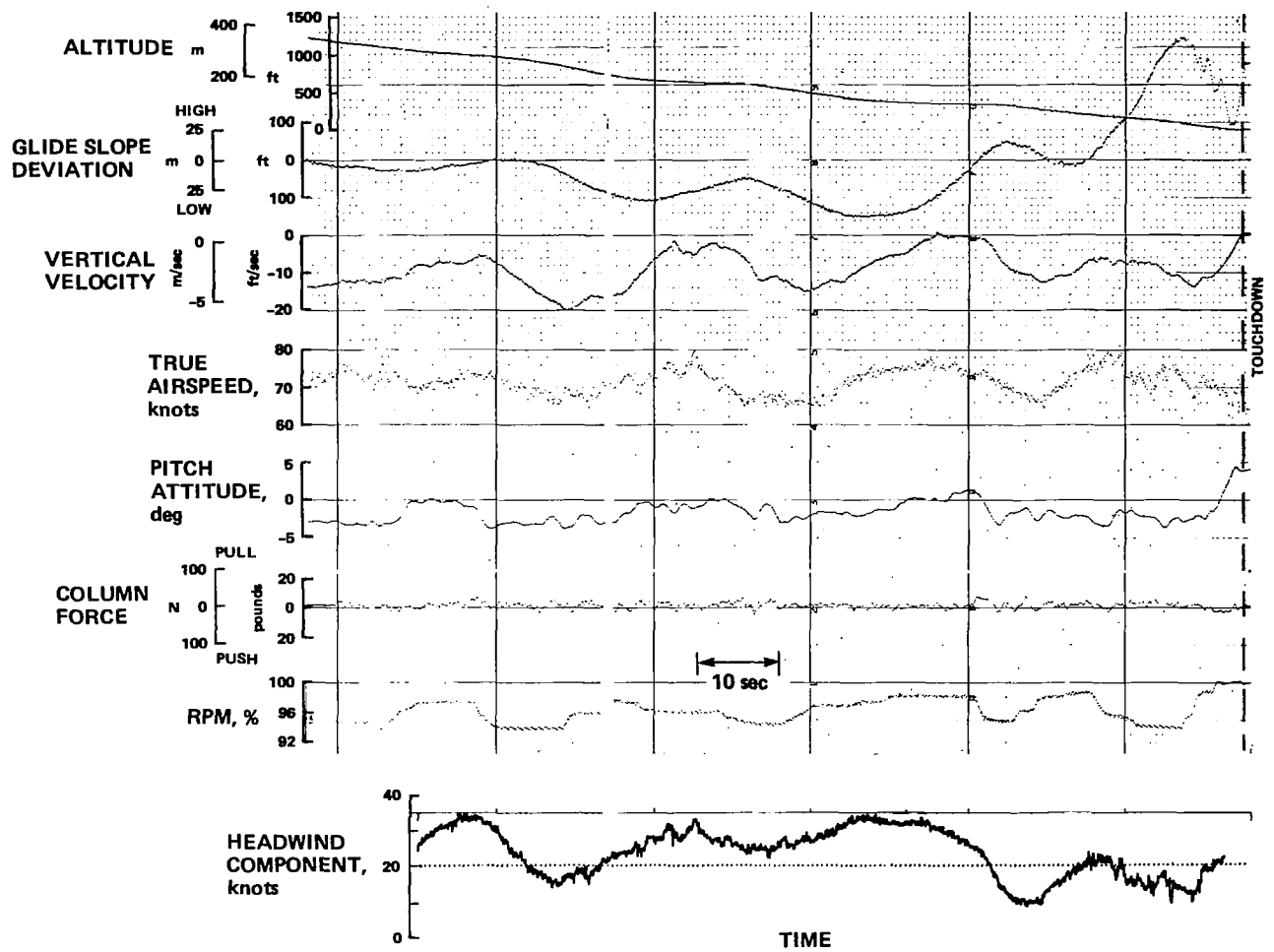


Figure 35.— Landing approach in turbulence for configuration 7 (long initial time response, conventional flightpath-airspeed coupling).

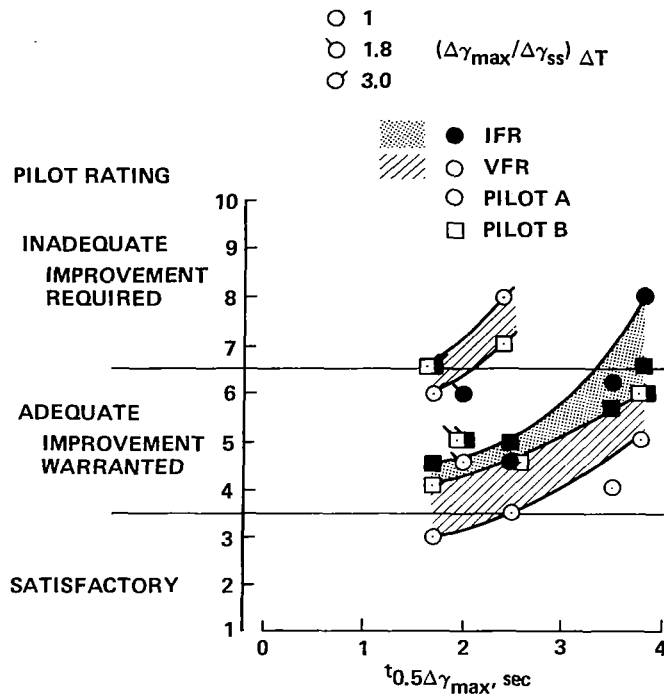


Figure 36.— Combined influence of flightpath overshoot and initial flightpath time response on pilot ratings of glide-slope tracking (light winds, no turbulence).

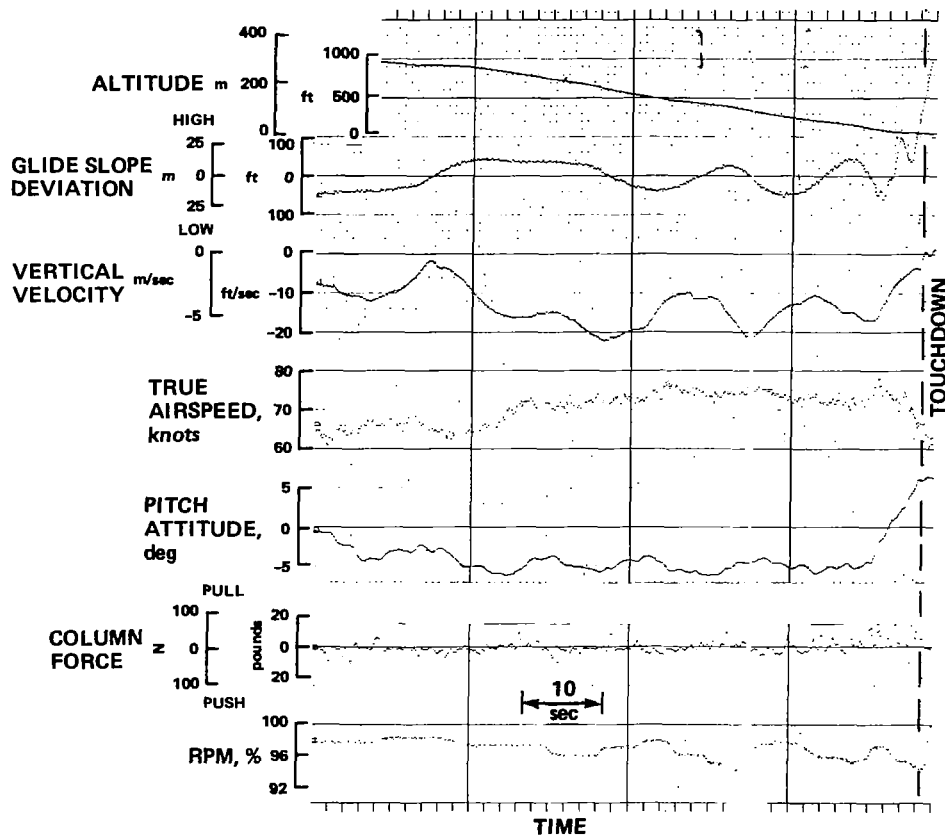


Figure 37.— Landing-approach time history for configuration 9 (long initial time response, large flightpath overshoot and flightpath-airspeed coupling).

Configuration 1, it will be recalled, is characterized by no flightpath overshoot or flightpath-airspeed coupling and by a reasonably short initial response time ( $t_{0.5\Delta\gamma_{\max}} = 2.5$  sec). Pilot ratings for this configuration ranged from 4-1/2 to 5 for the instrument approach task. With the flight director available to provide commands for the throttle, column, and wheel controls, the configuration was judged to be fully satisfactory and was given pilot ratings from 2 to 3. Attention required for the instrument scan was reduced and the overall workload was considered to be minimal. A time history of a landing approach is shown in figure 38. Smooth glide-slope corrections are evident, little throttle control activity exists, and speed excursions are minimal.

Configuration 6 is also characterized by minimal path overshoot or path-speed coupling; however, its initial time response is long enough to make it inadequate for an instrument approach (PR from 6-1/2 to 8). By reducing the instrument scan workload and providing some lead information for flightpath control with the throttles to overcome the lag in flightpath response, the flight director made possible an improvement to a pilot rating of 5. An indication of the behavior of the aircraft during an approach for this configuration is provided in figure 39. Light turbulence is present. Glide-slope tracking is improved over that without the flight director (presented in fig. 29). However, some oscillatory flightpath behavior is still evident, though at a higher frequency appropriate to the flight-director/airframe combination. This oscillatory response could likely be reduced further by adjusting the flight director gains to provide additional effective flightpath phase margin; e.g., by increasing the path deviation rate gain. However, time did not permit further assessment of the flight director for this configuration.

A final point worth noting in this section: the pilots considered the flightpath angle information on the EADI useful enough to warrant a 1/2- to 1-unit improvement in their ratings over those given for configuration 6 during glide-slope tracking with the aid of a conventional instantaneous vertical speed indicator.

## Flare Control

Flare evaluations were performed by using either pitch attitude or thrust as the primary control of descent rate and touchdown position. When the flare was performed with a pitch rotation, a moderate reduction in thrust was occasionally performed to complete the landing at the desired location on the runway. When the flare was accomplished with thrust control, an open-loop pitch rotation was performed to establish the landing attitude. Under some circumstances the flare could be successfully performed by using coordinated application of the pitch and thrust controls.

*Flare with pitch*— The pilots' assessments of the flare with pitch indicated that the dominant influence on this maneuver was the ability to adequately check the sink rate before touchdown. Figure 40 illustrates the effect on pilot rating of variations in flightpath response to pitch,  $\Delta\gamma_{\max}/\Delta\theta_{ss}$ . It is apparent that the pilots preferred that flightpath follow pitch attitude in a ratio approaching 1:1 in the short term, and that they were quite sensitive to reductions in this response capability. If they were unable to change flightpath appreciably with reasonable changes in pitch attitude (as constrained by airframe geometry limits) and with comfortable rotation rates, their ratings were significantly degraded. They also expressed a sensitivity to the initial normal acceleration and considered it as a factor in their assessment of the flare capability. Inadequate ratings for flare with pitch alone were obtained for  $\Delta\gamma_{\max}/\Delta\theta_{ss} < 0.5$ . Satisfactory ratings could be achieved with  $\Delta\gamma_{\max}/\Delta\theta_{ss} > 0.7$ .

Pilot comments for the satisfactory configuration (12) indicated that it could be flared with a gentle rotation and that repeatable landing performance could be achieved. Figure 41 shows a time history of a representative flare maneuver for configuration 12. A pitch rotation of about  $8^\circ$  was sufficient to check the sink rate from 4.6 m/sec (15 ft/sec) to 1.8 m/sec (6 ft/sec) at touchdown. No assist with thrust was required, and in fact, a reduction in thrust was performed prior to touchdown. Pitch rates were less than 3 deg/sec. Figures 42 and 43 provide flare-control profiles and sink-rate profiles for configuration 12 that indicate the usage of the pitch control as well as the control of sink rate as a function of altitude. The flares tended to be initiated at altitudes of about 9-10 m (30-35 ft), and a steady pitch rotation was held to the point of touchdown to arrest the sink rate to acceptable levels. No oscillatory control tendencies can be observed.

The flare for the inadequate heave response configuration (14) could not be controlled acceptably by pitch rotation alone. Pilot comments revealed their awareness of the substantially reduced heave response to pitch. Figure 44 shows an example of a flare performed with configuration 14 with little initial application of thrust. A pitch rotation of  $11^\circ$  at rates exceeding 3.5 deg/sec was performed to check the sink rate from 3.2 m/sec (10.5 ft/sec) to 0.6 m/sec (2 ft/sec). No attempt was made in this case to complete the landing within the touchdown zone since the pilot was primarily concentrating on the ability to control sink rate with some precision. Note that the pilot started to increase thrust less than a second prior to the initial touchdown. The aircraft rebounded into the air and the pilot then applied maximum continuous thrust (99% rpm) to cushion the final touchdown. Flare profiles and sink-rate profiles shown in figures 45 and 46 reveal the large magnitude pitch rotation that is required if the flare is attempted with little or no assistance with thrust. The flare is also

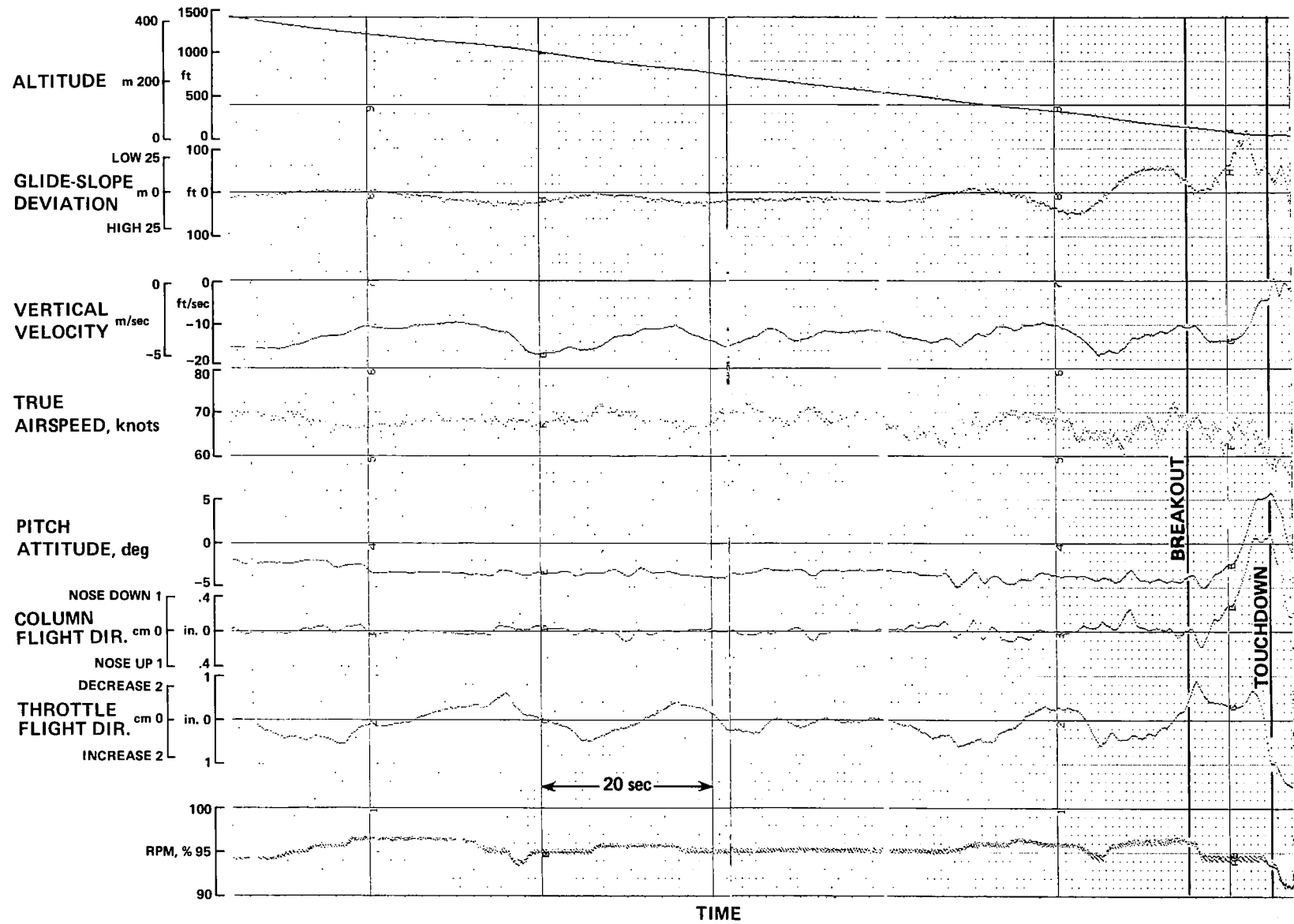


Figure 38.— Landing approach time history for configuration 1 (no flightpath overshoot or flightpath-airspeed coupling; with three-cue flight director).

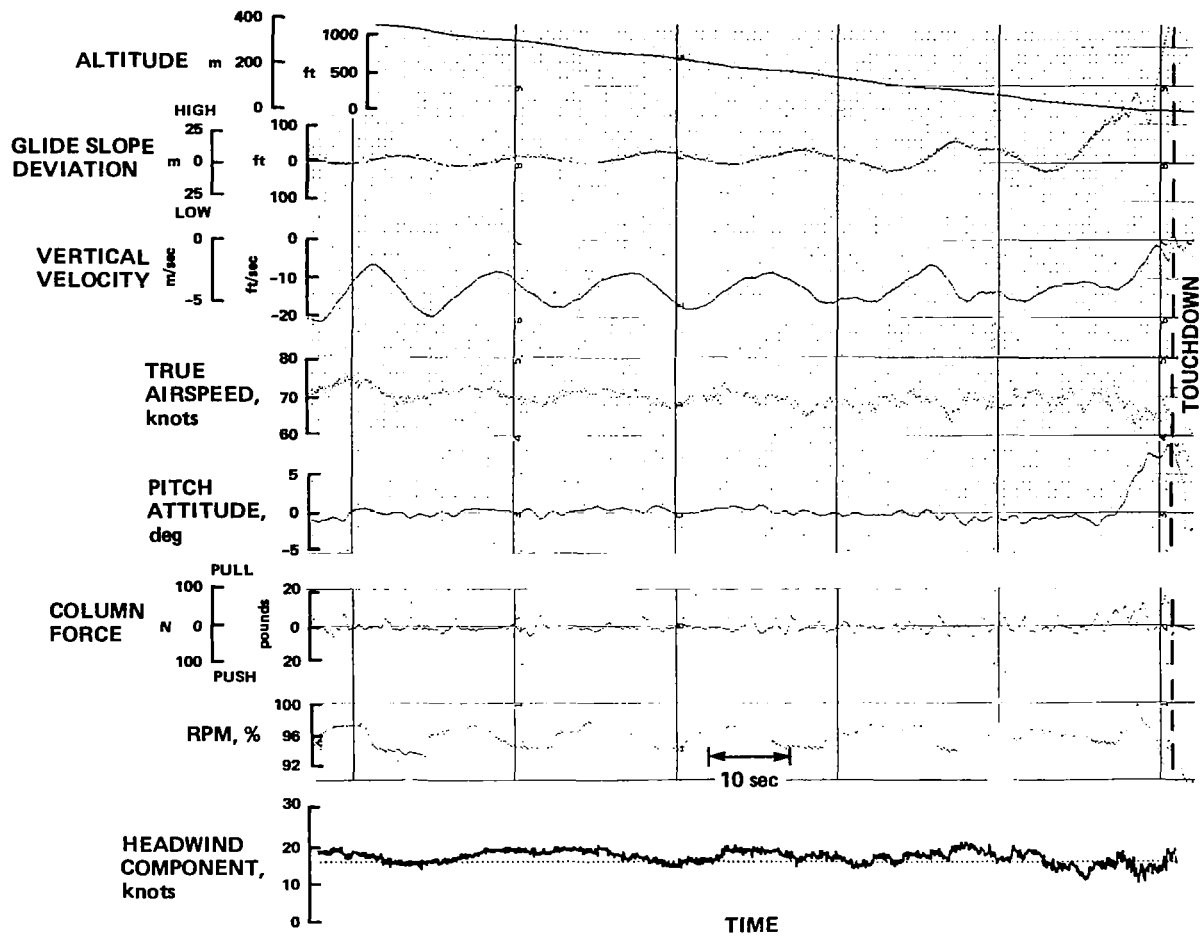


Figure 39.— Landing approach in turbulence for configuration 6 (low heave damping, long initial response time; with three-cue flight director).

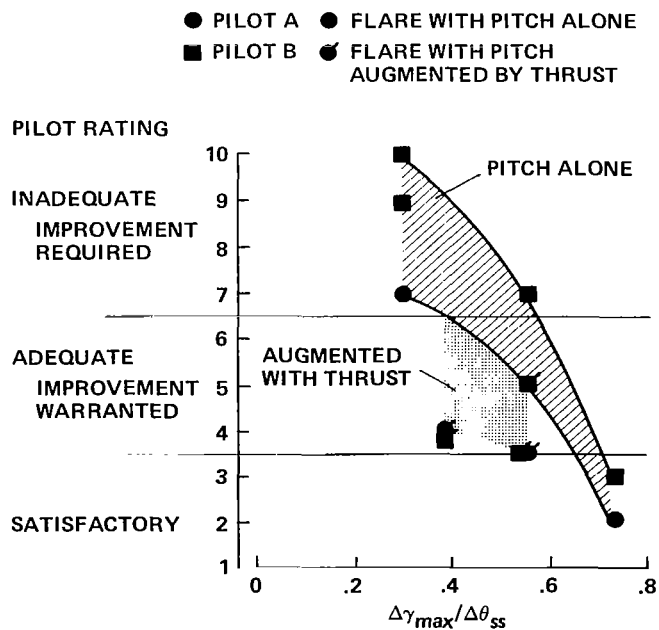


Figure 40.— Influence of initial flightpath response to pitch attitude on pilot rating of flare control.

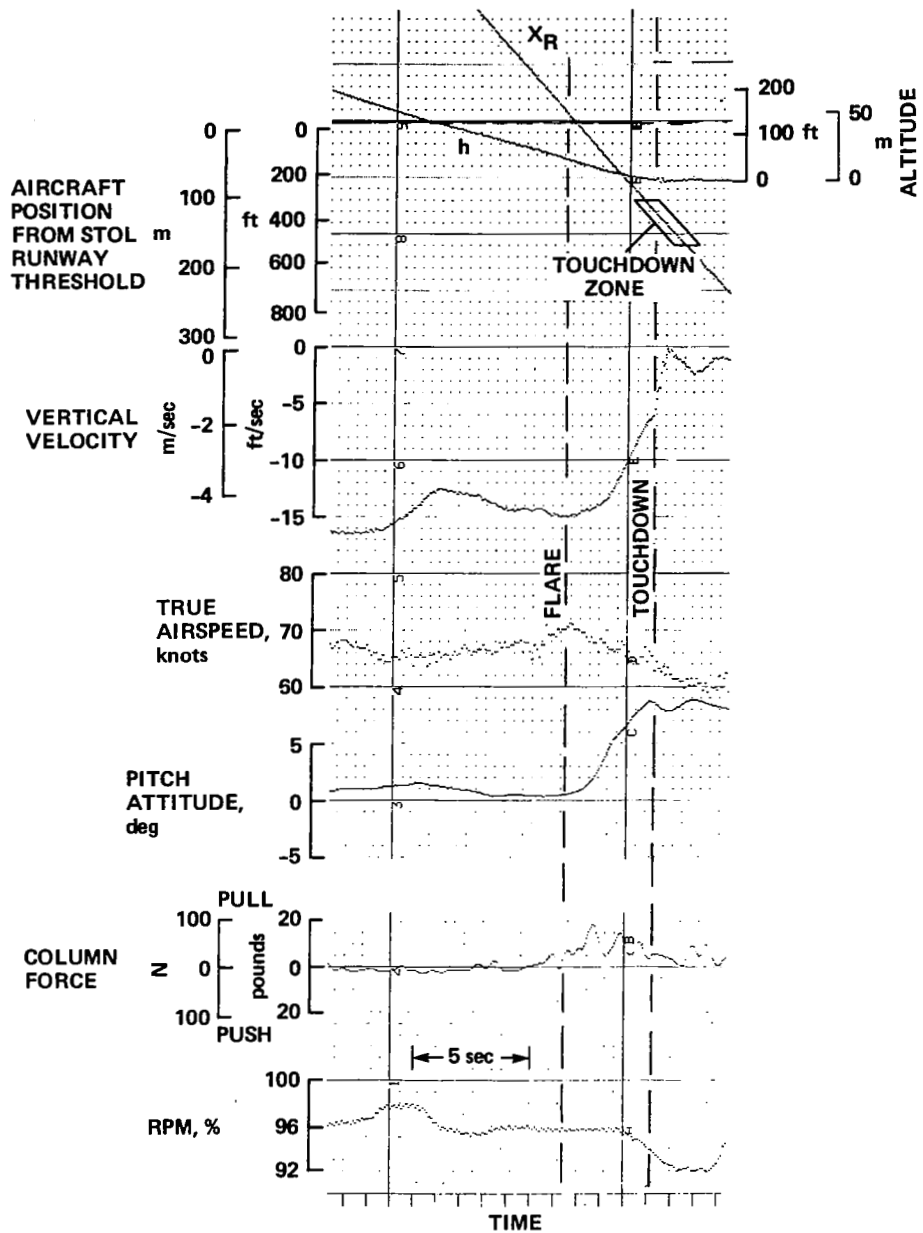


Figure 41.— Landing-time history for configuration 12 (satisfactory initial flightpath response to pitch).

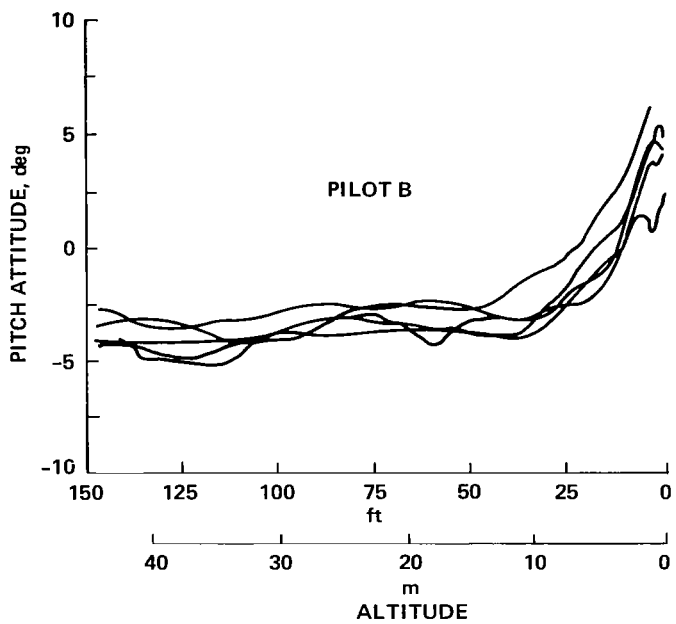
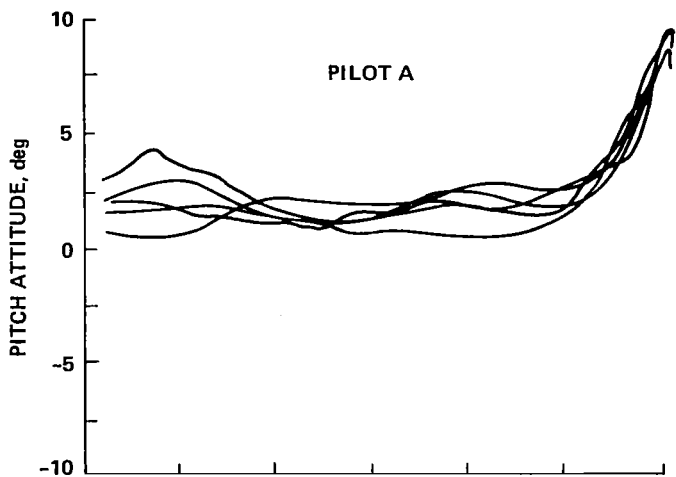
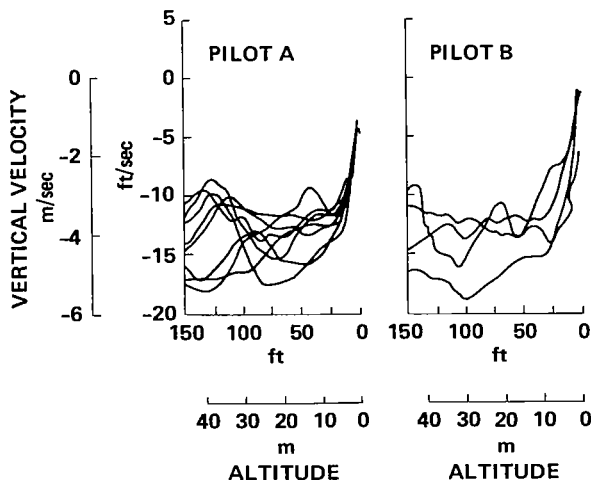


Figure 42.— Flare-control profiles for configuration 12 (satisfactory initial flightpath response to pitch).

Figure 43.— Sink-rate profiles for configuration 12 (satisfactory initial flightpath response to pitch).



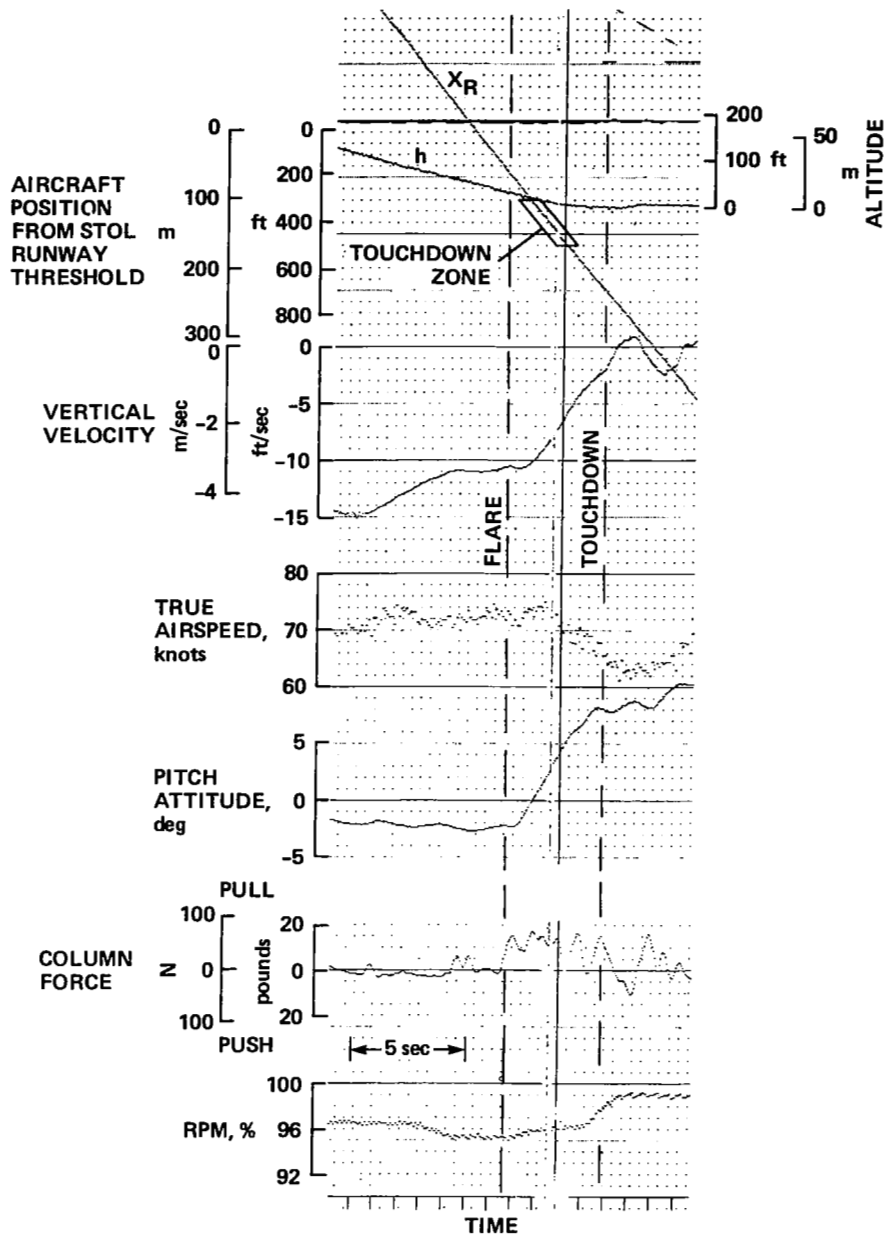


Figure 44.— Landing time history for configuration 14 (inadequate initial flightpath response to pitch).

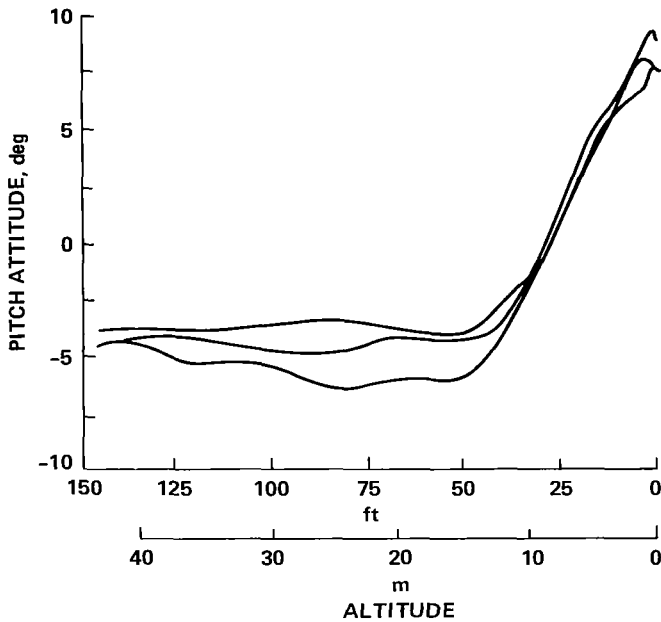


Figure 45.— Flare-control profiles for configuration 14 (inadequate initial flightpath response to pitch).

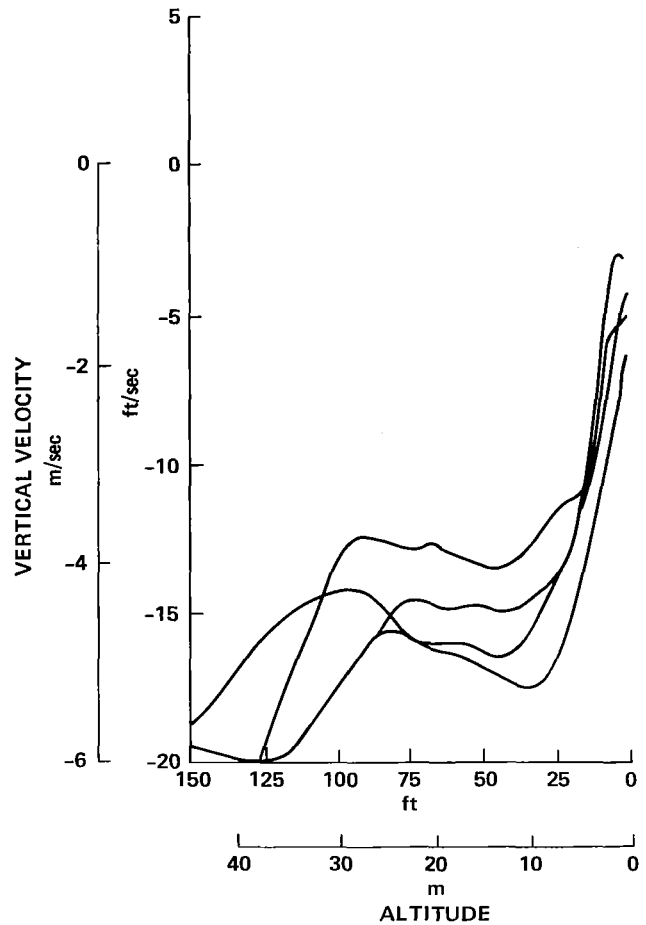


Figure 46.— Sink-rate profiles for configuration 14 (inadequate flightpath response to pitch).

initiated at a slightly higher altitude than for the best configuration, in this case closer to 12 m (40 ft).

Configurations with adequate but unsatisfactory heave response to pitch (configurations 11 and 13) could be successfully controlled in the flare by coordinated application of the pitch and thrust controls. In some cases, this technique consisted of a step increase in thrust prior to flare initiation to assist in reducing high sink rates or a gradual reduction to complete the landing; pitch control was used to further modulate the sink rate. In other instances, the two controls might be modulated simultaneously during the flare. Configurations 11 and 13 encompassed values of  $\Delta\gamma_{\max}/\Delta\theta_{ss}$  of 0.38 to 0.55 and, as shown in figure 40, received pilot ratings from 3-1/2 to 5. The shaded region extrapolates these results to the boundary for adequate flare control.

Figure 47 shows an example of a flare for configuration 13. In this case, a fairly significant thrust increment is made part way through the flare, followed by an even larger reduction in thrust in the 2 sec before touchdown. A steady

pitch rotation is used to initiate the flare, and it is relaxed somewhat toward the end of the flare to avoid floating beyond the touchdown zone. This particular configuration ( $\Delta\gamma_{\max}/\Delta\theta_{ss} = 0.38$ ) and flare technique were given a rating of 4 by the evaluation pilot.

*Flare with thrust*— Although configuration 14, which had the poorest heave response to pitch ( $\Delta\gamma_{\max}/\Delta\theta_{ss} = 0.29$ ), was rated inadequate for flare control with pitch alone, it was possible to perform the flare successfully by using thrust predominantly for sink-rate control. An example landing in which thrust was the primary flare control for this configuration is shown in figure 48. A quite large thrust increment is used to reduce the initial sink rate of 4.6 m/sec (15 ft/sec), and this level of thrust is sustained until touchdown. Although a pitch rotation is initiated early and at an unusually high altitude of 25 m (80 ft), this is done primarily to establish a landing attitude that will clear the nose wheel. Once this attitude is achieved, the rotation is stopped by the pilot. Note that the sink-rate control authority is substantial with this amount

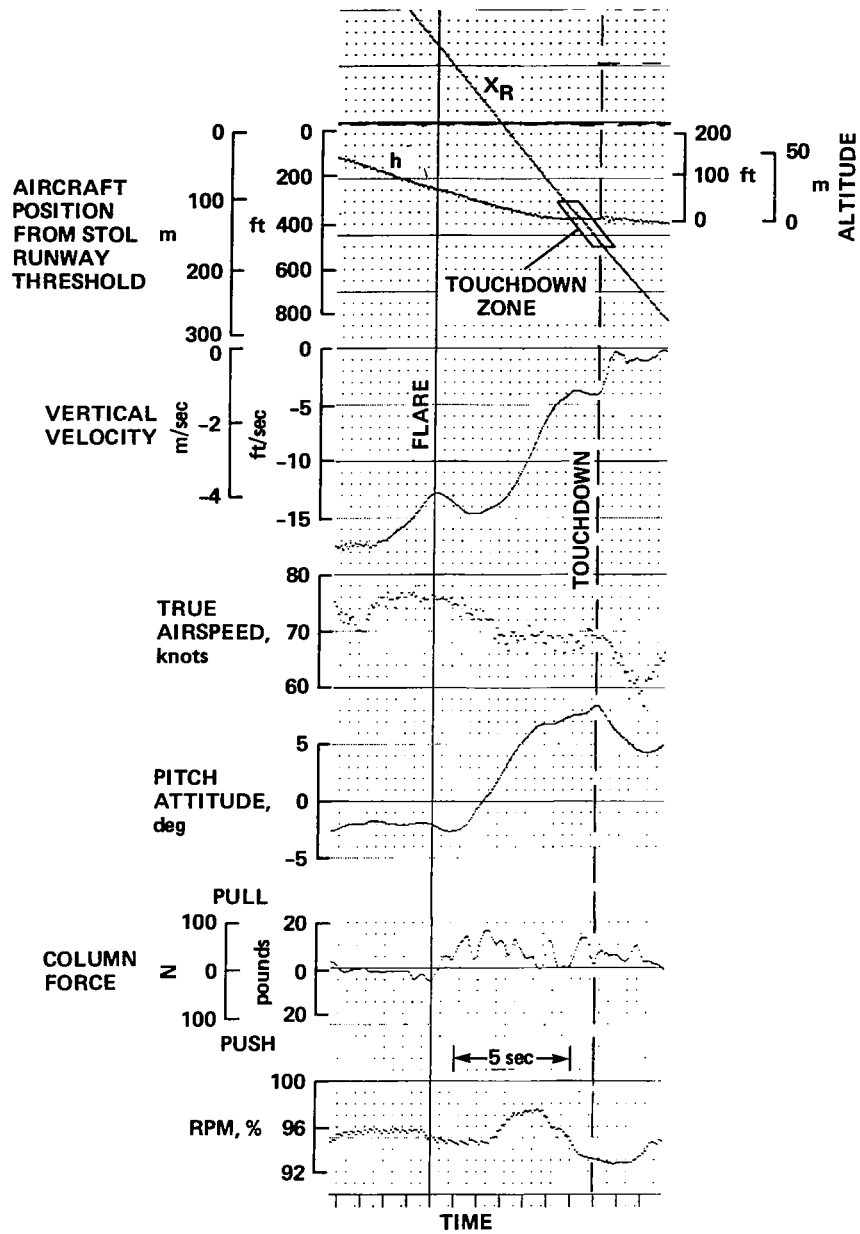


Figure 47.— Landing-time history for configuration 13 (coordinated pitch and thrust control for flare).

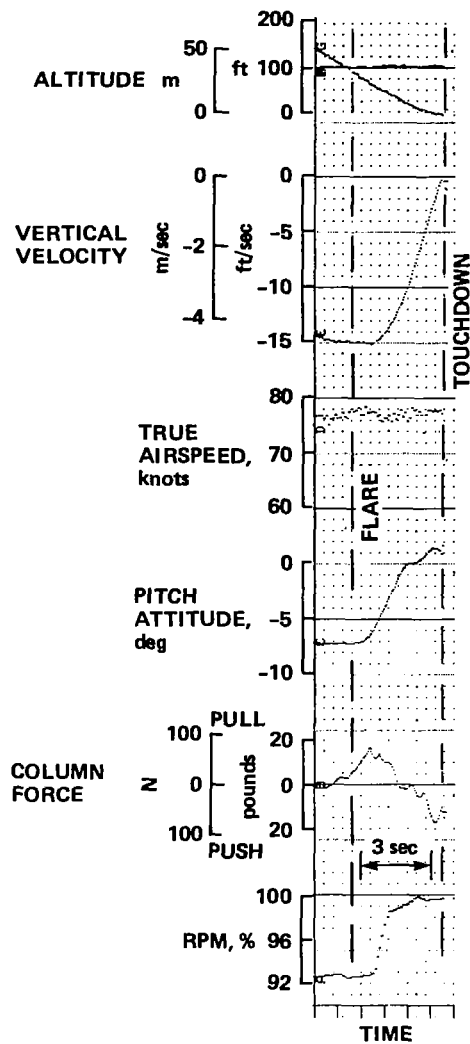


Figure 48.— Landing-time history for configuration 14 (primary flare control with thrust).

of thrust application and ensures a sink rate to the target of 1 to 2 m/sec (3.3 to 6.6 ft/sec). Figures 49-51 give examples of flare profiles from several landings with this configuration. The extent to which thrust is modulated just prior to and during the flare is apparent in figure 49. Large inputs and reversals in thrust control are used during the last 30 m (100 ft) before touchdown, with noticeable increases in activity during the last 9 m (30 ft). Pitch rotations (fig. 50) are initiated at about 12 m (40 ft) and are continued through an increment of about  $8^\circ$  before touchdown. In figure 51, the effective sink-rate arrestment still begins at about 9 to 10 m (30 to 33 ft) and is performed without any oscillatory tendencies to the point of touchdown. Pilot ratings for this configuration are shown in figure 52 as a function of the initial flightpath response time that was noted in previous discussions to be a significant factor for

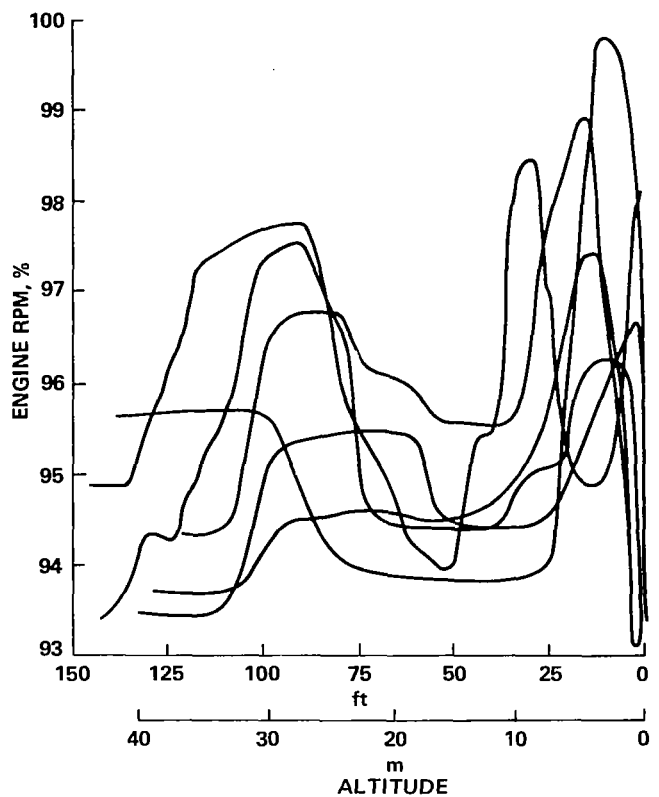


Figure 49.— Primary control of the flare with thrust for configuration 14.

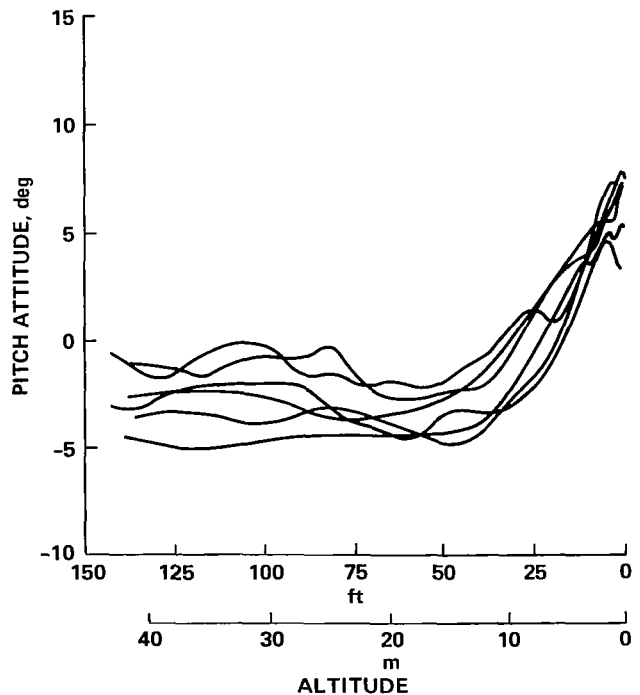


Figure 50.— Secondary control of the flare with pitch attitude for configuration 14.

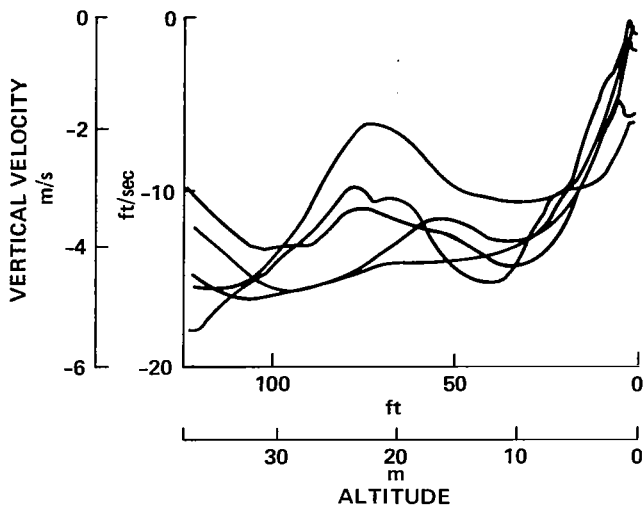


Figure 51.— Sink-rate profile for configuration 14 (primary control of flare with thrust).

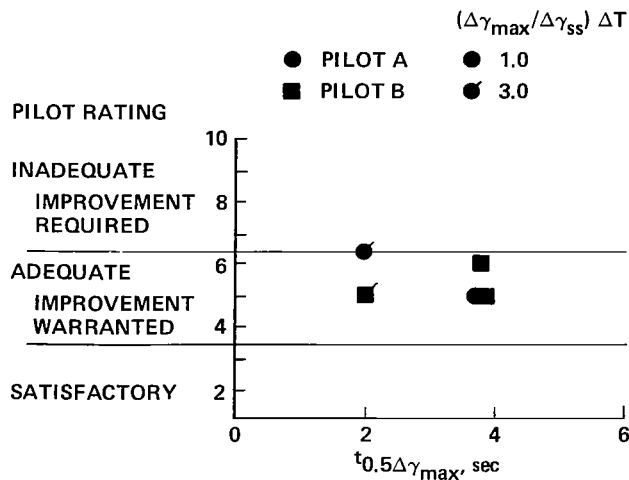


Figure 52.— Influence of initial flightpath time response on pilot ratings of flare control with thrust.

path control during the approach. No flightpath overshoot or path-speed coupling exist for the unflagged symbols in figure 52. Although the pilots felt that the flare could be executed successfully for this configuration by using thrust, the relatively slow initial response associated with low vertical velocity damping ( $Z_w = -0.2 \text{ sec}^{-1}$ ) and a somewhat sluggish engine response ( $\omega_E = 2.7 \text{ rad/sec}$ ) gave the pilots an impression of only marginally adequate flare control, and led to ratings from 5 to 6. In general, the pilots did not have enough confidence in their ability to consistently achieve the desired flare performance and they were unwilling to give this configuration more acceptable ratings. Simi-

lar ratings were given to a configuration with shorter initial response time, but with substantial flightpath overshoot (flagged symbols in fig. 52).

Measurements of landing precision are shown in figure 53 for the configurations (11, 12, 14) ranging from satisfactory to inadequate heave response and for flares performed either primarily with pitch or with thrust control. Dispersions in touchdown point are slightly less for the configuration for flare control with pitch alone (configuration 12) than for the other two. The pilots also tended to land the pitch-alone configuration consistently toward the

CONFIGURATION	11 ———	12 - - - - -	14 ———
FLARE TECHNIQUE	PITCH + THRUST	PITCH PRIMARY	THRUST PRIMARY
NUMBER OF LANDINGS	18	22	18
MEAN TOUCHDOWN DISTANCE	156 m 514 ft	113 m 372 ft	144 m 473 ft
MEAN TOUCHDOWN SINK RATE	1.2 m/s 3.8 f/s	1.4 m/s 4.5 f/s	1.3 m/s 4.2 f/s

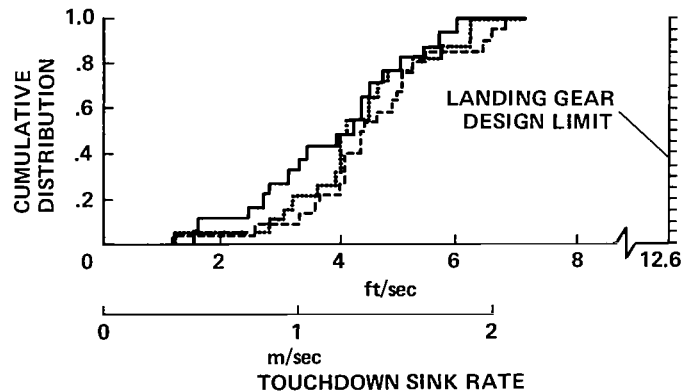
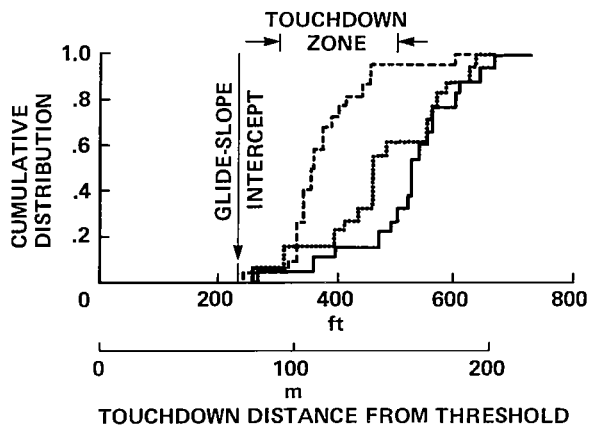


Figure 53.— Comparison of landing performance.

beginning of the touchdown zone. Since the flare maneuvers for the configurations with poor heave response were initiated at a slightly higher altitude, their touchdown dispersions fall toward the end of the zone. The pilots did not feel that these differences were significant to their precision of control of the touchdown. Dispersions in touchdown sink rate were virtually identical for these three configurations. Mean values were about 1.2 m/sec (4 ft/sec) and provided a substantial margin from the landing gear design limit. Considering the results of the landing performance analysis, as well as the evaluation pilot's comments, the primary influence on the pilots' assessments of these configurations is considered to be the compensation required of the pilots to achieve this performance.

Considering the configurations with variations in the long-term flightpath washout in response to pitch, as long as the capability exists to check the sink rate adequately with rotation or thrust, the time for a flightpath correction to bleed off ( $t_{0.1} \Delta\gamma_{max}$ ) does not appear to have a significant influence on flare control or landing precision. Pilot ratings for these configurations are presented for the values of initial flightpath response and  $d\gamma/du$  in figure 54. There were no changes in ratings or pilot comments when  $d\gamma/du$  and the long-term washout were changed for those configurations

in which flare was controlled predominantly with pitch. For the cases in which it was necessary to perform the flare with thrust to achieve adequate flying qualities, the long-term time response to pitch would not be expected to be a significant factor. Example time histories are shown in figures 55 and 56 for landing flares for two configurations (15, 16) with adequate short-term heave response that operates either in the drag bucket or rather far on the backside of the drag curve. In figure 55, a flare is performed with a configuration (15) that effectively operates in the drag bucket and with a long flightpath washout time interval ( $t_{0.1} \Delta\gamma_{max} = 13$  sec). The flare is initiated with pitch and is assisted with thrust only to the extent that the throttles were retarded toward the end of the flare to complete the landing. Adequate sink-rate control is available with pitch; no floating tendencies were observed, nor could they be provoked during any of the landings with this configuration without a significant abuse of the control technique. For the configuration (16) that operates well on the backside of the drag curve, figure 56 shows a time history of a landing in which the pilot intentionally overflares the aircraft at the initiation of the landing and prolongs the maneuver to see if the aircraft has a tendency to develop high sink rates (fall out) during the latter stage of the flare. No change in thrust is made during the first 8 sec of the maneuver. Significant speed bleed off occurs from the initiation to touchdown (67 to 47 knots) and the sink rate begins to build up following the initial arrestment. However, it is still possible to check this buildup with a small additional rotation and a single-step application of thrust. For the purpose of investigating this behavior, no attempt was made to terminate the flare in time to land in the touchdown zone. Compared with a normal flare duration of 4 to 7 sec, this maneuver was abnormally long (10.8 sec).

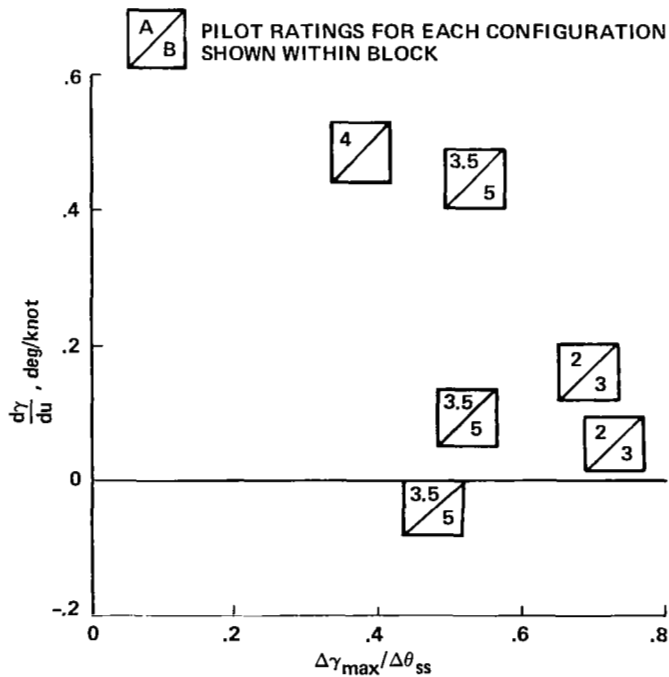


Figure 54.— Influence of initial and long-term flightpath response to pitch on pilot ratings of flare control.

To further illustrate the influence of short- and long-term heave response characteristics on the flare, a comparison of time histories for a simulation of a representative flare maneuver with variations of these characteristics is provided in figure 57. The maneuver consists of a steady pitch rotation of 1.2 deg/sec for a duration of 7 sec. Heave-response characteristics range from  $0.4 \leq \Delta\gamma_{max}/\Delta\theta_{ss} \leq 0.7$  and  $0.0 \leq d\gamma/du \leq 0.4$  deg/knot. It is evident that the dominant effect on the ability to change sink rate over this interval is the initial flightpath response magnitude. In comparison, the change in long-term flightpath response has little effect on the touchdown sink rate. For this representative flare maneuver, the reduction in touchdown sink rate varies from 1.3 to 3.2 m/sec (4 to 10.5 ft/sec) for the range of initial response magnitudes, compared with a variation of 1.5 to 2.3 m/sec (5 to 7.5 ft/sec) for a range of long-term response times that encompasses operating conditions of  $d\gamma/du$  from nearly neutral to steep backside (0.4 deg/knot).

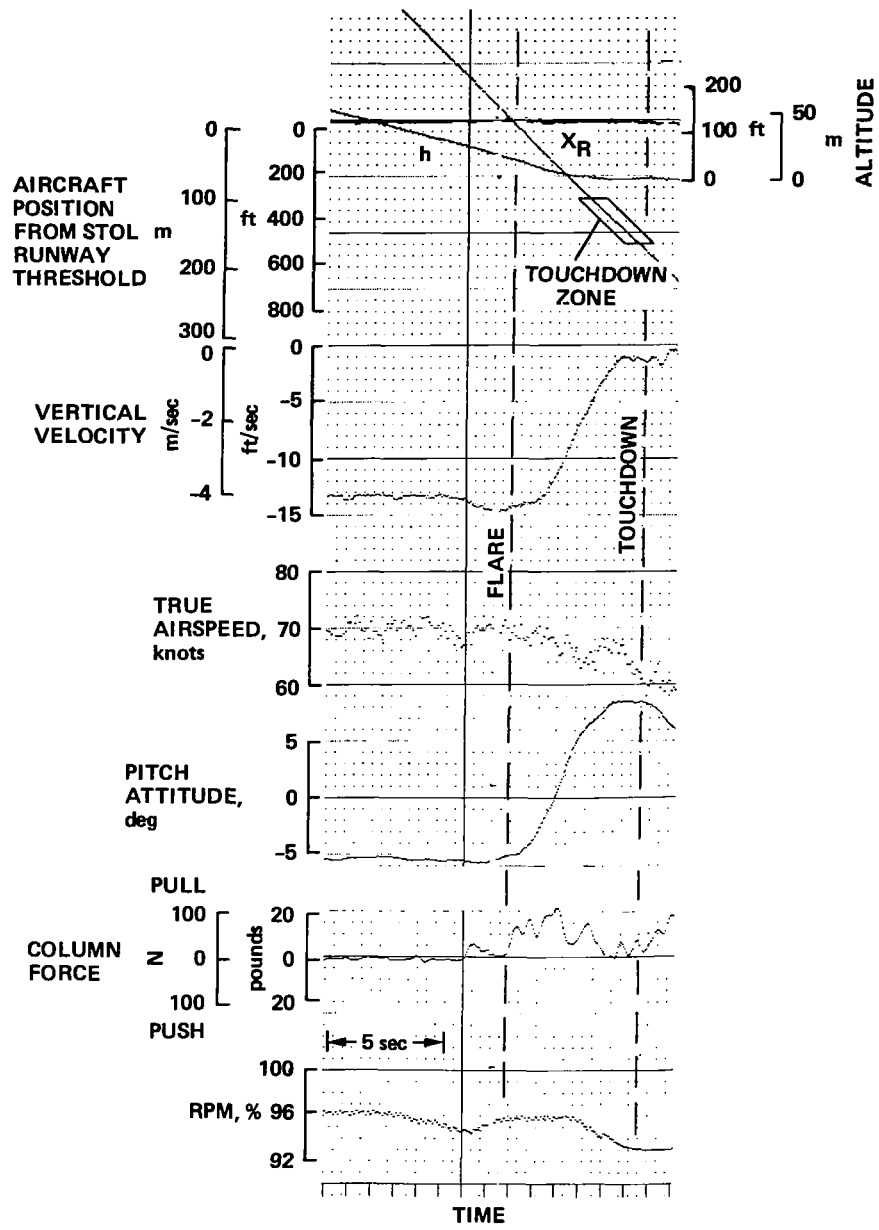


Figure 55.— Landing-time history for configuration 15 ( $d\gamma/du \cong 0$ ).

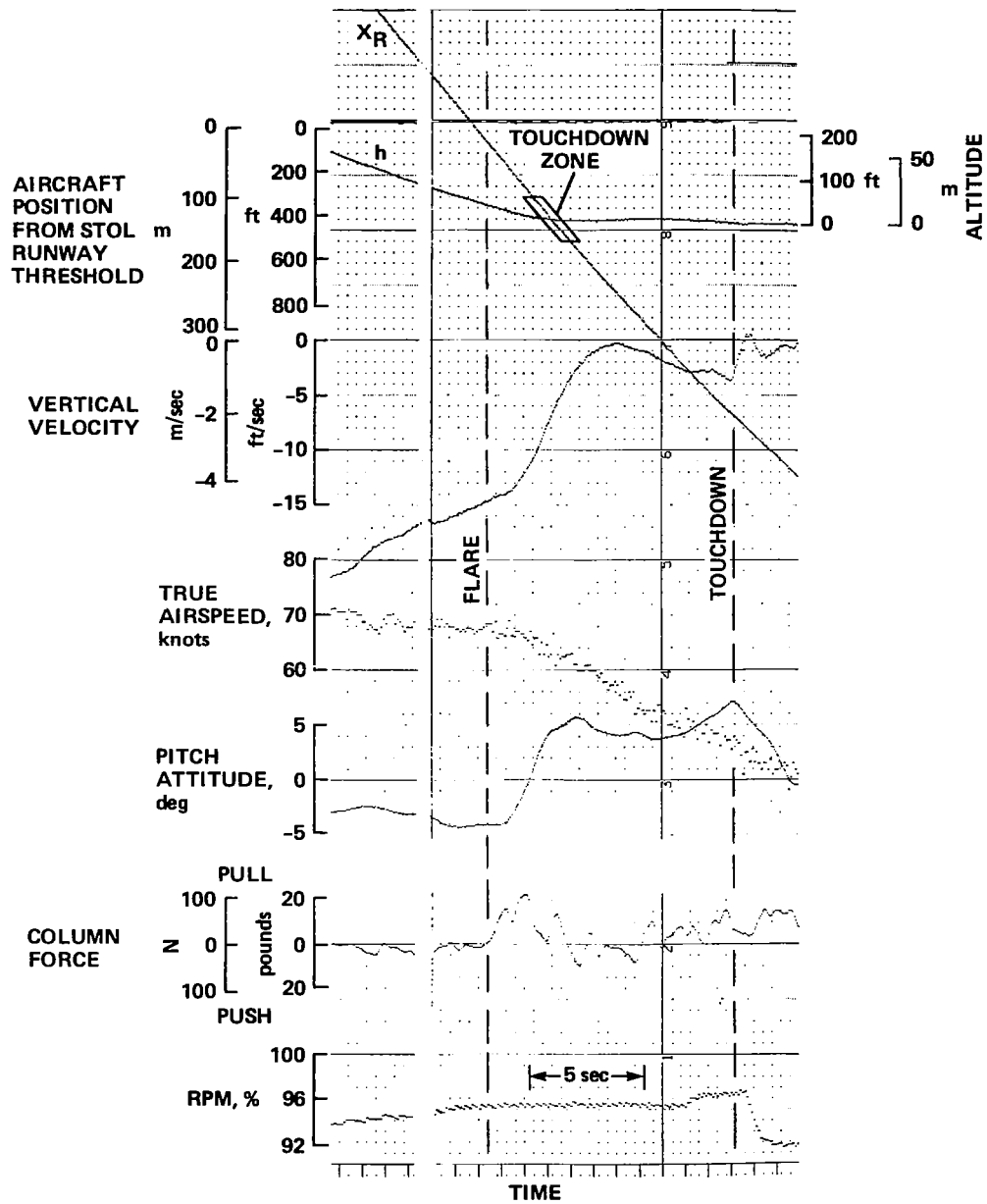


Figure 56.— Landing-time history for configuration 16 ( $d\gamma/du = 0.44$ ).

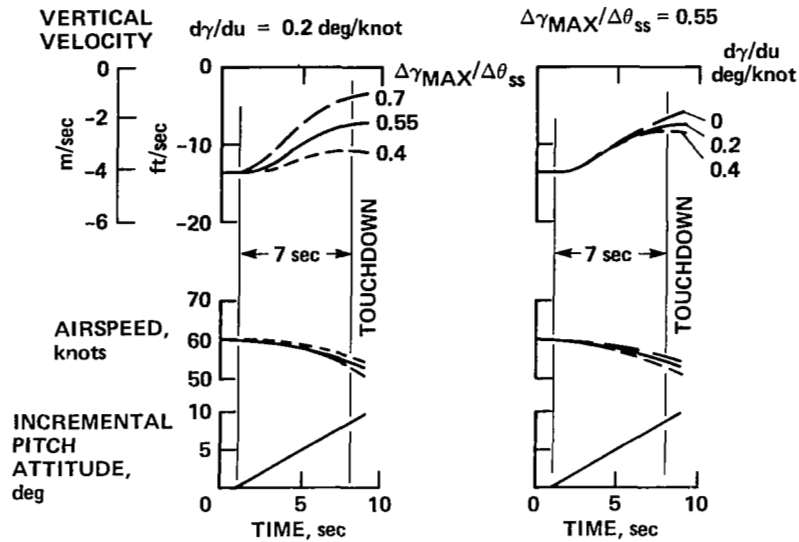


Figure 57.— Influence of initial and long-term flightpath response on flare control with pitch attitude.

## IMPLICATIONS FOR DESIGN CRITERIA

### Glide-Slope Control

From the results of this flight-research program, as well as from data acquired during flight experiments (ref. 10) and during experiments on the Ames Research Center's Flight Simulator for Advanced Aircraft (refs. 7, 9), it is possible to establish flying-qualities criteria for glide-slope control associated with a precision instrument approach. Based on these collected results and analyses, the criteria should be concerned with flightpath overshoot and the initial flightpath time response to the throttle control. The criteria thus apply to the class of powered-lift STOL aircraft that operate on the backside of the drag curve and rely on control of engine thrust and possibly another normal-force control device for use in glide-slope tracking (e.g., the McDonnell-Douglas YC-15). For powered-lift aircraft that utilize extensive lift and drag control augmentation to make the aircraft respond to the pilot's controls as if it were operating on the frontside of the drag curve (e.g., the Boeing YC-14), more appropriate criteria are contained in references 14 and 19.

To assess criteria for flightpath overshoot, data collected from the flight experiments of reference 10 and from the simulator experiments of reference 7 are compared with the IFR flight data of figure 23 of this report. This comparison is shown in figure 58. Some unpublished data obtained in flight experiments with the Princeton variable stability Navion and transmitted to the authors by D. R. Ellis are also included in this figure. The limited data available from reference 10 agree quite well with the results of this experi-

ment, considering that the spread of data in this experiment would be degraded up to 1 unit for operation in light to moderate turbulence. The Princeton Navion data, obtained in light turbulence, are no more than 1 unit from the data range of this experiment. The simulator data obtained in smooth air are from 1-1/2 to 2 units better than the flight data from this program and from those of reference 10. Part of this difference can be attributed to the effect of light turbulence on the results of this report, perhaps as much as 1/2 to 1 rating unit based on the turbulence sensitivities apparent in the data of reference 10. Based on the general impression of the evaluation pilot who participated in both the flight and simulation experiment, the remaining difference in rating may be attributed to a more critical view of the glide-slope tracking task during the latter stage of the approach in flight compared with the simulator, where the landing could not be performed with a degree of accuracy comparable to that demanded in flight. The attention required of the pilot for both glide-slope and localizer tracking was such that even the best configuration was rated unsatisfactory for the instrument approach with raw MLS guidance.

Considering these data, if the aircraft's flying qualities are to be judged adequate for the IFR glide-slope tracking task, flightpath overshoot should not exceed 2.0 to 2.5 for operation in turbulence in the light to moderate range. This criterion applies for otherwise good initial time response characteristics. (It should be emphasized that pilot ratings that are in the marginally adequate range reflect a situation in which deficiencies in the aircraft's characteristics require extensive pilot compensation to achieve adequate performance of the specified task. Because it is unlikely that such

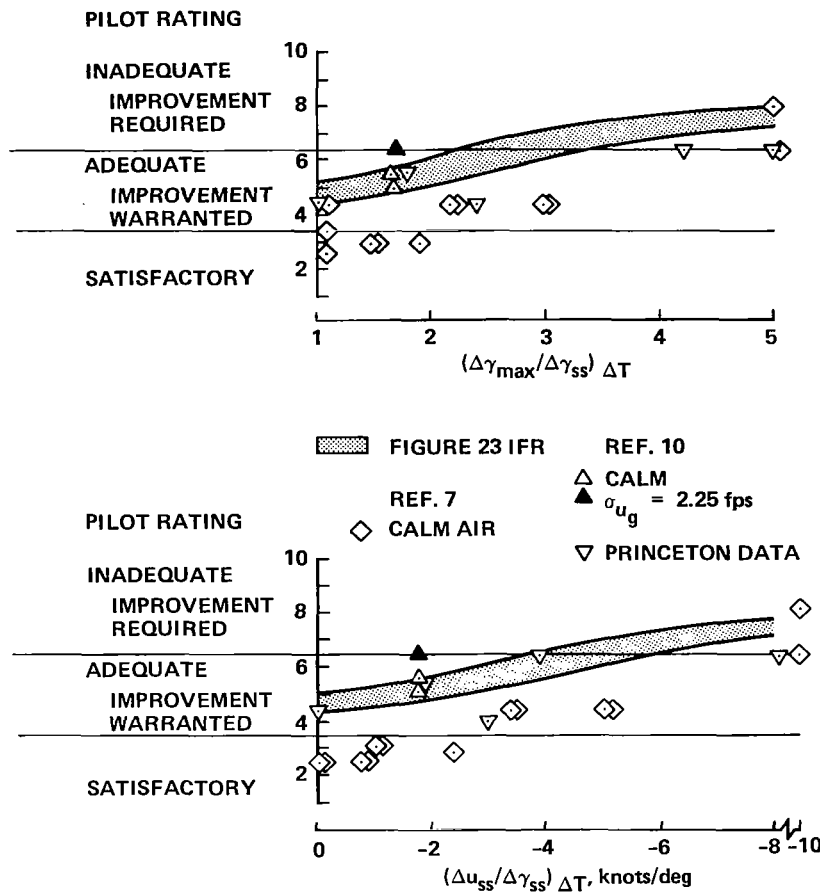


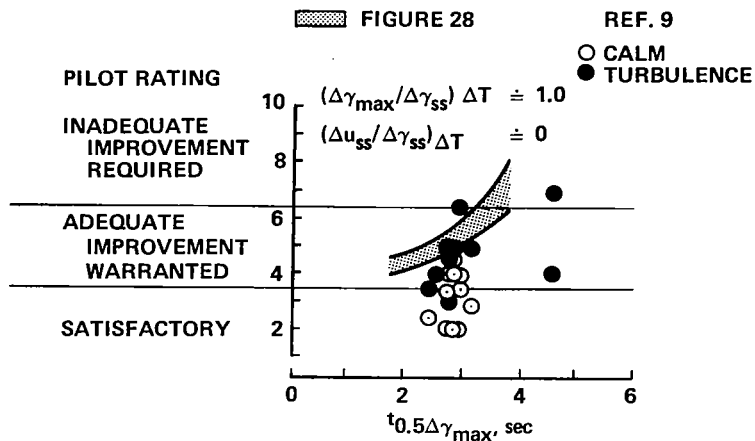
Figure 58.— Comparison of pilot rating data of glide-slope tracking for variations in flightpath overshoot and flightpath-airspeed coupling.

characteristics could be accepted for routine operation, design improvements should be strongly encouraged when characteristics fall on or near the associated boundary.) Since the configurations with flightpath overshoot were, in most cases, accompanied by flightpath-airspeed coupling, and since this coupling had some influence on the pilots' ratings for this task, the corresponding pilot rating data are also shown in relation to the amount of coupling for each configuration. In light of pilot concerns about the influence of this coupling on margins and landing performance, as well as the effort required to suppress its influence on path control, the amount of coupling should be kept less than  $-5.0$  knots/deg to ensure adequate flying qualities.

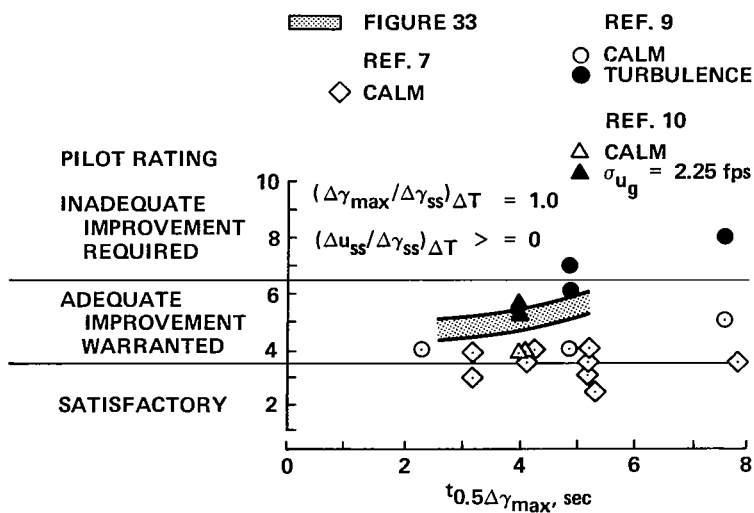
Criteria for the initial flightpath time response, as defined by  $t_{0.5} \Delta\gamma_{\max}$ , can be derived from the data of figures 28 and 33 and from references 7, 9, and 10. A comparison of these data is shown in figure 59, in which two situations are distinguished. The first, as shown in figure 59(a), is the case of no flightpath-airspeed coupling. Although the simulator results of reference 9 show satisfac-

tory ratings for operation in calm air, those data for relatively light turbulence agree well with the results presented previously in figure 28. For this level of turbulence, the initial time response should be less than 3.5 to 4.0 sec for adequate flying qualities. Operation in moderate turbulence would reduce this initial response time to between 3.0 and 3.5 sec, as noted in the preceding section (Discussion of Results). The value of  $t_{0.5} \Delta\gamma_{\max}$  recommended in reference 9 as acceptable for a certification criterion for short-term flightpath response is 3 sec; it is consistent with the conclusions drawn from figure 59(a).

For the case of conventional flightpath-airspeed coupling (positive  $(\Delta u_{ss}/\Delta\gamma_{ss}) \Delta T$  in response to throttle), data on initial time response are presented in figure 59(b) from figure 33, as well as from references 7, 9, and 10. Once again, the simulator data for calm-air operation are more favorable than the flight results. However, the data from the various flight and simulation programs agree quite well for operation in light turbulence. Under the circumstances where it is possible to augment the short-term response



a) NO FLIGHTPATH - AIRSPEED COUPLING



b) CONVENTIONAL FLIGHTPATH - AIRSPEED COUPLING

Figure 59.— Comparison of pilot-rating data of glide-slope tracking for variations in initial time response.

with a coordinated pitch input that also serves to maintain the nominal approach speed, the initial time response to the throttles can be increased to 6 or 7 sec for acceptable flying qualities. This value would be reduced to 5 to 6 sec for operation in moderate turbulence, as noted in the preceding section.

Combined influences of overshoot and initial response on design criteria can be extracted from figures 36 and 58. Three groups of data, indicated by the shaded regions shown in figure 60, separate adequate from inadequate flying qualities, and they serve to define a more general boundary encompassing the range of overshoot and initial response time. It can be observed that overshoot ratios exceeding 3.0 and initial response times exceeding 3.5 sec

cannot be tolerated, in general. For the region between these limits, a trade-off of overshoot and response time is illustrated by the cross-hatched area. As noted previously, it does not appear possible to adjust these characteristics to achieve satisfactory flying qualities for an instrument approach, using raw data guidance. It has been demonstrated in the flight experiments reported herein and in the simulator experiments in reference 10 that satisfactory flying qualities can be achieved by employing a properly designed flight director for added approach guidance with configurations that have essentially no path overshoot or path-speed coupling and acceptable initial time response. Thus, the addition of a flight director or a well-designed integrated situation display is likely to be a requirement for fully satisfactory flying qualities.

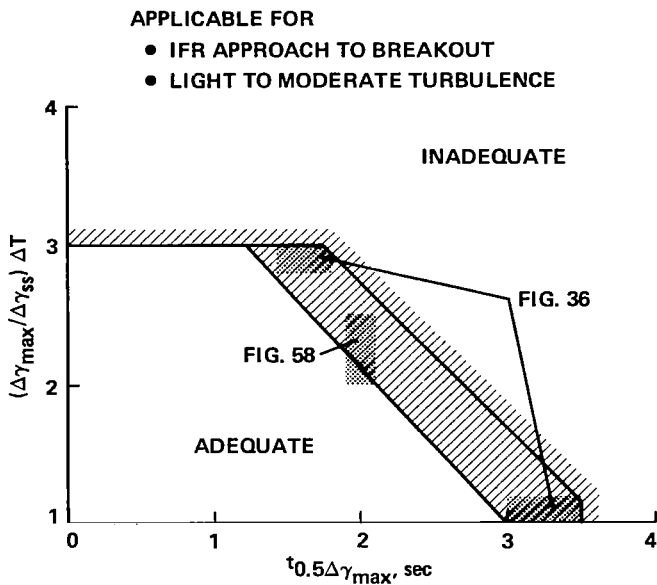


Figure 60.— Combined influence of flightpath overshoot and initial response time on adequacy of glide-slope control.

### Flare Control

Criteria for aircraft response characteristics pertinent to a full or partial flare maneuver must be related to the primary control used to perform the flare, pitch attitude or thrust (or an equivalent normal force control of sufficient authority). Application of a secondary control may be permitted, such as a step increase in thrust at flare initiation when pitch is the primary control for flare modulation, or an initial pitch rotation to the landing attitude when thrust is used for precise sink rate control.

When pitch rotation is the primary means of flare control, the initial magnitude of flightpath response to pitch is the characteristic on which a design criterion should be based. Data from figure 40 and reference 13 (as well as additional unpublished data from the Princeton Navion) serve to define the limits of this capability. These data are shown in figure 61, where the results from reference 13 correspond to flares augmented with thrust and the unpublished Princeton data correspond to flare with pitch alone. Results of these three flight experiments and the Ames Research Center's Quiet Short-Haul Research Aircraft (QSRA) are in good agreement and provide a basis for distinguishing the flightpath response to pitch attitude that is necessary to achieve adequate flare capability for this control technique. (The QSRA is a modified de Havilland C-8A Buffalo aircraft that incorporates an upper-surface blown high-lift system powered by four high by-pass ratio turbofan engines.) As suggested in the preceding section, satisfactory flare control can be expected if the short-term

flightpath response to pitch exceeds  $\Delta\gamma_{\max}/\Delta\theta_{ss} = 0.7$ . The limit on ability to adequately control the flare with a pitch rotation of reasonable magnitude is about  $\Delta\gamma_{\max}/\Delta\theta_{ss} = 0.55$ . When this capability becomes marginal or inadequate, it is possible to use an initial increment of thrust to augment the flare capability with pitch. This coordinated control technique appears to allow the flare with pitch to be performed adequately for configurations with initial flightpath to pitch response as little as  $\Delta\gamma_{\max}/\Delta\theta_{ss} = 0.4$ . When flightpath response to pitch falls below this value, it is clearly necessary to use thrust or another normal-force device as the primary flare control. The regions of  $\Delta\gamma_{\max}/\Delta\theta_{ss}$  appropriate to these various techniques are delineated at the bottom of the figure.

Subsidence of the flightpath response in the long term, associated with operation on the backside of the drag curve, does not appear to have an appreciable influence on flare control with pitch. Results of these flight experiments, the Princeton Navion data, and the findings of reference 9 support this conclusion.

In principle, when the flare is controlled with thrust, the response characteristics of concern would be expected to be the same as those for flightpath control on the approach.

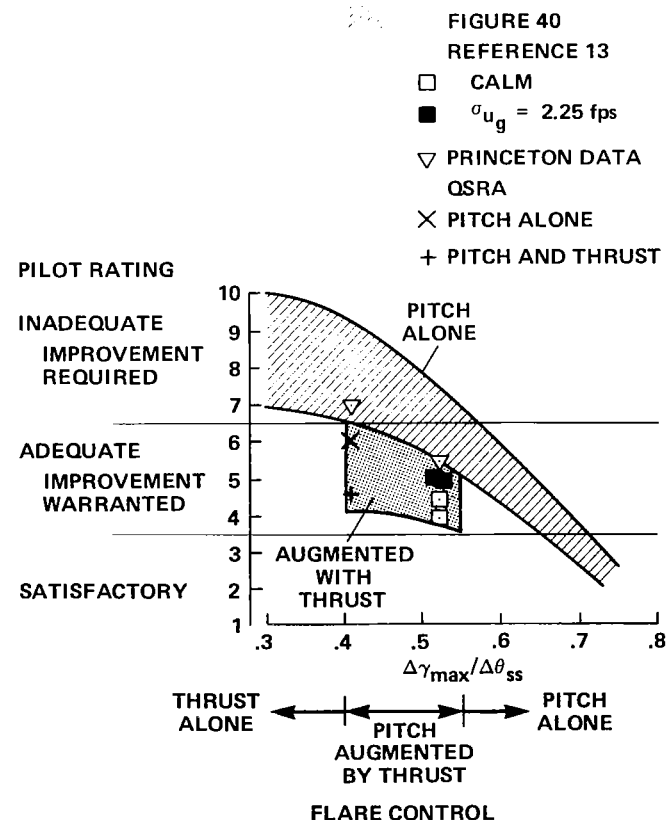


Figure 61.— Comparison of pilot-rating data of flare control for variations in flightpath response to pitch attitude.

However, given sufficient flightpath-control authority with thrust, the factor of most concern for flare control is the time required for flightpath to initially respond to a throttle control input. In this regard, the time response measure  $t_{0.5\Delta\gamma_{\max}}$  used for approach-path control is an appropriate metric. Long-term flightpath subsidence associated with path overshoot, and flightpath-airspeed coupling are of much less consequence since it is difficult to discern these characteristics over the relatively short duration of the flare.

Data from figure 52, flight data from reference 13, and simulation data from reference 9 all apply to flare with thrust and are presented for comparison in figure 62. The scatter in these data is somewhat greater than desired for a clear distinction to be made concerning limits on flare capability. The flight results from reference 13 and the bulk of the reference 9 simulation data give the impression that initial response times from 3 to 4 sec are necessary to achieve adequate flying qualities in the flare. It should be noted that values of  $t_{0.5\Delta\gamma_{\max}}$  for the reference 13 configurations were not specified in that report. Instead they were computed using the transfer-function factors and derivatives from reference 13 and the curves of figure 3 from this report. Thus, the accuracy that can be associated with their initial time response is more questionable than if measured from an actual time history. However, even if they were in error by 25%, they would still correspond well with the simulation results of reference 9. In that report, it was also found that an initial response time of 2.0 sec would suffice to provide acceptable flare response for airworthiness certification.

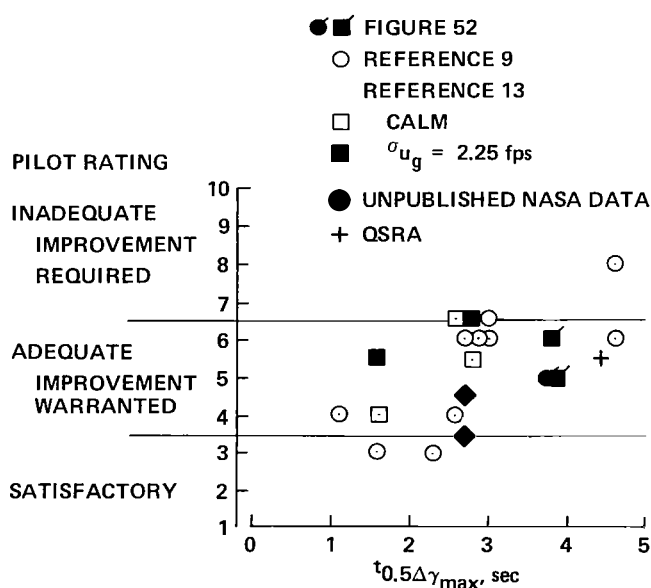


Figure 62.— Comparison of pilot-rating data of flare control with thrust for variations in initial flightpath time response to throttle.

The data from the flight experiments of this report and from those of the QSRA are more lenient in regard to flare response to thrust and suggest that adequate flying qualities (to be distinguished from those certifiable as airworthy) can be obtained with initial response times between 4.0 and 4.5 sec. Since this result is also more lenient than that for precision IFR approach path tracking, the glide-slope control criteria would govern the design for flightpath response to thrust. Unpublished data obtained at Ames Research Center from flight experiments conducted to substantiate the findings of references 9 and 15, indicated that satisfactory flying qualities can be obtained for the flare when the initial response is less than about 2.5 sec.

Discussion of response criteria for the flare would not be complete without consideration of the contributions of ground effect, particularly those concerned with lift perturbations in the flare. As noted in a previous section (Description of Flight Research Program), the results of the flight experiments reported herein were obtained for ground effects that consisted of up to an 8% lift increment (according to refs. 17 and 22). Based on the results of flight experiments presented in reference 24 on the influence of ground-effect magnitude and dynamic lag on flare control for a range of flightpath response characteristics, it can be seen that neutral to positive ground effect up to lift increments of 10% do not have an effect on the pilot's evaluation of flare characteristics for a representative powered-lift STOL aircraft configuration. Even lift decrements of up to 10% did not degrade the ratings more than 1/2 unit. Only for suckdown of 20% of the free-air lift did pilot ratings show a significant degradation. Data from the YC-15 flight-test program and analysis based on those results published in references 25 and 26 indicate that for approach operating conditions up to free-air lift coefficients of 4.0, lift increments in ground effect of up to 10% can be anticipated. Experience with the YC-14 is consistent with these predictions. Although a review of an extensive collection of wind-tunnel results in reference 27, as well as the predictive method of reference 25, suggests that it is possible that lift decrements may exist for free-air lift coefficients of 5 or greater, qualitative experience with the Ames Research Center's QSRA in approach operations at lift coefficients from 5.5 to 6 show no such evidence. The general impression obtained from a large number of STOL landings with this aircraft is that neutral to slightly positive lift ground effect exists for approach lift coefficients ranging from 5 to 6. In light of the collected flight experience from four operational aircraft, the specific results from the ground-effect experiment of reference 24, and the lack of any evidence of strong suckdown in ground effect, it is reasonable to assume that ground effect will have little influence on flying qualities for the flare and landing of a powered-lift STOL aircraft. However, if ground effect with lift decrements approaching 20% can be predicted with confidence for a new design, some degradation in flying qualities for the flare should be anticipated.

## CONCLUSIONS

A flight research program, conducted to assess requirements for flightpath and airspeed control for glide-slope tracking during a precision approach and for control of the flare and landing, particularly as applied to powered-lift STOL aircraft, has been described. Ames Research Center's Augmentor Wing Research Aircraft was used to make approaches on a  $7.5^\circ$  glide slope to landings on a  $30 \times 518$  m ( $100 \times 1700$  ft) STOL runway. The aircraft's research flight control system provided the capability for evaluating a wide range of flightpath and airspeed response characteristics. Results from these experiments, in combination with pertinent data from other sources, have been used to establish flying-qualities design criteria for the landing approach and flare-control tasks.

For glide-slope tracking, these results have defined criteria concerned with flightpath and airspeed response to the throttle control for a configuration with good attitude control characteristics. For powered-lift STOL aircraft, good attitude control is most likely to be obtained with pitch and roll attitude stabilization and command augmentation (rate-command/attitude-hold or attitude command), augmented Dutch roll damping, and turn coordination. Then, the response characteristics of primary concern are flightpath overshoot, initial flightpath response time, and flightpath-airspeed coupling. Design criteria for each of these characteristics to achieve adequate ( $PR < 6.5$ ) and satisfactory ( $PR < 3.5$ ) flying qualities for precision glide-slope tracking during an instrument approach in light turbulence down to the point of flare initiation are as follows:

- Flightpath overshoot ratios less than 2.5 to achieve adequate flying qualities for good initial time response characteristics
- Time for initial flightpath response to reach one half its peak value less than 3.5 sec to achieve adequate flying qualities for no overshoot

- Steady-state flightpath-airspeed coupling less than  $-5.0$  knots/deg for adequate flying qualities with good initial response
- Incorporation of a flight director or integrated situation display for fully satisfactory flying qualities with configurations having little or no overshoot or path-speed coupling.

An increase in turbulence may degrade pilot ratings from 1/2 unit for good control characteristics to 1-1/2 units for poor characteristics.

Criteria for flare control are associated with the primary control appropriate to the flare technique. For flares performed primarily with pitch rotation, the maximum initial flightpath response to pitch attitude is the most important factor to be considered. Long-term flightpath response associated with operation on the backside of the drag curve is of relatively little concern. When the pitch control alone is used to perform the flare, the ratio of the maximum short-term flightpath response to a step in pitch attitude must exceed approximately 0.55 for adequate flare control and about 0.7 for satisfactory flare control. If this ratio falls between 0.4 and 0.55, the flare can still be executed adequately with pitch if a step increment in thrust is used to initiate the maneuver. When the ratio is less than 0.4, the flare must be controlled primarily with thrust. An initial pitch rotation to the landing attitude may be performed if required. The criteria for flightpath response to the throttle is concerned with the initial response time. Adequate flying qualities may be achieved for initial response times less than 4.5 sec to reach the increment in flightpath response commanded by the throttle. Satisfactory ratings can be obtained for initial response times less than 3 sec. Variations in lift in ground effect are not likely to have a significant influence on flare control unless lift decrements exceed 10% of the approach lift coefficient.

Ames Research Center  
National Aeronautics and Space Administration  
Moffett Field, California 94035, August 25, 1981

## APPENDIX A

### TURBULENCE RESPONSE RELATIONSHIPS

References 9 and 10 describe the effect of atmospheric turbulence on glide-slope tracking. As noted in reference 9, the aircraft's flightpath response to horizontal and vertical gusts may be described by the following expressions, assuming that constant pitch attitude is maintained during the gust encounter:

$$\frac{\gamma}{u_g} = \frac{(-Z_u/V_o)s}{\Delta_{\theta=\text{const}}}$$

$$\frac{\gamma}{w_g} = \frac{(-Z_w/V_o)(s - X_u + X_w Z_u/Z_w)}{\Delta_{\theta=\text{const}}}$$

The range of frequencies of the turbulence spectrum over which the aircraft's flightpath shows significant response is determined by either  $\omega_{\theta}$  or  $1/T_{\theta 2}$ , the flightpath response bandwidth. The magnitude of the response to a unit disturbance is scaled by the derivative  $Z_u$  for horizontal gusts and by  $Z_w$  for vertical gusts.

When the pilot is engaged in controlling flightpath to track the glide slope in the presence of turbulence, these relationships that describe the effect of turbulence on flightpath response are modified to the extent that the characteristic roots of  $\Delta_{\theta=\text{const}}$  are altered by closed-loop

control of flightpath with thrust. If it is assumed that this closed-loop control is executed in a manner to provide a flightpath bandwidth between 0.5 and 1.0 rad/sec, the closed-loop roots can be approximated by

$$\Delta_{\theta=\text{const}} = (s + 1/T'_{\gamma T})(s + 1/T'_{\theta 2})$$

$\gamma \rightarrow \delta_T$

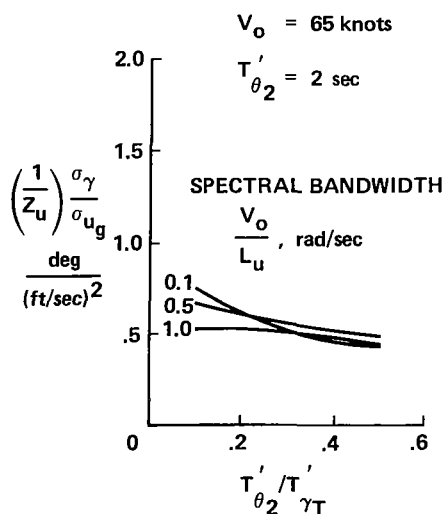
The modified transfer functions for flightpath response to horizontal and vertical gust become

$$\frac{\gamma}{u_g} = \frac{(-Z_u/V_o)s}{(s + 1/T'_{\gamma T})(s + 1/T'_{\theta 2})}$$

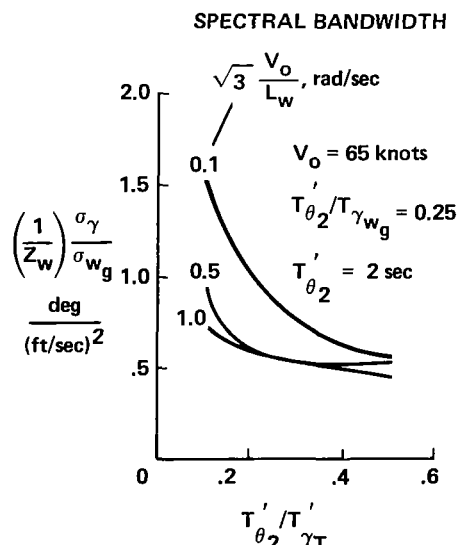
$$\frac{\gamma}{w_g} = \frac{(-Z_w/V_o)(s - X_u + X_w Z_u/Z_w)}{(s + 1/T'_{\gamma T})(s + 1/T'_{\theta 2})}$$

Contributions of turbulence to rms flightpath response are shown in figure 63. Considering typical values of  $Z_u$  and  $Z_w$  for powered-lift aircraft operating at STOL approach speeds, the flightpath disturbances due to horizontal and vertical gusts are of approximately the same magnitude.

Another form of atmospheric disturbance that deserves attention is the gradient of horizontal wind velocity, or wind shear. The transfer-function relationship in this case is



a) RESPONSE TO LONGITUDINAL GUSTS



b) RESPONSE TO VERTICAL GUSTS

Figure 63.— Contribution of longitudinal and vertical gusts to closed-loop flightpath control.

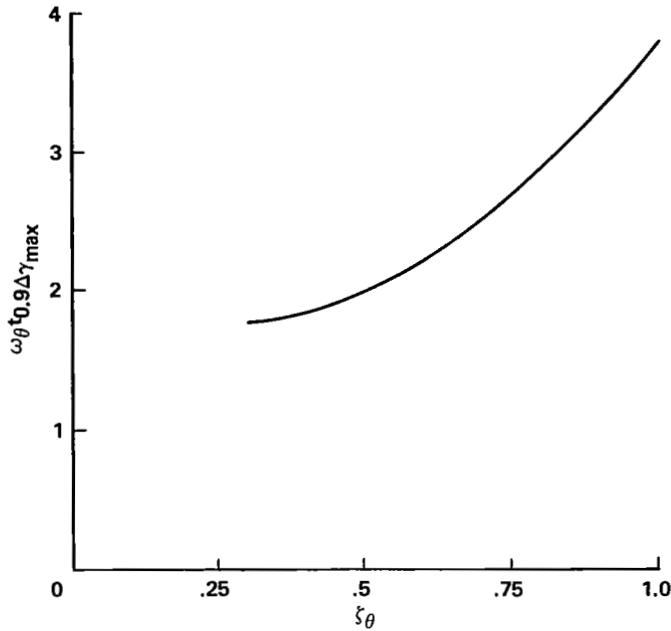


Figure 64.— Time to develop flightpath disturbance caused by a longitudinal wind gradient.

$$\frac{\gamma}{\dot{u}_w} = \frac{-Z_u/V_0}{\Delta\theta = \text{const}}$$

This response is characterized by the steady-state disturbance that develops in response to a sustained wind gradient and the time required for this disturbance to develop. From this transfer function it can be shown that the steady-state flightpath upset is described by

$$(\Delta\gamma_A)_{ss} = \frac{\dot{u}_w}{g} + \frac{d\gamma}{du} \frac{u}{\dot{u}_w} \dot{u}_w$$

where the first term in the expression is the change in flightpath required to counteract the inertial acceleration due to the wind shear, and the second term is the result of the change in lift-drag ratio associated with the airspeed excursion during the shear encounter. Thus the primary influence of the aircraft's configuration on the response to wind shear is associated with operation on the backside of the drag curve and with the steady-state airspeed disturbance, which is

$$\frac{u}{\dot{u}_w} = \frac{2\zeta_\theta}{\omega_\theta} - T_{u_g}$$

$$1/T_{u_g} = -Z_w + Z_u X_w / X_u$$

The time response can be characterized by the time interval required for the disturbance to reach 90% of its steady-state value. Figure 64 illustrates the contributions to this time factor. It appears that for representative powered-lift aircraft characteristics ( $\zeta_\theta \doteq 0.9$ ,  $\omega_\theta \doteq 0.3$  rad/sec) the flightpath disturbance is established in about 10 sec. Under circumstances of unattended operation or when the pilot is not sufficiently aware that wind shear is being encountered, the flightpath disturbance may develop fully and, it occurs at low altitude, to a dangerous extent. However, if the pilot has sufficient information concerning the aircraft's situation during the approach, particularly good quality vertical speed or flightpath information, and if the aircraft has sufficient performance capability to counter the disturbances, then there should be little difficulty in traversing such wind gradients. However, if the aircraft is operated using only the current generation cockpit instruments, such as the IVSI, airspeed, and raw data glide-slope deviation indicators, and if the aircraft's performance capability in the landing configuration is marginal, then wind-shear encounters may prove troublesome or even dangerous for STOL approach and landing operations.

## APPENDIX B

### DOCUMENTATION OF EVALUATION CONFIGURATIONS

Table 5 presents the longitudinal stability derivatives of the basic aircraft for the nominal approach configuration, from which the various glide-slope and flare-control configurations are derived. Tables 6 and 7 provide the data from

which the pertinent flightpath and airspeed response characteristics were extracted. Figures 65 and 66 show the time histories of the glide-slope and flare control configurations, respectively, from which the response data were derived.

TABLE 5.—LONGITUDINAL STABILITY DERIVATIVES  
FOR THE AUGMENTOR WING RESEARCH AIRCRAFT

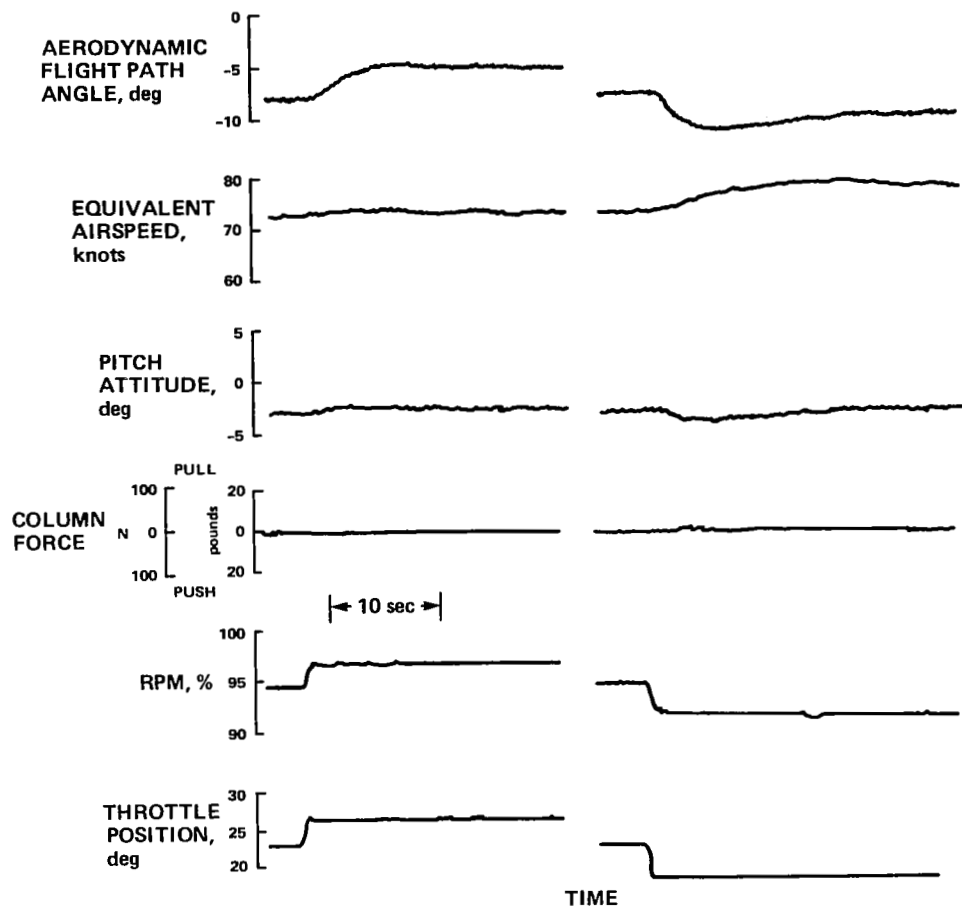
Gross weight = 19,522 kg (43,000 lb)	$N_H = 95\%$
$V_{c_o} = 70$ knots	$\delta_F = 65^\circ$
$\alpha = 3.6^\circ$	$\nu = 80^\circ$
	$I_{yy} = 281,000 \text{ kg}\cdot\text{m}^2$ (207,000 slug-ft <sup>2</sup> )
$X_u = -0.056 \text{ sec}^{-1}$	$Z_u = -0.36 \text{ sec}^{-1}$
$X_w = 0.11 \text{ sec}^{-1}$	$Z_w = -0.52 \text{ sec}^{-1}$
$\frac{X_q}{V_o} = 0.0073$	$\frac{Z_q}{V_o} = -0.079$
$\frac{X_{\delta_e}}{V_o} = 0.016 \text{ sec}^{-1}$	$\frac{Z_{\delta_e}}{V_o} = -0.062 \text{ sec}^{-1}$
$\frac{X_{\delta_\nu}}{V_o} = -0.05 \text{ sec}^{-1}$	$Z_{\delta_\nu} = 0$
$X_{\delta_c} = 0$	$\frac{Z_{\delta_c}}{V_o} = 0.0015 \text{ sec}^{-1}/\%$
$X_{\Delta T} = 0$	$\frac{Z_{\Delta T}}{V_o} = -0.0076 \text{ sec}^{-1}/\% N_H$
$M_u = 0$	$M_{\dot{\alpha}} = -0.43 \text{ sec}^{-1}$
$M_\alpha = -0.46 \text{ sec}^{-2}$	$M_{\delta_e} = -1.72 \text{ sec}^{-2}$
$M_q = -1.27 \text{ sec}^{-1}$	

TABLE 6.- GLIDE-SLOPE CONTROL CONFIGURATIONS

Config- uration	GW, lb	$V_{c_0}$ , knots	$\gamma_{A_0}$ , deg	$\Delta T$ , % $N_H$	$\Delta\gamma_{max}$ , deg	$\Delta\gamma_{ss}$ , deg	$\Delta u_{ss}$ , knots	$\frac{\Delta\gamma_{max}}{\Delta\gamma_{ss}}$ ,	$\frac{\Delta u_{ss}}{\Delta\gamma_{ss}}$ , knots/deg	$t_{0.5} \Delta\gamma_{max}$ , sec
1	42,700	73	-8	2.2	3.3	3.2	1.5	1.03	0.47	2.5
	42,500	73	-7.5	-3.2	-3.6	-2.1	5.5	1.71	-2.62	2.3
2	43,600	75	-8	2.6	2.85	1.6	-4.5	1.8	-2.8	2.0
	43,500	76	-7	-2.5	-3.5	-2.5	5.5	1.4	-2.2	2.2
4	42,500	67	-9	2.3	2.9	.2	-6	14.5	-30.0	1.7
	42,300	67	-7.5	-2.5	-3.7	-1.7	6	2.2	-3.53	1.8
6	42,600	75	-7.5	2.9	5.9	4.9	-1.5	1.2	-.31	3.8
7	42,000	71	-7.5	1.4	2.8	2.8	3.3	1.0	1.2	5.2
	41,900	73	-7	-2.1	-4.5	-4.5	0	1.0	0	2.6
8	42,000	75	-8.5	2.5	4.0	1.2	-6.3	3.33	-5.2	2.4
	41,900	73	-7	-1.1	-1.5	-4	3.0	3.75	-7.5	2.2
9	42,500	75	-7	2.3	2.9	1.0	-4.5	2.9	-4.5	2.0

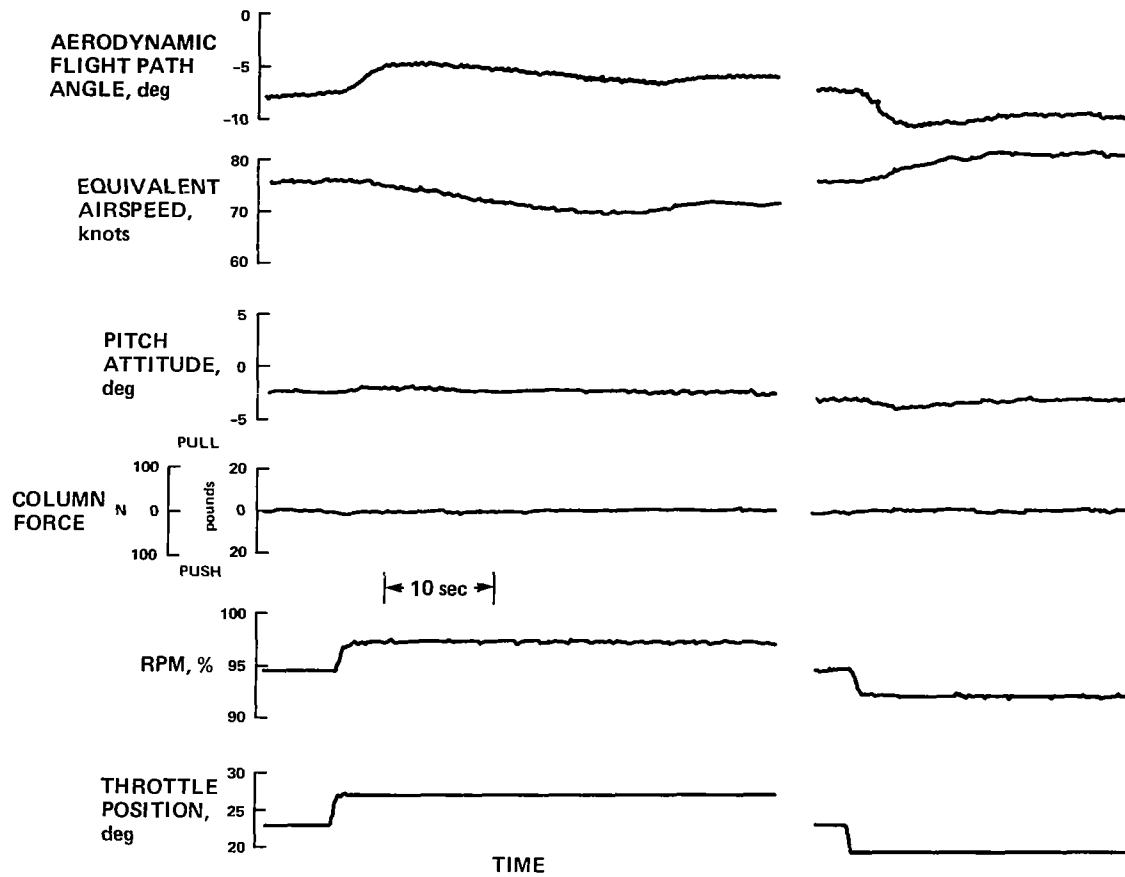
TABLE 7.— FLARE-CONTROL CONFIGURATIONS

Config- uration	GW, lb	$V_{c_0}$ , knots	$\gamma_{A_0}$ , deg	$\Delta\gamma_{\max}$ , deg	$\Delta\gamma_{ss}$ , deg	$\Delta\theta_{ss}$ , deg	$\Delta u_{ss}$ , deg	$\frac{\Delta\gamma_{\max}}{\Delta\theta_{ss}}$	$\frac{d\gamma}{du}$ , deg/knot	$\frac{\Delta u_{ss}}{\Delta\theta_{ss}}$ , knots/deg	$t_{0.1} \Delta\gamma_{\max}$ , sec
11	45,500	77	-7	2.6	-0.8	4.7	-8	0.55	0.1	-1.74	12.8
	45,300	75	-7.5	-3.2	---	-5.9	---	.54	---	---	---
	44,500	75	-8	---	.5	-2.9	8	---	.062	-2.76	10.1
12	44,300	77	-9	2.6	---	3.3	---	.79	---	---	---
	44,300	77	-9	---	-3	3.0	-8.5	---	.035	-2.83	22.4
	44,200	75	-9	-2.65	---	-3.5	---	.76	---	---	---
	44,200	75	-9	---	.0	3.0	9	---	.0	-3.0	16.8
13	43,000	68	-4	1.2	---	3.2	---	.38	---	---	---
	43,000	68	-4	---	-3.5	3.0	-7	---	.5	-2.33	6
14	43,800	77	-7.5	.95	---	3.0	---	.32	---	---	8.8
	43,700	74	-8	-2.1	1.2	-3.8	4.5	.55	.27	-1.2	13.6
15	44,000	69	-7.5	1.3	---	2.8	---	.46	---	---	---
	44,000	69	-7.5	---	.1	2.6	-3.3	---	-.03	-1.27	12.8
	43,800	68	-7.5	-2.0	---	-3.4	---	.59	---	---	---
	43,800	68	-7.5	---	-1.0	-3.25	-5.0	---	-.2	-1.54	---
16	43,700	68	-7	1.5	-3.5	2.9	-7.8	.52	.45	-2.69	11.2
	42,800	68	-7.5	-1.6	---	-2.8	---	.57	---	---	---
	42,800	68	-7.5	---	1.35	-2.5	13	---	.104	-5.2	---



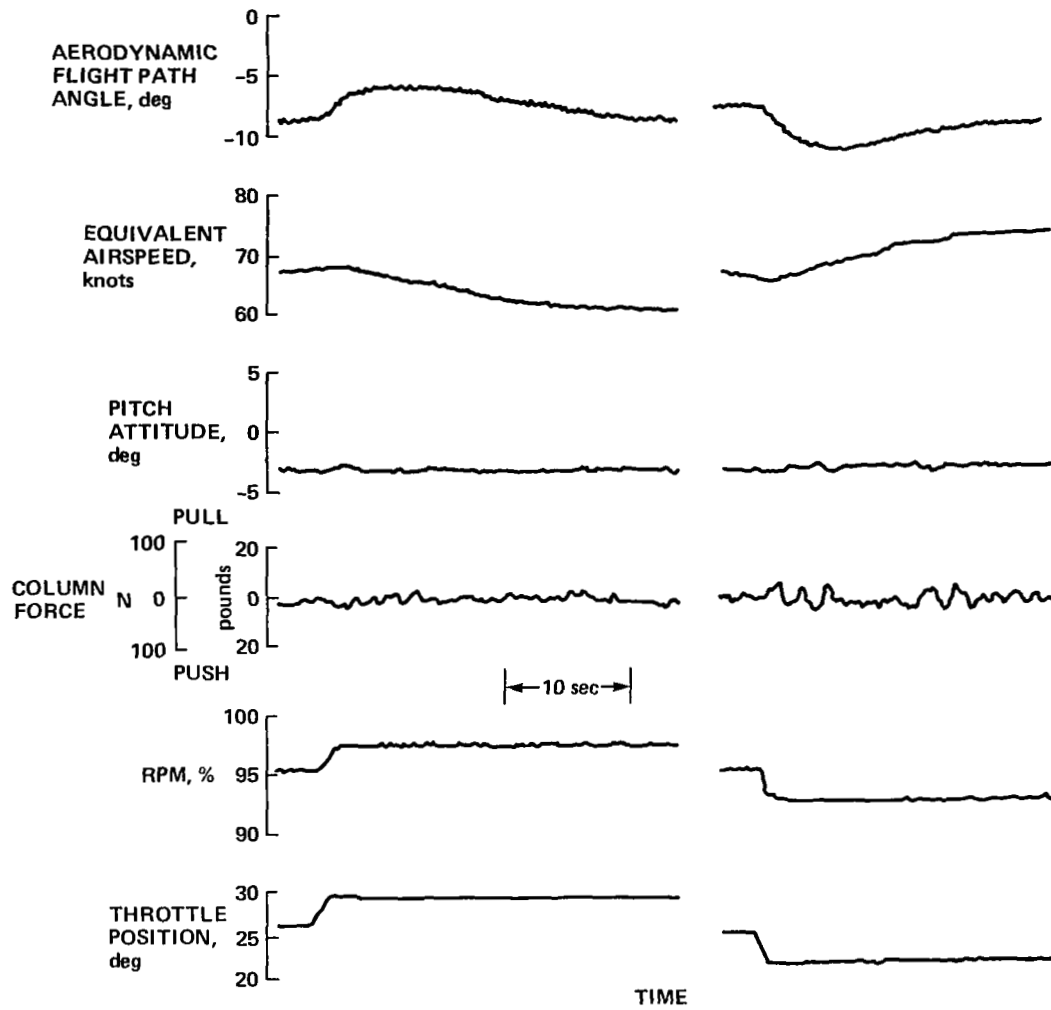
(a) Configuration 1.

Figure 65.— Longitudinal response to a step throttle input.



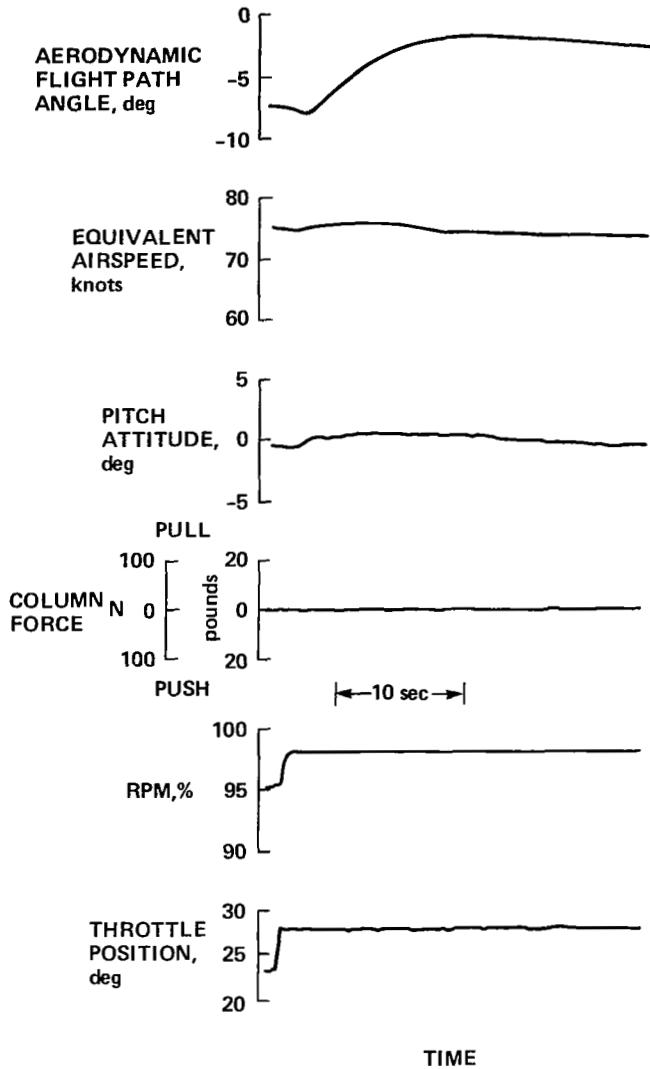
(b) Configuration 2.

Figure 65.— Continued.



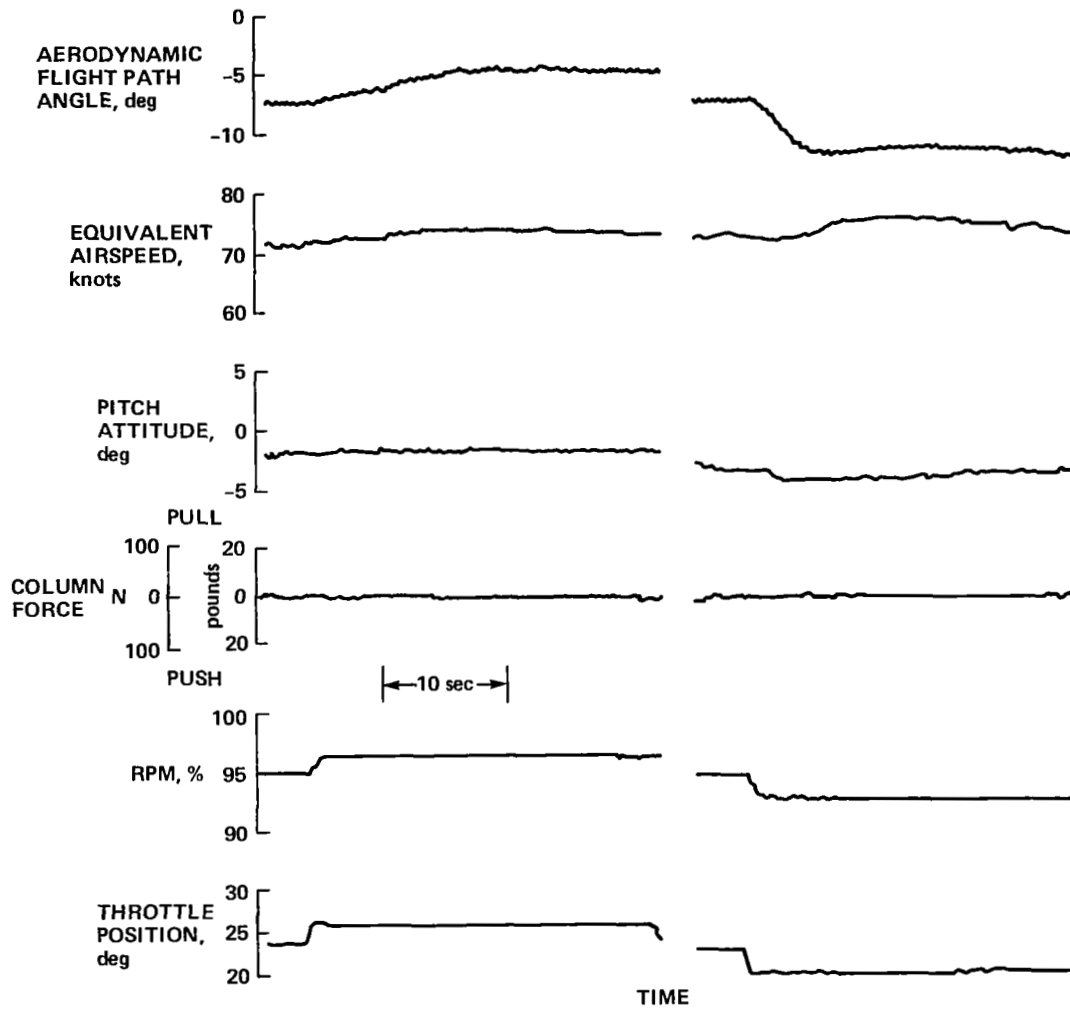
(c) Configuration 4.

Figure 65.— Continued.



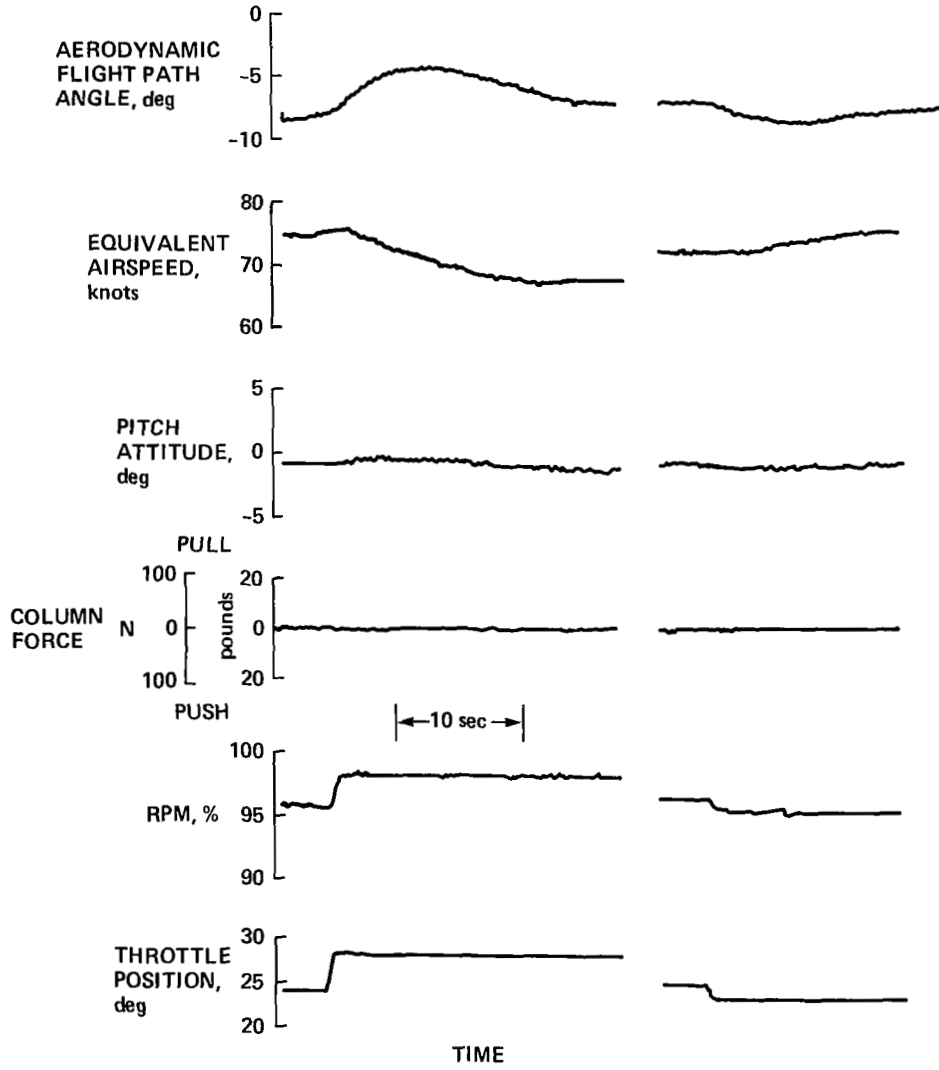
(d) Configuration 6.

Figure 65.— Continued.

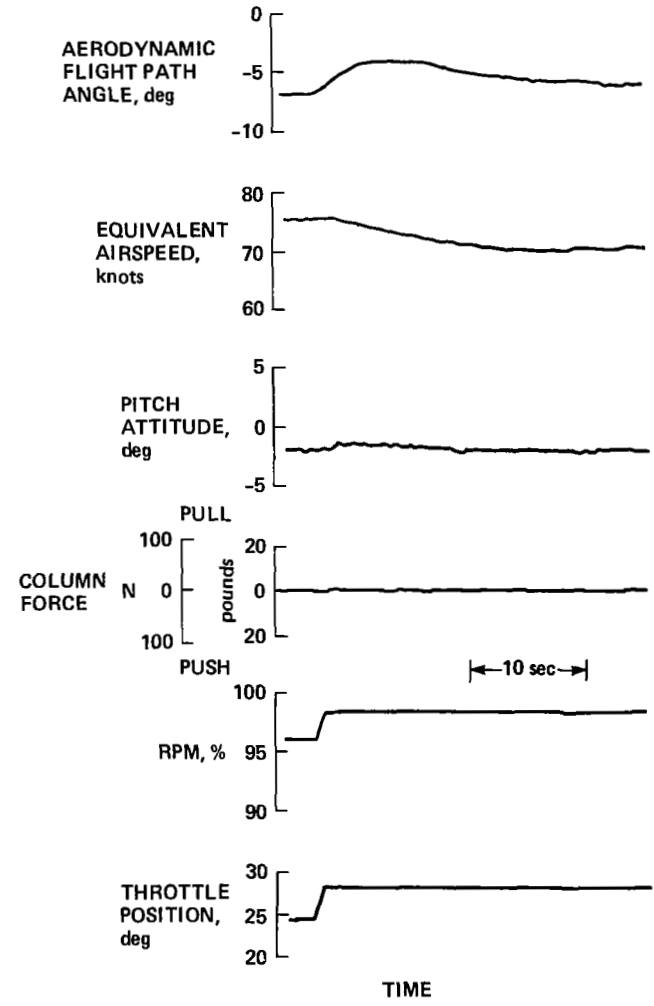


(e) Configuration 7.

Figure 65.— Continued.

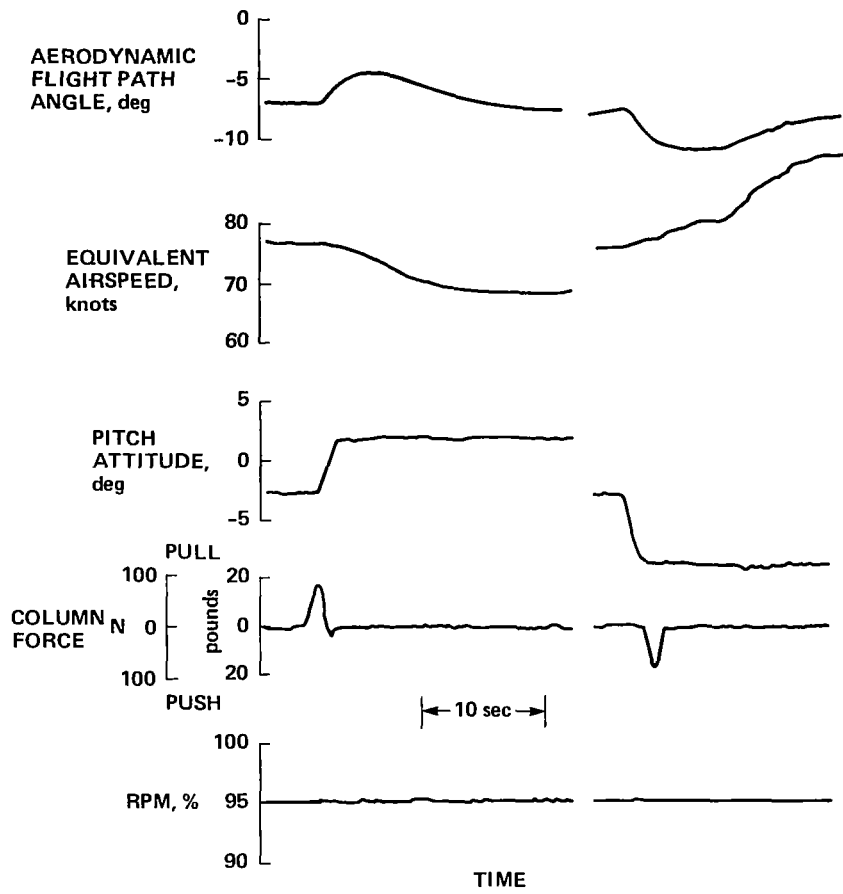


(f) Configuration 8.



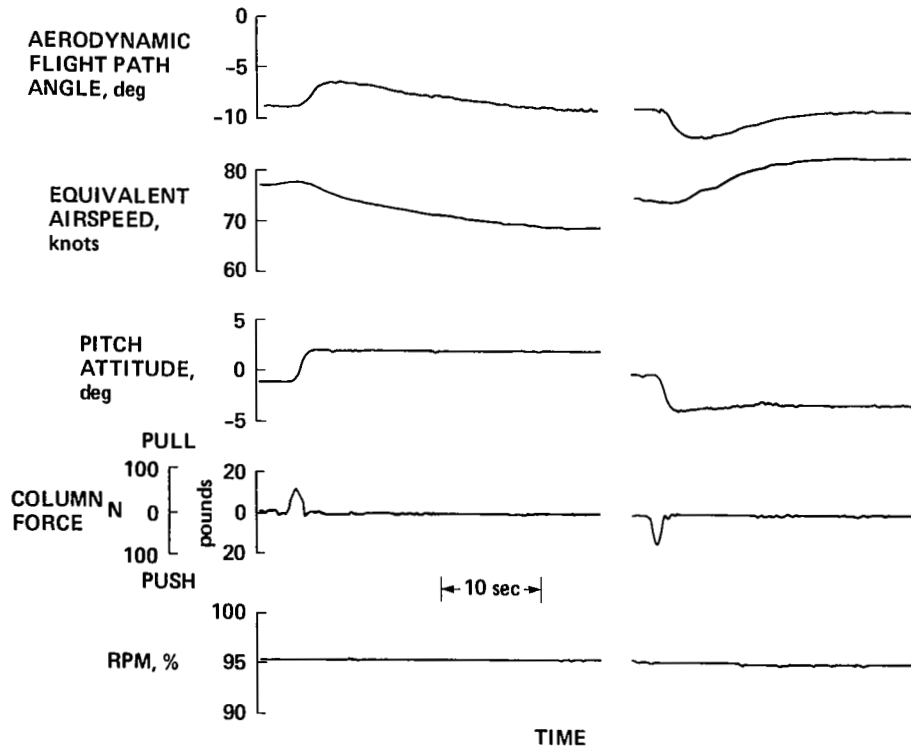
(g) Configuration 9.

Figure 65.- Concluded.



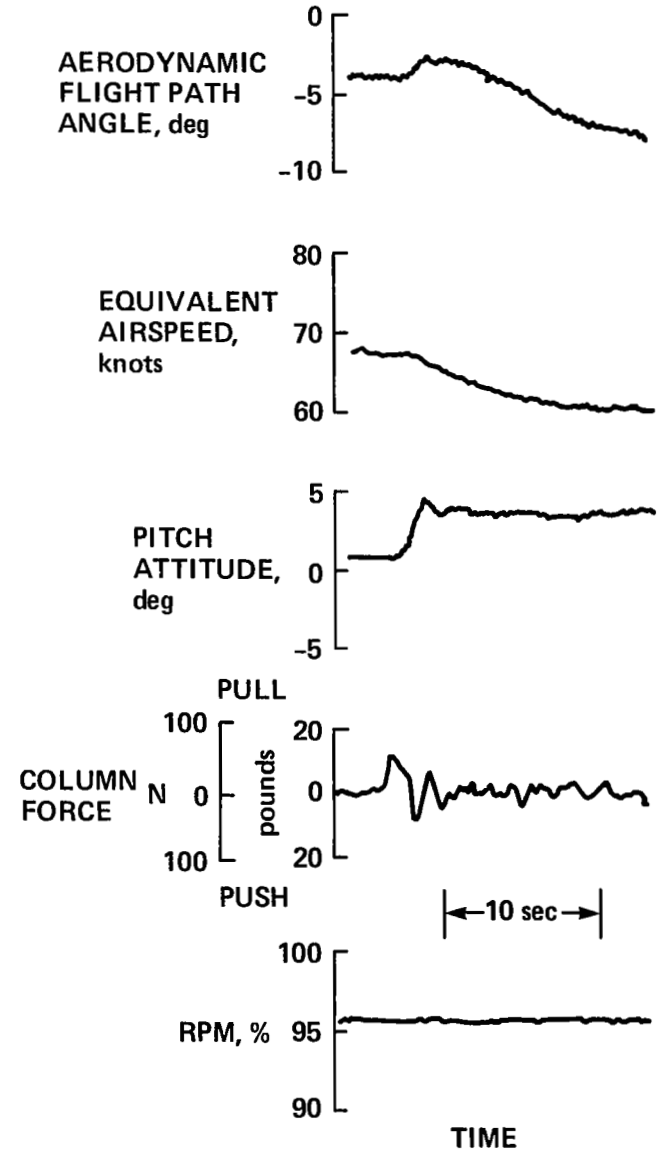
(a) Configuration 11.

Figure 66.— Longitudinal response to a step pitch input.



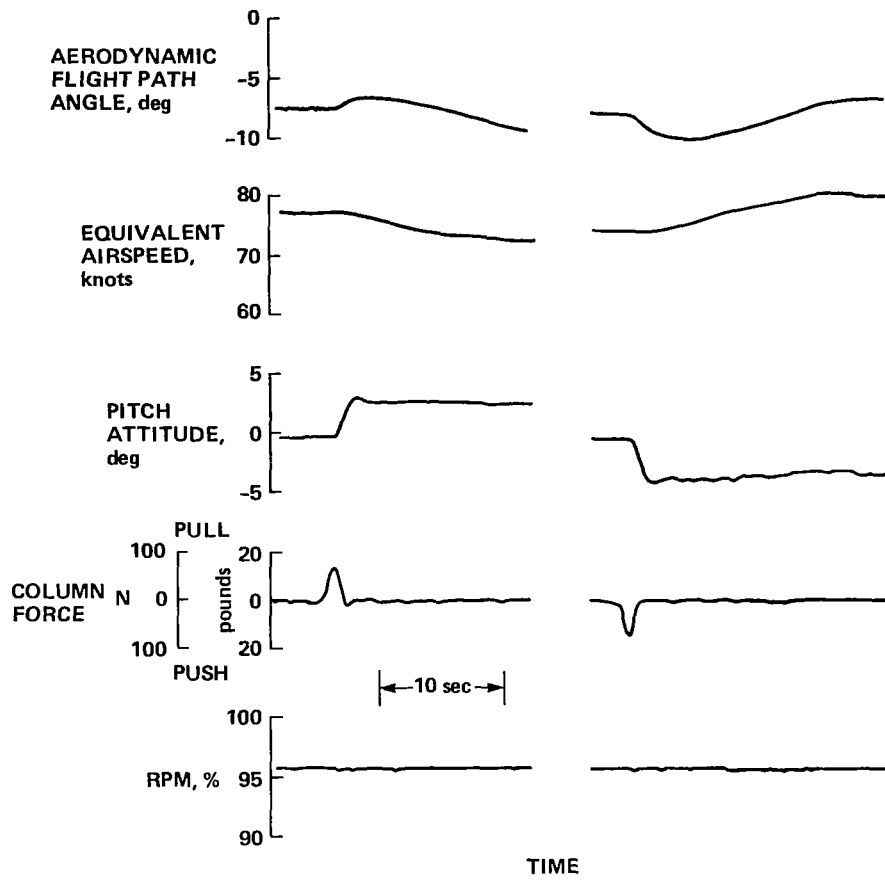
(b) Configuration 12.

Figure 66.— Continued.



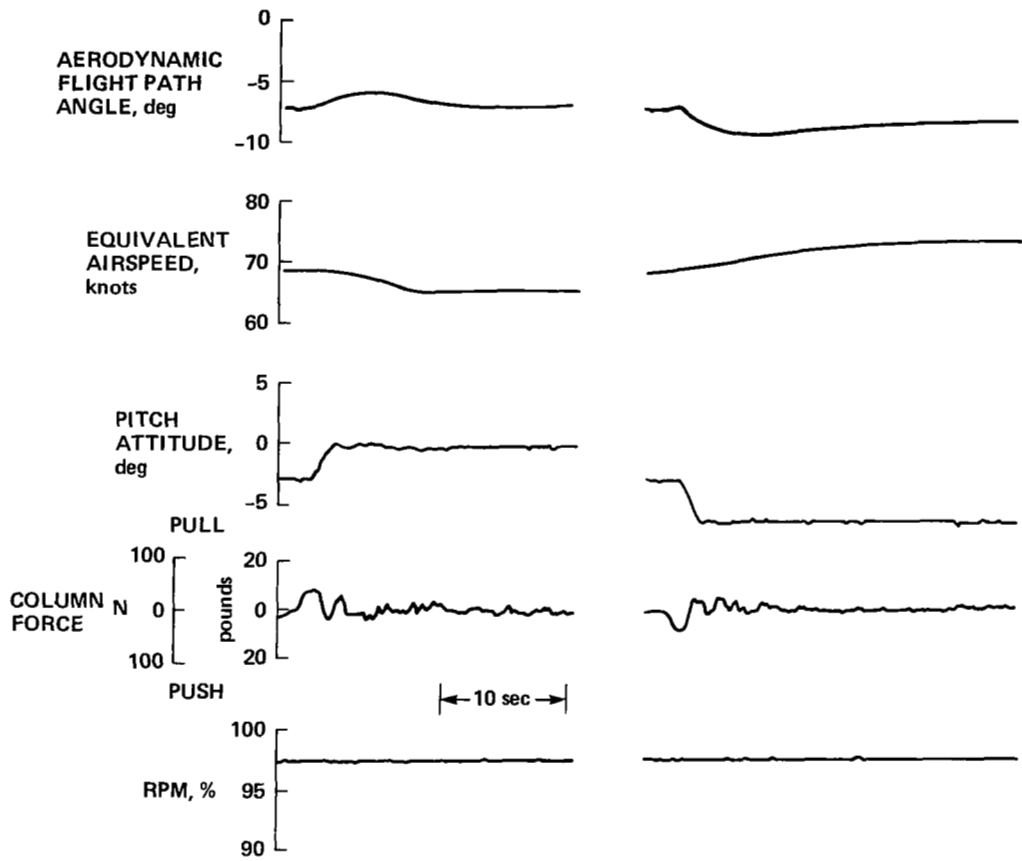
(c) Configuration 13.

Figure 66.— Continued.



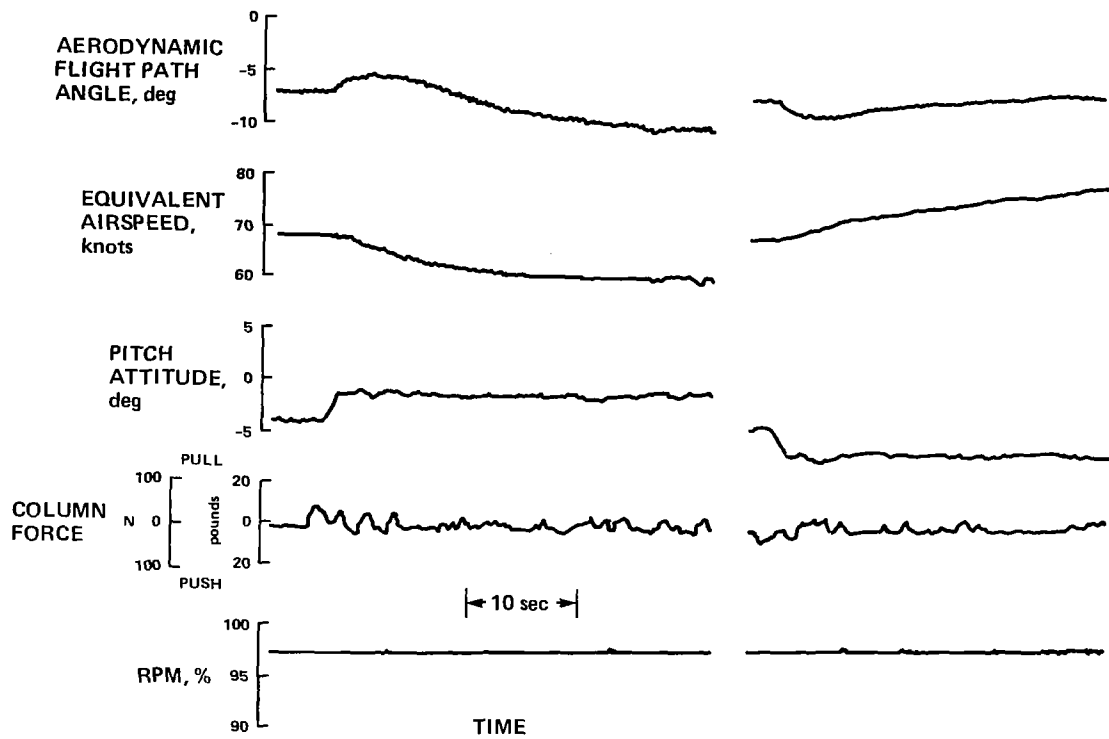
(d) Configuration 14.

Figure 66.- Continued.



(e) Configuration 15.

Figure 66.- Continued.



(f) Configuration 16.

Figure 66.— Concluded.

## APPENDIX C

### SUMMARY OF PILOT COMMENTS AND RATINGS

Tables 8 and 9 present the pilots' evaluations of each of the experimental configurations investigated in the flight research program. The tables include evaluations of glide-slope control configurations under VFR and IFR conditions in calm air and in turbulence (table 8) and flare-control configurations in winds and turbulence (table 9). Pilot commentaries accompany the opinion ratings. A summary of a range of wind conditions encountered for each

configuration is provided, including tower-reported winds for individual landings or for a series of landings. The most significant encounters of winds and turbulence, as derived from the wind extraction program, are also presented; they include sustained headwind gradients, their duration and time of encounter during the approach, and extremes of headwind and vertical gusts, as measured along the aircraft's flightpath.

TABLE 8.— SUMMARY OF PILOTS' EVALUATIONS AND WIND CONDITIONS FOR GLIDE-SLOPE TRACKING CONFIGURATIONS

Config-uration	Tower reported winds		Measured turbulence					Pilot ratings, VFR (IFR)		Pilot comments
			$\dot{U}_w$ knots/sec	$\Delta t$ , sec	$T_{TD}$ , sec	$u_{w \min}$ $u_{w \max}$ knots	$\pm w_{w \max}$ ft/sec	A	B	
	knots	deg								
1	5	320						3.5		Decoupling of flightpath and airspeed response allows approach to be made at more constant pitch attitude which simplifies tracking task. Glide-slope tracking reasonably good. No change to 1/2 to 1 rating unit change in pilot rating for shears and turbulence encountered. Most deficiencies associated with raw data instrument scan.
	10	360								
	25-30	310								
	37	320	0.8	8	20	9-24	18	3.5		
			-1.4	8	37			in turb		
			.8	7	45					
	30-38	320	1.4	8	22	10-30	12			
			1.0	7	75					
	5	320	1.0	7	18	0-7	6	(4.5)		
			-1.0	7	28					
	15	300							4 (4.5)	
	20-30	270							(4.5-5)	
	35-40	320							(5-5.5)	
	5	360	-1.1	9	20	-6 to 7	9		in turb	
			1.5	8	30					
			-1.5	7	60					
1 + flight director	20	320						(2-2.5)		Flight director does a good job. Makes IFR tracking significantly easier. Good glide-slope and localizer tracking performance. Pitch commands smooth and easy to follow. Throttle and lateral directors seem a little bit busy and perhaps too sensitive.
	20-25	320	-1.2	7	10	9-19	3			
	10	340							(3)	
	25	320								

TABLE 8.— CONTINUED

Config- uration	Tower reported winds		Measured turbulence					Pilot ratings, VFR (IFR)		Pilot comments
			$\dot{U}_w$	$\Delta t$	$T_{TD}$	$u_w$ min max	$\pm w_w$ max	A	B	
	knots/sec	sec	sec	knots	ft/sec					
2	5	360	-1.0	10	70	16-30	7.5	4.5 (6)	5 (5)  (5.5-6) in turb	Some difficulty with coupled flightpath- airspeed-angle-of-attack responses to thrust. Airspeed variations influence flightpath response and landing distance. Angle-of- attack variations influence safety margins. Sluggish flightpath response when correcting to glide slope from low offset. Easy to get low/slow due to path-speed coupling. Must either control attitude to hold airspeed to obtain acceptable flightpath response during glide-slope corrections, or accept degraded flightpath response if allowing pitch SCAS to hold attitude. Large attitude changes to hold speed. Pitch control required to hold speed while making path corrections with thrust is unconventional (nose-down change in attitude must be coordinated with an increase in thrust for a correction up to the glide slope, and vice versa. Workload evenly divided between glide-slope and localizer tracking tasks. Effects of turbulence and shears encountered degrade ratings by 1/2 to 1 rating unit. Reduced sink rate in strong headwinds compensates for effect of turbulence.
	30-38	320								
	5	360								
	8	360								
	25-30	270								
	30-40	310								
	35-42	320								
	20	350								
12	360									

TABLE 8.— CONTINUED

Config- uration	Tower reported winds		Measured turbulence					Pilot ratings, VFR (IFR)		Pilot comments
			$\dot{U}_w$	$\Delta t$ ,	$T_{TD}$	$u_w$ min max	$\pm w_w$ max	A	B	
	knots/sec	sec	sec	knots	ft/sec					
3	25-30	300	-1.0	9	20	14-23	6	6	6.5 (6.5)	Best to maintain constant attitude; otherwise large speed and angle-of-attack excursions occur. Flightpath overshoot and path-speed coupling apparent. Easy to get slow during glide-slope corrections. Acceptability depends on available path control authority. Can make 1-dot glide-slope corrections but response is sluggish. Marginally acceptable if enough flightpath control authority is available. If path corrections not accompanied by large attitude changes, path control is limited.
			-1.0	6	70	15-23	9			
	10 7	060 120	-1.0	6	30					
			-1.0	7	15					
4	25-30	300	-0.9	8	65	16-24	7	7	7	Unacceptable. Flightpath is not controllable. Large adverse path-speed coupling. Can only adequately conduct approach if glide-slope corrections are kept small. Corrections from 1-dot high or low causes airspeed excursions of 10-15 knots. Difficult to recover from low offset. Speed decays. Lowering nose to regain speed eventually reduces rate of descent, but very sluggish.
			1.0	8	32					
	11-15	300	1.5	8	15	15-24		>7		
5	calm calm 35-45	320	1.4	12	46	18-34	16	3-3.5	(4.5) (4.5-5) in turb	Glide-slope tracking OK. Not much different in turbulence. About the same as configuration 1 for IFR tracking.
			-0.8	18	33					
			1.2	10	15					
			-2.3	6	30	15-34	21			
			-1.5	6	20					

TABLE 8.— CONTINUED

Config- uration	Tower reported winds		Measured turbulence					Pilot ratings, VFR (IFR)		Pilot comments
			$\dot{U}_w$	$\Delta t$	$T_{TD}$	$u_w$ min max	$\pm w_w$ max	A	B	
	knots	deg	knots/sec	sec	sec	knots	ft/sec			
6	15	300						5		Must be accustomed to making large and rapid throttle corrections. Glide-slope control noticeably worse than configuration 1. Tend to overshoot when capturing glide slope. Tracking is oscillatory. Flightpath response is lightly damped. Initial impression is that response to throttles is too sensitive although that impression is discounted with more exposure to this configuration. Tracking is worse close in. Under IFR, it's difficult to determine appropriate glide-slope corrections that are compatible with flare into touchdown zone. Under visual conditions, pilot will begin to aim for touchdown zone earlier and make path adjustments accordingly. Effect of turbulence fairly negligible since ground speed and sink rate are reduced in strong headwind.
	35-44	320	2.0	9	50	10-32	18			
			-2.0	5	32					
			-1.0	9	25					
	10	090	-2.0	8	57	-1 to 8	9	(8)		
			1.4	6	40					
			-7	6	22					
	7-10	090	-1.0	9	45	-2 to 8	6		6	
	calm								(6)	
	35-40	320	1.5	10	46	13-28	18		(7)	
			-1.0	12	33				in turb	
			3.0	7	60	12-34	24		no $\gamma$ bar	
			-1.4	7	48				(6-1/2)	
			1.4	7	40				in turb	
		-3.3	6	20				with $\gamma$ bar		
		-2.0	9	50	9-32	27				
		2.0	9	40						
		-4.0	5	40	18-43	27				
		4.3	6	50						
		-2.5	6	30						
6 + flight director	25	320						(5)	Oscillatory flightpath behavior is still evident and glide-slope tracking still suffers.	

TABLE 8.— CONTINUED

Config- uration	Tower reported winds		Measured turbulence					Pilot ratings, VFR (IFR)		Pilot comments
			$\dot{U}_w$	$\Delta t$ ,	$T_{TD}$	$u_w$ min max	$\pm w_{w \max}$	A	B	
	knots/sec	sec	sec	knots	ft/sec					
7	5-10 10	350 090	1.0	8	28	-5 to 7	6	5.5 (5.5)		
			-1.0	10	18	-3 to 7	5			
	-1.0	7	60							
	1.0	7	40							
	35-40	320	1.5	7	60	6-38	15			
			1.0	10	10					
	10-20 20	300 270	-2.2	9	95	10-34	18			4.5 (4.5-5) (6) in turb
				1.0	17	83				
	40-45	320	-3.3	5	30					
			1.7	8	25					
	20	320	1.0	10	70	11-22	4			
			-1.0	8	22	12-22	6			
8	15	320	1.0	8	75	3-18	9	8		
			-0.8	10	62					
	0.8	15	50							
	calm								7	

TABLE 8.— CONCLUDED

Config- uration	Tower reported winds		Measured turbulence					Pilot ratings, VFR (IFR)		Pilot comments
			$\dot{U}_w$	$\Delta t$	$T_{TD}$	$u_w$ min max	$\pm w_w$ max	A	B	
	knots/sec	sec	sec	knots	ft/sec					
9	10	320	-1.0	7	12	6-15	6	5	Difficult to see much difference from configuration 6. Glide-slope tracking is oscillatory. Tend to overshoot glide slope and difficult to stabilize the approach. Flightpath-airspeed coupling noticeable but not excessive. Airspeed wanders quite a bit and it's difficult to coordinate pitch and throttle controls. Slow correcting from low offset.	
	15	320	-1.0	10	50	1-15	4			
	light and variable calm light and variable			1.0	10	18				5.5-6
10			-1.8	7	45	-3 to 8	4	6	Poor glide-slope tracking, but not as bad for overcontrolling as configuration 6. Tracking close in to breakout still difficult on instruments.	
	10-15 calm	090								4 (6-6.5)

TABLE 9.- SUMMARY OF PILOT'S EVALUATIONS AND WIND CONDITIONS FOR FLARE-CONTROL CONFIGURATIONS

Config- uration	Tower reported winds		Measured turbulence					Pilot ratings, VFR (IFR)		Pilot comments
	knots	deg	$\dot{U}_w$ knots/sec	$\Delta t$ , sec	$T_{TD}$ , sec	$u_w$ min max knots	$\pm w_w$ max ft/sec	A	B	
11	5 25-30 8 30-40 20	360 300 360 310 350						3.5	5 4	Flare-control technique – initiate and modulate flare with pitch rotation. Use discrete thrust inputs to compensate for high sink rates. Maintain positive sink rate to touch-down. Gradually reduce thrust when touch-down is assured. Landing precision reasonably good. Large pitch rotation required. Use of both pitch and thrust control not objectionable.
12	calm 35-42  calm 35-45	 320  320	 1.5 -2.5 -1.5  1.4 -0.8 1.2	 10 10 7  12 18 10	 50 40 15  46 33 15	 15-37  18-34	 21  16	2	3 4 in turb	Flare control primarily with pitch attitude. Good, comfortable flare capability.
13	10-15 calm  7-10	090  090	 -1.5 -1.1	 7 11	 7 11	 -7 to 10 -7 to 8		4	3-1/2-4 pitch + thrust 7-10 pitch alone	Response to pitch better than configuration 14. Necessary to coordinate thrust and attitude. Occasionally overcontrolled with thrust. Still inadequate for control with pitch alone.

TABLE 9.— CONTINUED

Config- uration	Tower reported winds		Measured turbulence					Pilot ratings, VFR (IFR)		Pilot comments
			$\dot{U}_w$	$\Delta t$	$T_{TD}$	$u_{w \min}$ $u_{w \max}$	$\pm w_{w \max}$	A	B	
	knots/sec	sec	sec	knots	ft/sec					
14	15	300						5 thrust primary	Must control flare with thrust. Flare control adequate with thrust, and about as good as for configuration 11. Occasionally requires nearly maximum thrust to arrest sink rate. Essentially no flightpath response to pitch. Good that aircraft responds primarily to only one control. Some degradation of rating in turbulence and wind shear.	
	10	350	-1.0	9	10	2-14	9	7 in turb		
			-1.5	6	45	0-14	10			
			-8	6	15					
	35-44	320	-2.0	5	32	10-32	18			
			-1.0	9	25					
	calm							5 thrust primary		
35-40	320	1.4	7	40	12-34	24	6 in turb			
		-3.3	6	20						
		-2.7	7	8	9-32	27				
		-4.0	5	40	18-43	27				
7-10	090	-2.5	6	30			9-10 pitch alone			
15	15 calm	300					3	5	Can't see much difference from configuration 11. Can't provoke poor flare by over-rotating or flaring early.	
16	20-30 calm	300					3.5	5	No difference from configuration 11. Flare entry conditions and turbulence mask any differences. Can't provoke poor flare by over-rotating or flaring early. Only slight tendency to drop in from an intentionally extended flare.	

TABLE 9.- CONCLUDED

Config- uration	Tower reported winds		Measured turbulence					Pilot ratings, VFR (IFR)		Pilot comments
			$\dot{U}_w$	$\Delta t$ ,	$T_{TD}$	$u_w$ min max	$\pm w_w$ max	A	B	
	knots	deg	knots/sec	sec	sec	knots	ft/sec			
17	calm							2	3	Same behavior as configuration 12. Good flare capability with pitch.
18	calm						5	Considerable thrust addition required to flare. Poor sink rate and touchdown control. Purposely over-rotated to try to provoke float. Only subtle difference from configuration 14.		
19	15	300					5	No difference in flare from configuration 14. May be some tendency to drop in after an unrealistically long float.		
20	10 calm	320	-1.0 1.5	7 6	12 10	6-15 -2 to 10	6 4	6.5		5

## APPENDIX D

### SYMBOLS

$AGL$	above ground level	$\dot{h}_F$	complementary filtered vertical velocity
$A_{uT}$	gain of the thrust-to-speed transfer function	IFR	instrument flight rules
$A_{\gamma T}$	gain of the thrust-to-flightpath transfer function	IVSI	instantaneous vertical-speed indicator
$A_{\gamma\theta}$	gain of the attitude-to-flightpath transfer function	$I_{yy}$	pitch moment of inertia
$a_x$	longitudinal body axis acceleration	$M_a$	pitching-moment derivative with respect to variable $a$ , $1/I_{yy}(\partial M/\partial a)$
$a_y$	lateral body axis acceleration	MODILS	prototype microwave landing guidance system
$a_z, n_z$	vertical body axis acceleration	$m$	aircraft mass
$c.g.$	center of gravity	$N_H$	high-pressure engine rotor rpm
DME	distance measuring equipment	PR	Cooper-Harper pilot rating
$D_\alpha$	drag derivative with respect to angle of attack, $1/m(\partial D/\partial \alpha)$	$p, p_B$	body axis roll rate
$dB$	decibel	$q, q_B$	body axis pitch rate
$d\gamma/du$	change of flightpath angle with air-speed for constant thrust	$r, r_B$	body axis yaw rate
EADI	electronic attitude-director indicator	SCAS	stabilization and command augmentation system
$F_{BO}$	electrical breakout force for column	$s$	Laplace operator
$F_c$	column force	$T$	line of constant thrust
$F_w$	wheel force	$T_{TD}$	time to touchdown
$F_p$	pedal force	$1/T_{u_g}$	real root of the numerator of the airspeed-to-longitudinal-gust transfer function
GW	gross weight	$1/T_{u_T}$	real root of the numerator of the thrust-to-air-speed transfer function
$g$	gravitational acceleration	$1/T_{\gamma T}$	real root of the numerator of the thrust-to-flightpath transfer function
HSI	horizontal situation indicator	$1/T_{\gamma_1}$	real root of the numerator of the attitude-to-flightpath transfer function
$h$	altitude		
$\dot{h}$	vertical velocity from barometric or radio altimeter		

$1/T_{\theta_1}, 1/T_{\theta_2}$	real roots of the attitude fixed longitudinal characteristic equation $\Delta\theta=\text{const}$	$w_g$	vertical gust
$t_{0.5}\Delta\gamma_{\text{max}}$	time to 50% of the peak flightpath response to a step change in thrust	$w_{w_{\text{max}}}$	maximum vertical wind velocity
$t_{0.1}\Delta\gamma_{\text{max}}$	decay time for flightpath response to a step change in pitch attitude	$X_a$	longitudinal force derivative due to variable $a$ , $1/m(\partial X/\partial a)$
$U_0$	initial longitudinal velocity for ground speed complementary filter	$X_R, Y_R, Z_R$	radar-measured position of aircraft in STOL runway coordinates
$\dot{U}_w$	rate of change of longitudinal wind (headwind shear with respect to time)	$\dot{X}_f$	complementary filtered inertial velocities
$U(\ )$	total longitudinal velocity for ( ) contribution	$\dot{X}_m$	raw radar-derived inertial velocities
$u$	perturbation airspeed	$\dot{X}_w, \dot{Y}_w, \dot{Z}_w$	components of wind velocity in STOL runway coordinates
$u_g$	longitudinal gust	$Z_a$	vertical force derivative due to variable $a$ , $1/m(\partial Z/\partial a)$
$u_{w_{\text{min}}}$ $u_{w_{\text{max}}}$	minimum and maximum values of headwind	$\alpha$	angle of attack
$V_c$	calibrated airspeed	$\alpha_0$	threshold angle of attack for throttle flight director
$V_{c_0}$	initial calibrated airspeed	$\dot{\alpha}$	rate-of-change of angle of attack
$V_F$	complementary filtered airspeed	$\beta$	angle of sideslip
VFR	visual flight rules	$\gamma$	flightpath angle
$V_G$	ground speed	$\gamma_A$	aerodynamic flightpath angle
$V_0$	initial airspeed, initial lateral velocity for ground speed complementary filter	$\gamma_0$	initial flightpath angle
$V_T$	true airspeed	$\Delta T$	incremental change in thrust
$V(\ )$	total lateral velocity for ( ) contribution	$\Delta t$	time duration of longitudinal wind gradient
$v$	perturbation lateral velocity	$\Delta\theta=\text{const}$	attitude-fixed longitudinal characteristic equation
$W_0$	initial vertical velocity for complementary filter	$(\Delta u_{ss}/\Delta\gamma_{ss})\Delta T$	ratio of change of steady-state airspeed to flightpath due to a change in thrust (constant pitch attitude)
$W(\ )$	total vertical velocity for ( ) contribution	$\Delta u_{ss}/\Delta\theta_{ss}$	ratio of change of steady-state airspeed to pitch attitude for constant thrust
$w$	perturbation vertical velocity	$\Delta y$	lateral deviation from localizer beam

$\Delta\beta/\Delta\phi$	ratio of peak sideslip to peak bank angle occurring during a turn entry maneuver	$\delta_w$	wheel position
$\Delta\gamma_{ss}$	steady-state flightpath perturbation	$\delta_{wBO}$	electrical breakout position for wheel
$(\Delta\gamma_{max}/\Delta\gamma_{ss})\Delta T$	ratio of peak-to-steady-state change of flightpath angle due to a change in thrust (constant pitch attitude)	$\zeta_E, \omega_E$	damping ratio and natural frequency of engine thrust response to throttle
$\Delta\gamma_{max}/\Delta T$	peak change in flightpath angle in response to a step change in thrust	$\zeta_\theta, \omega_\theta$	damping ratio and natural frequency of the attitude-fixed longitudinal characteristic equation (assuming a complex pair of roots)
$\Delta\gamma_{max}/\Delta\theta_{ss}$	peak change in flightpath angle in response to a step change in pitch attitude	$\theta$	pitch attitude
$\Delta\gamma_{ss}/\Delta\theta_{ss}$	ratio of change of steady-state flightpath angle to pitch attitude	$\theta_T$	effective thrust turning angle
$\delta_{A_{TOTAL}}$	sum of right and left aileron deflection	$\nu$	nozzle position
$\delta_{CH}$	inboard or outboard augmentor choke position	$\tau_E$	time constant for engine thrust response to throttle
$\delta_c$	column position	$\phi$	bank angle
$\delta_{cFD}$	column flight director bar deflection	$\psi$	heading angle
$\delta_e$	elevator position	$\omega_{BW}$	pilot's flightpath control bandwidth
$\delta_{eSAS}$	pitch SAS series servo position		amplitude ratio
$\delta_f$	flap position	( $\cdot$ )	derivative with respect to time, $d(\ )/dt$
$\delta_r$	rudder position	Subscripts:	
$\delta_p$	pedal position	$A$	aircraft velocity with respect to airmass
$\delta_{sp}$	spoiler position	$I$	aircraft velocity with respect to Earth
$\delta_T$	throttle position	$W$	velocity of airmass with respect to Earth

## REFERENCES

1. Chalk, C. R.; Neal, T. P.; Harris, T. M.; Pritchard, F. E.; and Woodcock, R. J.: Background Information and User Guide for MIL-F-8785B(ASG), Military Specification – Flying Qualities of Piloted Airplanes. AFFDL-TR-69-72, Aug. 1969.
2. Chalk, C. R.; Key, D. L.; Kroll, J. Jr.; Wasserman, R.; and Radford, R. C.: Background Information and User Guide for MIL-F-83300, Military Specification – Flying Qualities of Piloted V/STOL Aircraft. AFFDL-TR-70-88, March 1971.
3. Airworthiness Standards: Transport Category Airplanes. Federal Aviation Regulations, Part 25. June 1974.
4. Tentative Airworthiness Standards for Powered-Lift Transport Category Aircraft. Federal Aviation Administration, Aug. 1970.
5. V/STOL Handling Qualities, Part I. Criteria and Discussion. AGARD R-577-70, Dec. 1970.
6. Innis, Robert C.; Holzhauser, Curt A.; and Quigley, Hervey C.: Airworthiness Considerations for STOL Aircraft. NASA TN D-5594, 1970.
7. Franklin, James A.; and Innis, Robert C.: Flight-Path and Airspeed Control during Landing Approach for Powered-Lift Aircraft. NASA TN D-7791, 1974.
8. Allison, R. L.; Mack, M.; and Rumsey, P. C.: Design Evaluation Criteria for Commercial STOL Transports. NASA CR-114454, 1972.
9. Heffley, Robert K.; Stapleford, Robert L.; and Rumold, Robert C.: Airworthiness Criteria Development for Powered-Lift Aircraft – A Program Summary. NASA CR-2791, 1977.
10. Hoh, Roger H.; Craig, Samuel J.; and Ashkenas, Irving L.: Identification of Minimum Acceptable Characteristics for Manual STOL Flight-Path Control. Vol. 1 Summary, FAA-RD-75-123, June 1976.
11. Heffley, Robert K.: Closed-Loop Analysis of Manual Flare and Landing. *J. Aircraft*, vol. 13, no. 2, 1976, pp. 83-88.
12. Franklin, James A.; and Innis, Robert C.: Flight Evaluation of Flight-Path Control for the STOL Approach and Landing. *J. Aircraft*, vol. 15, no. 1, 1978, pp. 5-12.
13. Whyte, Patrick H.: An Exploratory Investigation of the STOL Landing Maneuver. NASA CR-3191, 1979.
14. Gerken, Gary: USAF Flying Qualities Requirements for a STOL Transport. ASD-TR-78-13, 1979.
15. Hynes, Charles S.; Scott, Barry C.; Martin, Paul W.; and Bryder, Ralph B.: Progress toward Development of Civil Airworthiness Criteria for Powered-Lift Aircraft. NASA TM X-73,124, 1976.
16. Quigley, Hervey C.; Innis, Robert C.; and Grossmith, Seth: A Flight Investigation of the STOL Characteristics of an Augmented Jet Flap STOL Research Aircraft. NASA TM X-62,334, 1974.
17. Vomaske, Richard F.; Innis, Robert C.; Swan, Brian E.; and Grossmith, Seth W.: A Flight Investigation of the Stability, Control, and Handling Qualities of an Augmented Jet Flap STOL Airplane. NASA TP-1254, 1978.
18. Neuman, Frank; Watson, DeLamar M.; and Bradbury, Peter: Operational Description of an Experimental Digital Avionics System for STOL Airplanes. NASA TM X-62,448, 1975.
19. Franklin, James A.; Innis, Robert C.; and Hardy, Gordon H.: Flight Evaluation of Stabilization and Command Augmentation System Concepts and Cockpit Displays during Approach and Landing of a Powered-Lift STOL Aircraft. NASA TP-1551, 1980.
20. Hoh, Roger H.; Klein, Richard H.; and Johnson, Walter A.: Development of an Integrated Configuration Management/Flight Director System for Piloted STOL Approaches. NASA CR-2883, 1977.
21. Kelly, James R.; Garren, John F. Jr.; and Deal, Perry L.: Flight Investigation of V/STOL Height-Control Requirements for Hovering and Low-Speed Flight under Visual Conditions. NASA TN D-3977, 1967.
22. Wingrove, Rodney C.: Parameter Estimation of Powered-Lift STOL Aircraft Characteristics Including Turbulence and Ground Effects. NASA TM X-62,382, 1974.

23. Cooper, George E.; and Harper, Robert P.: The Use of Pilot Rating in the Evaluation of Aircraft Handling Qualities. NASA TN D-5153, 1969.
24. Ellis, David R.: An In-Flight Simulation of Approach and Landing of a STOL Transport with Adverse Ground Effect. NASA CR-154,875, 1976.
25. Parks, Edwin K.: Flight-Test Measurement of Ground Effect for Powered-Lift STOL Airplanes. NASA TM 73,256, 1977.
26. Stevens, Victor C.; and Wingrove, Rodney C.: Ground Effects on STOL Aircraft. AIAA Paper 77-576, June 1977.
27. Campbell, John P.; Hassell, James, Jr.; and Thomas, J. L.: Recent Research on Powered-Lift STOL Ground Effects. AIAA Paper 77-574, June 1977.

1. Report No. NASA TP-1911	2. Government Accession No.	3. Recipient's Catalog No.	
4. Title and Subtitle DESIGN CRITERIA FOR FLIGHTPATH AND AIRSPEED CONTROL FOR THE APPROACH AND LANDING OF STOL AIRCRAFT		5. Report Date March 1982	6. Performing Organization Code
		8. Performing Organization Report No. A-8645	10. Work Unit No. 532-02-11
7. Author(s) James A. Franklin, Robert C. Innis, Gordon H. Hardy, and Jack D. Stephenson		11. Contract or Grant No.	
		13. Type of Report and Period Covered Technical Paper	
9. Performing Organization Name and Address Ames Research Center, NASA Moffett Field, Calif. 94035		14. Sponsoring Agency Code	
		12. Sponsoring Agency Name and Address National Aeronautics and Space Administration Washington, D.C. 20546	
15. Supplementary Notes Point of contact: James A. Franklin, M.S. 211-2, NASA-Ames Research Center, Moffett Field, California 94035, (415)965-5009, FTS 448			
16. Abstract <p>A flight research program was conducted to assess requirements for flightpath and airspeed control for glide-slope tracking during a precision approach and for flare control, particularly as applied to powered-lift, short takeoff and landing (STOL) aircraft. In some instances, the results are also pertinent to other types of aircraft that execute steep approaches to a flare and landing at low airspeeds. Ames Research Center's Augmentor Wing Research Aircraft was used to fly approaches on a 7.5° glide slope to landings on a 30 × 518 m (100 × 1700 ft) STOL runway. The aircraft's research flight control system made it possible to evaluate a wide range of flightpath and airspeed control characteristics. The dominant aircraft response characteristics that influence flying qualities for approach path tracking were determined to be flightpath overshoot, flightpath-airspeed coupling, and the initial flightpath response time. The significant contribution to control of the landing flare using pitch attitude was the short-term flightpath response. The limiting condition for initial flightpath response time for flare control with thrust was also identified. In general, the range of these characteristics that encompasses satisfactory to unacceptable flying qualities for the approach and landing was determined. Considering these data, as well as results of other flight and ground-based simulator programs, it is possible to define flying-qualities design criteria for glide-slope and flare control based on the aforementioned response characteristics.</p>			
17. Key Words (Suggested by Author(s)) STOL aircraft Handling qualities Approach and landing Flight research		18. Distribution Statement Unclassified - Unlimited  STAR Category - 08	
19. Security Classif. (of this report) Unclassified	20. Security Classif. (of this page) Unclassified	21. No. of Pages 98	22. Price* A05

\*For sale by the National Technical Information Service, Springfield, Virginia 22161